Numerical Methods for Pattern and Bifurcation Analysis in Complex Networks

Kirill Rogov

Numerical Methods for Pattern and Bifurcation Analysis in Complex Networks

Kirill ROGOV

Supervisors:
Prof. dr. H. Nijmeijer
Prof. dr. ir. W. Michiels
Dr. ir. E. Steur
Dr. A. Y. Pogromsky

Members of the
Examination committee:
Prof. dr. ir. R. Puers
(chair of preliminary defense)
Prof. dr. L.P.H de Goey
(chair of public defense)
Prof. dr. ir. G. Samaey
Prof. dr. ir. J.M.J. den Toonder
Prof. dr. E. Fridman

Dissertation presented in partial fulfillment of the requirements for the joint degree of Doctor (PhD): Mechanical Engineering at Eindhoven University of Technology (TU/e), and Doctor of Engineering Science (PhD): Computer Science at KU Leuven.

June 2021



The work described in this thesis was carried out in the UCoCoS project which has received funding from the EU Horizon 2020 research and innovation programme under the Marie Skłodowska-Curie grant agreement No 675080.

A catalogue record is available from the Eindhoven University of Technology Library.
ISBN: 978-90-386-5305-1

Printed by: ProefschriftMaken || www.proefschriftmaken.nl
Cover design by: ProefschriftMaken || Mercedes Benjaminse

© 2021 Kirill Rogov. All rights reserved.

Numerical Methods for Pattern and Bifurcation Analysis in Complex Networks

PROEFSCHRIFT

ter verkrijging van de graad van doctor aan de
Technische Universiteit Eindhoven en doctor in de
Ingenieurswetenschappen: Computerwetenschappen aan de KU Leuven,
op gezag van de
rector magnificus prof.dr.ir. F.P.T. Baaijens, voor een
commissie aangewezen door het College voor
Promoties, in het openbaar te verdedigen
op vrijdag 25 juni 2021 om 16:00 uur

door

Kirill Rogov

geboren te Sint-Petersburg, Rusland

Dit proefschrift is goedgekeurd door de promotoren en de samenstelling van de promotiecommissie is als volgt:

1e voorzitter:	prof. dr. L.P.H. de Goey (chair of public defense)
2e voorzitter:	prof. dr. ir. R. Puers (chair of preliminary defense)
1e promotor:	prof. dr. H. Nijmeijer
2e promotor:	prof. dr. ir. W. Michiels (KU Leuven)
copromotor:	dr. A.Y. Pogromsky
copromotor:	dr. ir. E. Steur
leden:	prof. dr. ir. G. Samaey (KU Leuven)
	prof. dr. ir. J.M.J. den Toonder
	prof. dr. E. Fridman (Tel-Aviv University)

Het onderzoek dat in dit proefschrift wordt beschreven is uitgevoerd in overeenstemming met de TU/e Gedragscode Wetenschapsbeoefening.

"Mathematics is the science of patterns, and nature exploits just about every pattern that there is."

Ian Stewart

Summary

Numerical Methods for Pattern and Bifurcation Analysis in Complex Networks

The thesis focuses on analyzing the phenomenon of pattern formation in (delay) coupled nonlinear systems. The starting points are works of Turing on morphogenesis and pattern formation, and Smale on determining conditions under which initially globally asymptotically stable systems being interconnected, exhibit emergent oscillatory behavior, possibly in a structured way (e.g. synchronous and partial synchronous oscillatory behavior). One of the major open questions concerns the prediction or analysis of oscillatory patterns in the neighbourhood of the bifurcation point of complex networked dynamical systems. In such complex networks, co-existence of several patterns is not rare and this makes common methods of analysis cumbersome to use. The thesis focuses on a numerical way of analysis, starting from the multivariable harmonic balance (MHB) method developed by Iwasaki. Iwasaki's work shows that the MHB method is a powerful tool for determining oscillatory profiles. However, it does not exploit network structures, which is important with respect to scalability to large networks, neither does it provide any information about the system's behaviour if the system is not in the neighbourhood of the bifurcation point.

In order to address the challenge described above, numerical approaches are developed based on the MHB method for networks of Lur'e systems with a more general structure and dynamics, which allow us to predict the oscillatory patterns appearing in the networks, even if some of them co-exist. The main contributions are:

1. *Equal amplitude oscillations.* The thesis introduces a semi-analytical - semi-numerical approach to predict oscillations with equal amplitudes in complex networks described by regular graphs. The approach determines a harmonic profile (frequency, amplitude, phases)

that is encoded in the largest eigenvalue and its corresponding eigenvector of the coupling matrix, and it successfully decouples the individual dynamics of the nodes and the topology of the network. The MHB method is efficient and provides very good approximations of oscillation patterns obtained by numerical simulation in the neighborhood of bifurcation points.

2. *General amplitude case.* A modification and generalization of the MHB method is proposed. The new approach allows to determine oscillatory profiles without restriction on amplitudes. The problem of determining an oscillatory profile is converted into an optimization problem. The interior point method is used to find optimal solutions. The optimization problem is, typically, a non-convex problem and multiple minima may exist, corresponding to the co-existence of oscillatory patterns. In order to solve these problems, we combine the optimization procedure with a multistart approach, which is feasible because of the small number of unknowns in the MHB setting. This approach keeps the accuracy of equal amplitude case approach and deals with co-existing modes.

3. *Pattern analysis in networks with time delays.* An MHB-method is developed for networks with time-delays. It is shown that the approach can be used as the initial data for a numerical bifurcation analysis. An oscillatory profile now consists of frequency, offset, amplitudes and phases. The optimization procedure is modified, and the convergence time is significantly decreased. In addition, it is demonstrated that the MHB approach can be used for basic bifurcation analysis and for an accurate prediction of phases and frequency of oscillations even out of the neighbourhood of the bifurcation point.

4. *Delay induced full synchronization.* In certain networks, full synchronization can be observed only in presence of time-delay in the coupling. In this thesis, this delay induced full synchronization phenomenon is studied in ring networks. Numerical analysis of this phenomenon is performed by means of the MHB approach and the bifurcation/continuation software package DDE-BIFTOOL. The analysis provides understanding of the phenomenon and pointed out the importance of usage the MHB and bifurcation analysis together in a complementary way for analysis of the behavior of complex networks.

Samenvatting

Numerical Methods for Pattern and Bifurcation Analysis in Complex Networks

Deze dissertatie spitst zich toe op de analyse van patroonvorming in netwerken van niet-lineaire systemen met tijdsvertragingen in de koppelingen. De uitgangspunten zijn het werk van Turing over morfogenese en patroonvorming, en dat van Smale over het bepalen van voorwaarden waaronder het koppelen van globaal asymptotisch stabiele systemen leidt tot oscillerend gedrag, mogelijk op een gestructureerde manier (zoals synchroon of gedeeltelijk synchroon oscillerend gedrag). Eén van de belangrijkste open vragen betreft het analyseren en voorspellen van oscillerende patronen in de buurt van bifurcatiepunten in complexe netwerken. In zulke netwerken kunnen verschillende oscillatie-patronen naast elkaar bestaan, wat het gebruik van de gangbare analysemethoden bemoeilijkt. Het onderzoek beschreven in deze disseratie gaat in op de numerieke analyse van dit fenomeen, op basis van de multivariabele harmonische balans (MHB) methode, ontwikkeld door Iwasaki. Iwasaki's werk toont aan dat de MHB-methode een krachtig hulpmiddel is voor het bepalen van oscillerende profielen. De methode baat echter de netwerkstructuur niet uit, wat belangrijk is met oog of schaalbaarheid van de algoritmen naar grote netwerken toe, en ze levert geen informatie over het gedrag van het netwerk als het zich niet in de buurt van een bifurcatiepunt bevindt.

Om bovenstaande hoofdvraag te beantwoorden, zijn er numerieke benaderingsmethoden ontwikkeld op basis van de MHB-methode, die toepasbaar zijn op netwerken met een meer algemene structuur en dynamica. Deze methoden zijn in staat om oscillerende patronen die in deze netwerken optreden te voorspellen, zelfs wanneer sommige naast elkaar bestaan. De belangrijkste onderzoeksbijdragen beschreven in deze dissertatie zijn:

1. *Oscillaties met gelijke amplitudes.* Er is een semi-analytische, semi-

numerieke methode ontwikkeld om oscillaties met gelijke amplitudes te voorspellen in complexe netwerken die worden beschreven door een regulier netwerk. Onze aanpak resulteert in een harmonisch profiel (frequentie, amplitude, faseverschuivingen) dat gecodeerd is in de grootste eigenwaarde van de koppelingsmatrix en de bijbehorende eigenvector. Hierbij worden de individuele dynamica van de deelsystemen en de topologie van het netwerk ontkoppeld. De MHB-methode is efficiënt en levert zeer goede benaderingen op van de oscillatiepatronen verkregen met een numerieke simulatie in de buurt van bifurcatiepunten.

2. *Oscillaties met verschillende amplitudes.* De MHB-methode is aangepast en breder toepasbaar gemaakt. Een nieuwe benadering maakt het mogelijk om oscillerende profielen te bepalen zonder beperking op de grootte van de amplitudes. Het bepalen van een oscillatieprofiel wordt omgezet naar een optimalisatieprobleem, waarvoor we een interior point methode gebruiken. Het optimalisatieprobleem is in het algemeen niet convex, en er kunnen meerdere oplossingen zijn, wat co-existentie van verscheidene oscillerende patronen kan impliceren. Daarom is de optimalisatieprocedure gecombineerd met een multistart-strategie, die haalbaar is vanuit rekenkundig standpunt vanwege het klein aantal onbekenden in de MHB methode. Het algoritme is even nauwkeurig als dat voor het geval van gelijke amplitudes, en het blijft toepasbaar wanneer verschillende patronen gelijktijdig voorkomen.

3. *Patroonanalyse in netwerken met tijdsvertragingen.* De MHB-methode is uitgebreid naar netwerken met tijdsvertragingen. Er is aangetoond dat de benadering kan worden gebruikt als initiële data voor een numerieke bifurcatieanalyse. De bovenvermelde optimalisatieprocedure is aangepast en de convergentie van het algoritme is aanzienlijk versneld. Bovendien is aangetoond dat de MHB-benadering gebruikt kan worden voor elementaire bifurcatieanalyse en voor het nauwkeurig voorspellen van de frequentie van oscillaties, zelf ver weg van bifurcatiepunten.

4. *Volledige synchronisatie in netwerken, geïnduceerd door tijdsvertragingen.* In bepaalde netwerken kan volledige synchronisatie enkel voorkomen wanneer er tijdsvertraging is in de koppelingen. In deze dissertatie is dit fenomeen bestudeerd in ringnetwerken. Een numerieke analyse is uitgevoerd door middel van een combinatie

van de MHB-methode en het bifurcatie/continuatie softwarepakket DDE-BIFTOOL. De analyse heeft geleid tot belagnrijke inzichten in het fenomeen en toont het belang van het gebruik van zowel de MHB-methode als bifurcatieanalyse voor complexe netwerken aan.

Contents

Summary **i**

Samenvatting **iii**

Contents **vii**

List of Figures **xi**

List of Tables **xv**

1 Introduction **1**
1.1 Emergent behavior of complex systems 1
1.2 Pattern formation in complex networks 4
1.3 Objectives, contributions and outline 8
1.4 List of Publications 11

2 Preliminaries **13**
2.1 Nomenclature 13
2.2 Stability of ordinary differential equations 14
2.3 Passive and semipassive systems 16
2.4 Retarded functional differential equations 18
2.5 Elementary Hopf Bifurcation theory 21
2.6 Harmonic balance method 23

3 Pattern Analysis in diffusively coupled Lur'e systems **27**
3.1 Introduction 27
3.2 Problem setting 29

3.2.1 Networks of interconnected Lur'e systems 30
3.2.2 Conditions for oscillatory behavior 31
3.2.3 Describing Function Approximation 33
3.2.4 Problem formulation 34
3.3 Pattern Prediction by Multivariable Harmonic Balance . . . 34
3.3.1 Multivariable Harmonic Balance 35
3.3.2 Deriving the MHB equation 37
3.3.3 Equal amplitude case 39
3.3.4 General amplitude case 43
3.4 Numerical examples 46
3.4.1 Results for the equal amplitude case 47
3.4.2 Results for the general amplitude case 51
3.5 Concluding remarks 58

4 Delay Coupled Systems: Bifurcation and Pattern analysis 59
4.1 Introduction 59
4.2 Problem setting 62
4.2.1 Networks of delay coupled Lur'e systems 62
4.2.2 Conditions for oscillations 64
4.2.3 Critical values of time delay 67
4.2.4 Problem of pattern analysis in delay-coupled systems 69
4.3 Multivariable Harmonic Balance for delay coupled systems . 70
4.3.1 Equal amplitude case 72
4.3.2 General amplitude case 75
4.4 Numerical examples 76
4.4.1 Network with a supercritical Hopf bifurcation 77
4.4.2 Network with a subcritical Hopf bifurcation 84
4.5 Concluding remarks 91

5 Delay Induced Full Synchronization: A case-study 93
5.1 Introduction 93
5.2 Network representation 95
5.3 Delay Induced Full Synchronization 99
5.4 Analytical and numerical analysis of the case-study 105
5.4.1 Stability Analysis of Synchronized Equilibria 106
5.4.2 Pattern analysis by MHB 109
5.4.3 Numerical Bifurcation Analysis 114
5.5 Concluding remarks 120

6 Conclusions and Future directions 123
6.1 Conclusions 123
6.2 Future directions 127
6.2.1 The generalized MHB method 127
6.2.2 Network structure synthesis 128
6.2.3 Local controller for networks with coexisting patterns128

References 131

Acknowledgments 145

Curriculum Vitae 148

List of Figures

1.1 A visual, organizational map of complex systems broken into seven sub-groups created by Hiroki Sayama, D.Sc. Taken from [Wikimedia Commons]. 2
1.2 Patterns in structures. Left: spirals of prime numbers. Taken from [Vectorworks Forum]. Center: structure of a snowflake by Alexey Kljatov, CC BY-SA 4.0, [Wikimedia Commons]. Right: pattern of liquid crystal structure by Minutemen, CC BY-SA 3.0, [Wikimedia Commons]. 4

2.1 Supercritical Hopf bifurcation in the plane. Stable limit cycle for $\sigma = -1$. 22
2.2 Subcritical Hopf bifurcation in the plane. Unstable limit cycle for $\sigma = 1$. 23

3.1 An example of the network consisting of dynamical systems. 30
3.2 Linear system L_K. 36
3.3 Loop Transformation reorders the structure of the network in order to apply the MHB method. 37
3.4 Ring-like networks of diffusively coupled systems displaying oscillations with equal amplitudes 39
3.5 Oscillatory patterns with equal amplitudes in ring-like networks (left fig.: 3-node network, right fig.: 4-node network). Network dynamics is given in Section 3.4. 40
3.6 Networks of identical diffusively coupled systems displaying oscillations with unequal amplitudes. 43

3.7 Oscillatory patterns with unequal amplitudes (left fig.: 6-node network, right fig.: 8-node network). Network dynamics is given in Section 3.4. 44
3.8 Error between the MHB method and ODE simulations for three- and four-node networks for $\gamma_{3,4} = 1.01\bar{\lambda}_{3,4}$. Inner plots represent zoomed-in sections for the presentation purposes. 50
3.9 Objective Function cross-section of α_1 and α_2 for clockwise and counterclockwise waves. Since both wave-like solutions has equal amplitudes α_1 and α_2, they are shown as a single point. Fval is the objective function value. 53
3.10 Objective Function cross-section of ϕ_2 and ϕ_3 for both solutions. 54
3.11 Comparison of the MHB method and ODE simulation for network represented by Γ_8 for different coupling strength. . 57

4.1 An example of the directed network consisting of dynamical systems. 64
4.2 Network structure for numerical examples. 77
4.3 Rightmost characteristic roots computed for fixed $\gamma_{min} = 0.6481$ and $\tau_c = 1.5304$. 80
4.4 Rightmost characteristic roots computed for fixed $\gamma = 0.7129$ and $\tau_c = 1.5304$. 81
4.5 Network behavior obtained by simulating DDEs. 81
4.6 Ring network structure with N nodes. 83
4.7 Rightmost characteristic roots computed for fixed $\gamma_{min} = 2.5376$ and $\tau_c = 4.7643$. 86
4.8 Bifurcation curves in (τ, γ) parameter space. 86
4.9 Branch of periodic solutions that emerges from the subcritical Hopf bifurcation. 89
4.10 Oscillatory profiles of the periodic solutions represented by red dots in Fig. 4.9. 90

5.1 Network structure for the case study. 96
5.2 Block scheme representation of the network. 98
5.3 Rightmost characteristic roots computed for fixed $\gamma = 0.7110$ and $\tau_{c1} = 0.4364$. 100
5.4 Rightmost characteristic roots computed for $\gamma = 0.7110$ and $\tau = 1.5$. 101
5.5 Output of direct simulation of the given network for a pair of parameters $\gamma = 0.7110$ and $\tau = 1.5$. 102

5.6 Rightmost characteristic roots computed for $\gamma = 0.7110$ and $\tau = 3.5$. 103
5.7 Delay Induced Full Synchronization. Output of direct simulation of the given network for a pair of parameters $\gamma = 0.7110$ and $\tau = 3.5$. 104
5.8 Rightmost characteristic roots computed for $\gamma = 0.7110$ and $\tau = 6$. 104
5.9 240 phase shift rotating wave. Output of direct simulation of the given network for a pair of parameters $\gamma = 0.7110$ and $\tau = 6$. 105
5.10 Rightmost characteristic roots computed for $\gamma = 0.7110$ and $\tau = 2.8$. 110
5.11 Output of direct simulation for a pair of parameters $\gamma = 0.7110$ and $\tau = 2.8$. The full synchronization regime. 111
5.12 Output of direct simulation for a pair of parameters $\gamma = 0.7110$ and $\tau = 2.8$. The $2\pi/3$ phase shift travelling wave regime. 112
5.13 Rightmost characteristic roots computed for $\gamma = 0.7110$ and $\tau = 5.3$. 113
5.14 Stability of the branch of trivial equilibria for $\gamma = 0.7110$. Note that in the bottom right part of the figure, the numerical artifact is observed. 115
5.15 Branches of periodic solutions. 120 wave mode and full synchronization mode. The purple dots represent computed periodic solutions from which form the branches. 116
5.16 Rightmost characteristic roots computed for double Hopf bifurcation at $\gamma = 0.7045$ and $\tau = 2.8191$. 117
5.17 Bifurcation diagram in (γ, τ)-parameter space. Red vertical line is $\gamma = 0.7110$. Golden region 3 contains three coexisting modes, namely $120, 240$ and FS. 118
5.18 Rightmost characteristic roots at $\gamma = 0.95$ and $\tau = 4$. 119

List of Tables

3.1 Multi-stable oscillatory profiles of the network represented by matrix Γ_3. 48
3.2 Comparison of the MHB method and ODE simulation of the network represented by matrix Γ_3. 48
3.3 Oscillatory profile and comparison of the MHB method and ODE simulation of the network represented by matrix Γ_4. . 48
3.4 Amplitudes and frequency of oscillatory profiles of the network represented by matrix Γ_6. Multi-stability. 52
3.5 Phases of oscillatory profiles of the network represented by matrix Γ_6. Multi-stability. 52
3.6 Comparison of the MHB method and ODE simulation applied to the network represented by matrix Γ_6. Multi-stability. 52
3.7 Oscillatory profile of the network represented by matrix Γ_8. 55
3.8 Comparison of the MHB method and ODE simulation applied to the network represented by matrix Γ_8. 55
3.9 Comparison of the MHB method and ODE simulation for 8-node network vs. coupling strength. 56

4.1 Oscillatory profiles of the network extracted from the DDE simulation, computed by the general MHB method and by the EAC MHB method. 82
4.2 Comparison of the DDE simulation, and the general MHB method and special case of the MHB method outputs. 82
4.3 Computational time of EA MHB, MHB and dde23 and comparison of the numerical MHB approach and the direct simulation. 83

4.4 Stable and unstable co-existing oscillatory patterns which are computed by the MHB method. 87
4.5 Comparison of the DDE simulation and the MHB method outputs. 87
4.6 Stable oscillatory patterns computed by the EAC MHB method. 91
4.7 Comparison of the DDE simulation and the EAC MHB method outputs. 91

5.1 Oscillatory pattern computed by the MHB method for $\gamma =$ 0.7110 and $\tau = 1.5$. 101
5.2 Oscillatory pattern computed by the MHB method for $\gamma =$ 0.7110 and $\tau = 3.5$. 103
5.3 Oscillatory pattern computed by the MHB method for $\gamma =$ 0.7110 and $\tau = 6$. 103
5.4 Two stable coexisting oscillatory patterns which are computed by the MHB method for $\gamma = 0.7110$ and $\tau = 2.8$. 111
5.5 Comparison of the DDE simulation and the MHB method outputs. 112
5.6 Two stable coexisting oscillatory patterns which are computed by the MHB method for $\gamma = 0.7110$ and $\tau = 5.3$. 113
5.7 Bifurcation points and types of bifurcation. 114
5.8 Three coexisting patterns simultaneously computed by the MHB method. 119

Chapter 1

Introduction

1.1 Emergent behavior of complex systems

Complex systems are everywhere, ranging from gene regulatory networks in a cell to food webs in an ecosystem, and from an individual human brain to the Internet and social media, among thousands of other examples. Emergent behavior of such systems should be understood as a behavior of a complex system that does not depend on only the behavior of the individual parts, but is driven by their relationships (connections) with others. Thus the emergent behavior cannot be predicted by the analysis of only the individual parts of the system. In order to predict, analyse, or/and control it, both the individual parts and interconnections between them must be thoroughly studied.

Complex systems are networks of a large number of dynamic components, or nodes, which interact with each other and evolve through self-organization [1][2]. Scientists from the center of collective behavior of complex systems at Binghamton University and State University of New York created a map organizing the complex system phenomenology in 7 sub-groups (Fig. 1.1). Note that different groups can be defined and there might be some overlap between the groups. Such a classification shows the omnipresence of complex systems in different scientific fields and the importance of investigating the emergence phenomenon and its consequences. The emergent behavior of complex systems, resulting in different phenomena, is observed and studied in many scientific fields, such as biology, neuroscience, social science, physics, chemistry, material

science, control engineering, etc. The processes by which organisms form groups [3] and *act collectively* like ant colonies [4] and different flocks of birds showing amazing collective motion (murmuration) [5][6], are biological examples of the phenomenon of emergent behavior. Another interesting example in this field is the emergence of self-ordered motion in systems of particles with biologically motivated interaction [7]. In communication theory, the emergent behavior of cognitive radio is consid-

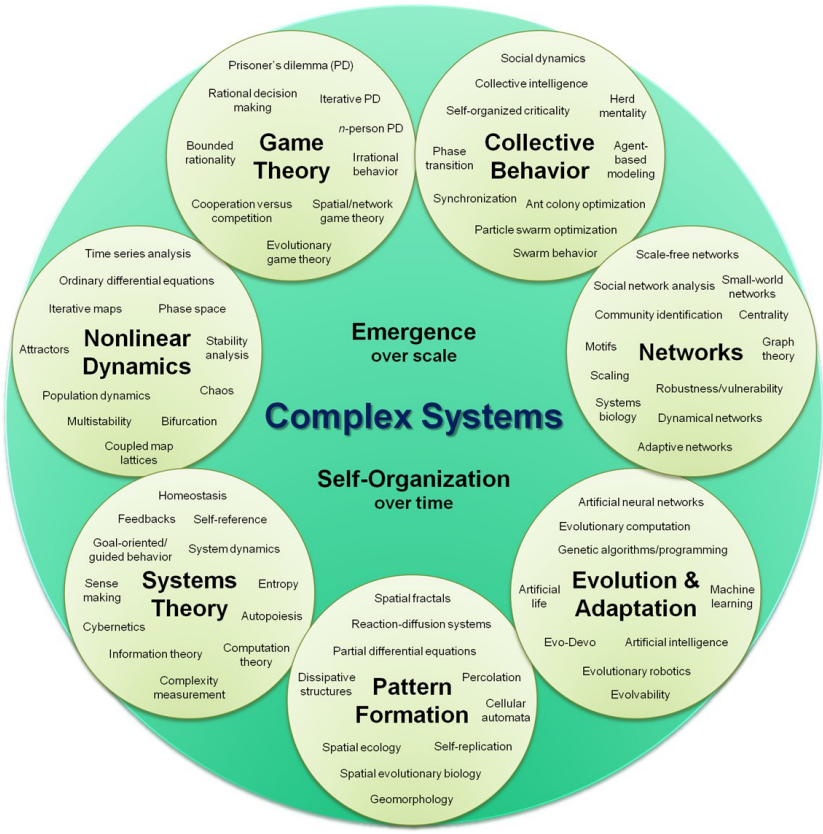


Figure 1.1: A visual, organizational map of complex systems broken into seven sub-groups created by Hiroki Sayama, D.Sc. Taken from [Wikimedia Commons].

ered as an *evolutionary game*, which depends on the degree of freedom of coupling that may exist between the interactions of different players (i.e. transmitters) operating in the environment of a cognitive radio [8]. Social scientists consider the emergent behaviour as the phenomenon which explains complexity of human performance, *self-organization* of human beings in groups, their social *collective behavior* [9], and, for example, the sociology of disasters [10]. Another example of emergent behavior in social networks is presented in [11] and describes the emergence of altruistic or cooperative behavior due to the spatial organization of players which is actively studied in the field of game theoretical approaches [12]. In physics and material science, emergent behavior is presented, for instance, as a *pattern formation* phenomenon in liquid crystals [13], *self-organized pattern formation* describing topological evolution in dense granular materials [14] and *collective behavior* of nano- and micro motors [15]. The phenomenon of emergence can result in scaling of random networks explaining the mechanisms behind the growth of large scale networks, for example the World Wide Web [16]. Mathematicians also develop approaches to use emergent behavior in order to improve different models, such as models for the reproducing behavior of crowds in order to improve collision avoidance [17][18] and gain better understanding of topology evolution of large scale networks [19].

In the fields of control engineering and computer science, the phenomenon of emergence is a subject of intensive study in network theory, multi-agent systems, swarm behavior, neuronal network, cybernetics and many other sub-fields. Many novel approaches in artificial intelligence, collective intelligence and collective robotics involve the theory of complex systems, such as emergent semantics in complex networks [20] and autonomous self-organization [21]. Modelling a collection of neurons of the cortex also shows the importance of investigating the emergent behavior in computational biology due to unexpected phenomena which are observed when neurons are coupled [22]. Understanding the complex systems behavior helps scientists and engineers to discover and develop novel and efficient control strategies for systems including a constellation of satellites [23], flocks of autonomous vehicles [24] and other formations [25][26][5]. Motivated by these applied works and the omnipresence of complex systems, emergent behavior and related phenomena have become popular subjects of study for physicists, biologists, sociologists, mathematicians and engineers. See for instance, the special issues [27][28][29][30][31] and the references therein.

It goes without saying that such a colossal topic cannot be covered by one thesis and it is not a purpose. In this thesis, the focus is on the phenomenon of *pattern formation*, which occurs in *complex networks*. Pattern formation can be a special case of emergent behavior. A short overview of this phenomenon is presented in the following section.

1.2 Pattern formation in complex networks

The main focus of the thesis is the phenomenon of *pattern formation* in *complex networks*. Patterns should be understood as a complex organization of structure or behavior in both space and time. Spirals of prime numbers in polar coordinates [32], fractal structures of snowflakes [33], liquid crystals structure [13], topologies of self-growing networks [34] and formation of the stars [35] and galaxies [36] are the examples of patterns in structures. See Fig. 1.2 for visual examples. Different synchronous regimes, which are observed in nature and artificial systems, are refereed to as behavioural patterns. Most common of them are: *synchronization*, *partial synchronization* and various types of travelling or *rotating waves*. Synchronization can be described as the phenomenon where "things" keep happening simultaneously for an extended period of time [37] [38]. The



Figure 1.2: Patterns in structures. Left: spirals of prime numbers. Taken from [Vectorworks Forum]. Center: structure of a snowflake by Alexey Kljatov, CC BY-SA 4.0, [Wikimedia Commons]. Right: pattern of liquid crystal structure by Minutemen, CC BY-SA 3.0, [Wikimedia Commons].

synchronization phenomenon is ubiquitous. A flock of birds moving south as a single organism [39], frogs singing or fireflies light up in unison [40],

agreement in frequency of rotation of power generators in power networks [41], synchronization of oxytocin neuronal networks [42] and even the time-correlated orbit and spin of our natural satellite - the moon [43] are examples of synchronization. The phenomenon of incomplete synchronization is usually called cluster synchronization or partial synchronization. It refers to the synchronization of only part of the nodes in a network or to the occurrence of groups or clusters of agents that work together in a synchronous manner. A typical example of clustering concerns the neuron synchronous activities in segments or clusters of the human brain [44]. Such kind of synchronization is widely present in so-called chimera systems, which describe the coexistence of coherence and incoherence in systems of coupled oscillators [45]. Chimera states are observed in a variety of networked systems such as chemical oscillators [46], electronic circuits [47], nonlinear optical experiments [48], neuron networks with fractal topology [49], etc. Another example of partial synchronization consists of human beings forming groups, for example in an orchestra [50]. Rotating or travelling waves are special kind of patterns which can be observed in complex networks and can be interpreted as a wave propagation of activity of the nodes of a network. It is a fundamental type of pattern formation in ring or linear formations of networks, which occurs in many biological systems, e.g., the motion of a leach [51], the segmentation clock [52], or brain wave activities in the cortex [53]. Complex rotating waves are also observed in coupled electrochemical [54] and electromechanical oscillators [55].

Complex networks and patterns, which occur in such networks, induce a large variety of applications in many fields. Controlled synchronization is widely used in, for instance, power systems to perform control of grid-connected voltage converters [56] and in encrypted communication schemes via synchronization of chaotic systems [57]. In medicine, the understating and control of synchronization and partial synchronization of segments of the brain can help people with epilepsy to predict and even possibly to control the seizures [58][59]. Another important application of different synchronous modes is the cooperation or coordination of robot manipulators [60][61]. In automotive engineering, synchronization also finds its place. For example, a platoon motion of vehicles, which is a cluster or string of synchronized vehicles, results in a significant reduction of aerodynamics drag and may lead to lower fuel consumption [62]. Travelling or rotating waves, which, among others, are observed in Central Pattern Generators (CPGs), can be used to reproduce the complex motion of many

organisms like leeches, snakes, cats or dogs, and applications for them are found in robotics and bioengineering [63][64][65].

A number of theories have been put forward with the goal to reveal the principles of pattern formation [66], but few of them are as universal as the theory of reaction-diffusion systems first proposed by Alan Turing [67]. In his research, the author "suggests that a system of chemical substances reacting with each other and diffusing through a tissue is adequate to account for the main phenomenon of morphogenesis". Several concepts related to the chemical basis of morphogenesis (development of patterns), spatial chemical patterns, and what is now called diffusion-driven instability or Turing's instability are introduced. The theory clarifies the complex self-organizing mechanisms resulting in the phenomenon of pattern formation using simple reactions of just two diffusively coupled components. This very simple network (in comparison to nowadays studied networks) of two coupled systems shows fascinating properties, such as, formation of self-organized patterns in the absence of initial asymmetries, a large variety of patterns (e.g. spots and stripes [68]) generated by varying the parameters (e.g. reaction and diffusion values) and robustness of these patterns to perturbations [69].

In the absence of spatial degrees of freedom a reaction-diffusion system can be reduced to a set of coupled nonlinear ordinary differential equations (ODEs) [70]. A nonlinear analysis of diffusion-driven instability in coupled ODE systems is performed in [71]. This article presents an example of two models of biological cells, coupled via a membrane, which takes the role of diffusive coupling. Each cell is inert or dead by itself, in a sense that the system is globally asymptotically stable. However, when the cells are coupled via diffusion, "the cellular system pulses (or expressed perhaps overdramatically, becomes alive!) in the sense that the concentration of enzymes in each cell will oscillate infinitely" [71]. The important question of determining conditions under which the diffusive coupling leads to oscillatory behavior in complex networks, is posed in that research. Answers to this question are provided in [72], [73], and [74]. The author derived conditions under which coupled systems show oscillatory behavior, and highlighted properties of the systems which are needed for this kind of behavior. Since the individual systems are globally asymptotically stable, the interconnections between the nodes are responsible for the change of dynamical behavior. An important result, which justifies the statement above, is presented in [75]. In that work, the authors present conditions

under which a network of systems which are globally asymptotically stable by themselves, being diffusively coupled display different synchronous regimes, such as partial synchronous oscillations. In [76] a similar phenomenon of cluster synchronization is described for a neuronal network. These conditions are related to the coupling strength between the agents of the network and the network topology. When the largest eigenvalue of the coupling matrix exceeds some threshold, the network equilibrium loses its stability via a *Hopf bifurcation* and an oscillatory patterns emerge [77][78]. The Hopf bifurcation changes the dynamics of the network from a stable equilibrium to oscillatory patterns. However, there are some open questions that are not answered in these papers. One of them concerns the prediction of oscillatory patterns in the networks. Another question arises from the fact that different oscillatory patters may coexist, which can occur in networks with diffusive coupling, such as clockwise and counterclockwise rotating waves in ring networks. This coexistence may induce multi-stability of the network. In the presence of the multi-stability, the application of common analytical methods, such as the direct Lyapunov method [79] (the Lyapunov-Krasovskii method in case of delay-coupled systems [80]), becomes highly nontrivial.

The above-mentioned studies all consider diffusive coupling [81], which is (usually) symmetric and delay-free. In [82], conditions for oscillations in networks with delay coupling are presented. In that research, the coupling function for a single system in a network is defined as a weighted difference of the time-delayed output of its neighbours and its own non-delayed output. Physically, the adopted delay model represents the time that a signal takes to propagate from its source to its destination, while the systems have access to their own outputs instantaneously. Such time-delay coupling functions appear, among others, in a network of neurons [83], electrical circuits [84], and networked control systems [85]. The coupled systems via the time-delay coupling may exhibit all previously discussed kinds of oscillatory patterns. The problem of analysis of coexisting patterns is even more important for delay-coupled systems due to a more complex behavior which depends on more parameters, namely the coupling strength and the time-delay. For this number of parameters, the analysis of a Hopf bifurcation, which may be the origin of oscillatory patterns, becomes cumbersome. The problem of (coexisting) pattern analysis in coupled systems is discussed in, for instance, [86][87][88].

1.3 Objectives, contributions and outline

In the previous sections, the phenomenology of pattern formation, various of applications and different approaches to study patterns occurring in complex networks are presented. A large number of applications in different scientific fields where oscillatory patterns are observed in complex network, necessitates fast methods of analysis. For standard methods this analysis can be numerically challenging. It motivates to develop numerically efficient algorithms aiming at the prediction of patterns in complex networks. The thesis addresses the problem of developing efficient tools for the analysis of oscillatory patterns, which occur in networks, by means of semi-analytical and numerical approaches. The prediction and analysis of oscillatory patterns in this thesis should be understood as a numerically efficient computation of oscillatory profiles (frequency, offset, amplitudes and phases) that approximate periodic solutions, which are observed in the networks. The focus of the thesis is on networks of nonlinear systems of Lur'e type, which are globally asymptotically stable if they are uncoupled, and start exhibiting various (stable, unstable, coexisting) oscillatory patterns, if they are interconnected into networks. A Lur'e system is a linear dynamical systems with an output based nonlinearity. Interactions in such networks can be represented by different types of coupling functions, for example the coupling can be with time-delay or delay free and diffusive. Depending on the coupling type, the networks can show different behavior. This leads to the need of the tools, which are able to analyze the behavior of the network for different types of coupling.

The individual nodes are globally asymptotically stable and start oscillating only when the coupling strength is increased from zero (in the time delay case a network usually also needs a non-zero delay to oscillate). This means that varying the interaction parameters in the coupling the network agents change their behavior from stable network equilibria to stable limit cycles (or vise versa, oscillation dead), which implies that a bifurcation occurs in such networks. We focus on the case where a Hopf bifurcation causes the instability of the network equilibria and leads to the occurrence of locally stable limit cycles. According to the normal form theory [77], the oscillations are sinusoidal-like in the neighbourhood of a bifurcation point. It motivates to develop a new approach, based on the harmonic balance method, for pattern analysis in such networks, which is one of the goals of this thesis. In order to deal with the nonlinearity in the system model, the latter is replaced by an approximation using the

describing function approach [89]. It is worth mentioning that the method of harmonic balancing is not limited to only small amplitude scenarios and for systems in which a Hopf bifurcation occurs. The harmonic balance method for a multivariable nonlinear system is called the Multivariable Harmonic Balance (MHB) and was first presented for the analysis of coupled central pattern generators in [90]. The method presented in [90] is not directly applicable for networks of nonlinear Lur'e systems and limited to the delay-free case. One of the goals is to overcome these limitations, since the approach is numerically efficient, simple to use, and scalable in a sense that for some cases the networks structure can be exploit to crucially decrease the computational complexity. Another goal of the thesis is to investigate the possibilities and limits of the MHB method, for instance, applicability for time-delay systems, ability to handle coexisting patterns, and detecting unstable periodic solutions.

The main contributions of the research presented in this thesis are:

- A novel method for pattern analysis in networks of nonlinear systems with delay-free coupling is developed. The method is based on the harmonic balancing technique and the describing function method.
- Mathematical and computational tools for pattern analysis of delay-coupled nonlinear systems, based on the MHB approach, are developed. Bifurcation theory and the MHB method are used in a complementary way in order to analyse and detect coexisting stable and unstable oscillatory regimes.
- The phenomenon of delay induced full synchronization is introduced and analysed. The observed phenomenon shows that the fully synchronized motion for some networks can be achieved by varying only the time-delay parameter, while the coupling parameter remains fixed. It is shown how the developed tools for the pattern analysis complement and support the bifurcation analysis in studying complex network behavior.

The thesis is organized as follows.

- Chapter 2 contains preliminary results, which are used in some or all following chapters. The basic stability theory is introduced for ODEs and DDEs. Concepts of passive and semipassive systems and elementary Hopf bifurcation theory are presented in the chapter. An introduction to the harmonic balance method is given.

- Chapter 3 presents a method for pattern analysis in networks of diffusively coupled nonlinear systems of Lur'e form. For this, the MHB equations are derived for interconnected Lur'e systems, where two cases are considered, namely the equal amplitude case (all amplitudes have the same magnitude) and the general amplitude case. The equal amplitude case can be solved semi-analytically, which is shown in the chapter. This semi-analytical approach exploits the network structure and shows the scalability property of the MHB method. For the general amplitude case, a numerical optimization routine is developed. In order to show the efficiency of the MHB technique the results of both methods are validated using simulations of the coupled systems and computational time is compared.

- Chapter 4 introduces the tools for pattern and bifurcation analysis of delay-coupled Lur'e systems. The MHB approach is modified and complemented by additional methods (e.g. a method for computing critical delays, based on solving a generalized eigenvalue problem) for delay-coupled systems. In order to show different possibilities of the MHB method, two networks with sub-critical and supercritical Hopf bifurcations are considered as examples. In order to verify the MHB results, the output is compared with the simulations and supported by a bifurcation analysis by means of the package `ddebiftool`.

- Chapter 5 describes a phenomenon, which is observed in delay-coupled nonlinear systems, presented as the first example in Chapter 4. By varying the value of the time-delay parameter, the network shows different oscillatory modes, including the full synchronization mode, which cannot occur for such network in the delay-free case. The phenomenon is called *delay induced full synchronization*. The network behavior is analysed in both ways, analytical and numerical, in order to determine and to describe the underlying mechanism of the phenomenon.

- Chapter 6 contains the conclusions of the thesis and recommendations for future research.

1.4 List of Publications

This thesis is mostly based on conference and journal papers, either published or accepted. The present section summarizes the relations between the papers and the chapters in this thesis.

Chapter 3 contains results presented in:

- K. Rogov, A. Pogromsky, E. Steur, W. Michiels, and H. Nijmeijer. "Pattern Prediction in Networks of Diffusively Coupled Nonlinear Systems". In: *IFAC-PapersOnLine* 51.33 (2018). 5th IFAC Conference on Analysis and Control of Chaotic Systems CHAOS 2018, pp. 62 –67
- K. Rogov, A. Pogromsky, E. Steur, W. Michiels, and H. Nijmeijer. "Pattern Analysis in Networks of Diffusively Coupled Lur'e Systems". In: *International Journal of Bifurcation and Chaos* 29.14 (2019), p. 1950200

Chapter 4 contains results presented in:

- K. Rogov, A. Pogromsky, E. Steur, W. Michiels, and H. Nijmeijer. "Pattern Analysis in Networks of Delayed Coupled Nonlinear Systems". In: *2020 European Control Conference (ECC)*. 2020
- K. Rogov, A Pogromsky, E. Steur, W. Michiels, and H. Nijmeijer. "Detecting coexisting oscillatory patterns in delay coupled Lur'e systems". In: *Chaos: An Interdisciplinary Journal of Nonlinear Science* 31.3 (2021), p. 033114

Chapter 2

Preliminaries

2.1 Nomenclature

The symbol $\mathbb{R}$ denotes the set of real numbers $(-\infty,\infty)$, $\mathbb{R}_{>0}(\mathbb{R}_{\geq 0})$ stands for the set of positive (non-negative) real values. The symbol $\mathbb{C}$ denotes the set of complex numbers. The notation $\mathbb{C}_+$ corresponds to the open right half plane, $\{z\in\mathbb{C}:\mathrm{Re}(z)>0\}$. The symbol j stands for the imaginary unit, $j^2=-1$. For a positive integer k we let I_k denote the identity matrix of the size $k\times k$ and $\mathbf{1}_k$ denotes the column vector of length k with all entries equal to 1. The notation $|\cdot|$ denotes Euclidean norm, i.e. $|x|=\sqrt{x_1^2+x_2^2+...+x_n^2}$. The symbol $\otimes$ stands for the Kronecker product of two matrices, i.e. letting the matrix $A\in\mathbb{R}^{n\times m}$ and $B\in\mathbb{R}^{p\times l}$, then the matrix $A\otimes B\in\mathbb{R}^{np\times ml}$ is given by

$$A\otimes B=\begin{pmatrix} a_{11}B & a_{12}B & \cdots & a_{1m}B\\ a_{11}B & a_{12}B & \cdots & a_{2m}B\\ \vdots & \vdots & \ddots & \vdots\\ a_{n1}B & a_{n2}B & \cdots & a_{nm}B\end{pmatrix},$$

where a_{ij} is the ij^{th} entry of the matrix A.
The symbol $\oplus$ stands for the Kronecker sum, i.e. $A\oplus B=A\otimes I_B+I_A\otimes B$. The symbols $^\top$ and * stand for the transposition and conjugate transposition, respectively. For a natural number r, C^r stands for a set of r-times continuously differentiable functions. Given positive integers p, q, for $\mathscr{X}\subset\mathbb{R}^p$ and $\mathscr{Y}\subset\mathbb{R}^q$ we denote the space of C^r continuous functions from $\mathscr{X}$ into $\mathscr{Y}$ as $C^r(\mathscr{X},\mathscr{Y})$. For the sake of simplicity, C^0 is denoted as C. If the derivatives

of a function of all ($r = \infty$) orders exist then the function is called smooth and if the derivatives exist up to some sufficiently high order then it is called sufficiently smooth. A function $V : \mathscr{D} \to \mathbb{R}_{\geq 0}$, where $\mathscr{D} \subset \mathbb{R}^n$ contains 0, is called positive (semi)definite, denoted by $V(\cdot) > 0$ ($V(\cdot) \geq 0$), if $V(0) = 0$ and $V(x) > 0$ ($V(x) \geq 0$) for all $x \in \mathscr{D} \setminus \{0\}$. It is radially unbounded if $\mathscr{D} = \mathbb{R}^n$ and $|x| \to \infty$ implies that $V(x) \to \infty$. If the quadratic form $x^\top P x$ where $P = P^\top$ is a symmetric matrix, is positive (semi)definite, then the matrix P is positive (semi)definite and denoted by $P > 0$ ($P \geq 0$).

2.2 Stability of ordinary differential equations

In this section, the definitions of stability of ordinary differential equations, which are used through the thesis, are given. Consider a system of ordinary differential equation,

$$\dot{x}(t) = f(t, x(t)), \tag{2.1}$$

where $x \in \mathbb{R}^n$ is a state, $f : \mathbb{R} \times \mathbb{R}^n \to \mathbb{R}^n$ is a continuous in t and locally Lipschitz continuous in x for all $t \geq t_0$. The dot notation stands for the derivative with respect to t. A solution to (2.1) on interval $[t_0, t_0 + T]$ is a function $x(t)$ that satisfies (2.1) on the given interval. A solution to (2.1) through (t_0, x_0), denoted by $x(t; t_0, x_0)$, is a solution to (2.1) for which $x(t_0; t_0, x_0) = x_0$. If the initial conditions are clear from the context, for the sake of brevity, the solution will be denoted by $x(t)$. The assumptions on f guarantee the local existence and uniqueness of solutions.

Definition 2.1 *(Lyapunov Stability [95]). Suppose that $f(t, 0) = 0$ for all $t_0 \geq 0$. Then the trivial trivial solution $x \equiv 0$ is*

i) stable if for any number $\epsilon > 0$ and any $t_0 \in \mathbb{R}_{\geq 0}$, there is $\delta = \delta(\epsilon, t_0) > 0$ such that $|x_0| < \delta$, implies that $|x(t; t_0, x_0)| < \epsilon$ for all $t \geq t_0$;

ii) uniformly stable if it is stable and the number δ can be selected independently of t_0;

iii) asymptotically stable if it is stable and there is a number $\bar{\delta} = \bar{\delta}(t_0) > 0$ such that $|x_0| < \bar{\delta}$, implies that $|x(t; t_0, x_0)| \to 0$ as $t \to \infty$;

iv) uniformly asymptotically stable if it is uniformly stable and there is a number $\bar{\delta} > 0$ such that for any $\epsilon > 0$ there is a $T = T(\epsilon) > 0$ such that $|x_0| < \bar{\delta}$ implies $|x(t; t_0, x_0)| < \epsilon$ for all $t \geq t_0 + T$;

v) exponentially stable if there are positive constants m and α such that $|x(t;t_0,x_0)| \leq m\exp(-\alpha(t-t_0))|x_0|$ for all $t \geq t_0$.

Note that all definitions above are given in the sense of Lyapunov and for *local* cases. They become *global* if the definitions hold for all $x_0 \in \mathbb{R}^n$ [96].

The stability of an equilibrium point of an ordinary differential equation can be ensured by evaluating a suitable Lyapunov function.

Theorem 2.1 *(Lyapunov's second method, [97]). Consider (2.1) and suppose that $f(t,0) = 0$ for all $t \geq t_0$. Let $u, v, w : \mathbb{R}_{\geq 0} \to \mathbb{R}_{\geq 0}$ be continuous non-decreasing functions, $u(s)$ and $v(s)$ are positive for $s > 0$, and $u(0) = v(0) = 0$. Suppose that there exists a positive definite function $V \in C^1(\mathbb{R} \times \mathscr{D}, \mathbb{R}_{\geq 0})$ such that*

$$u(|x|) \leq V(t,x) \leq v(|x|) \text{ for all } t, x$$

and

$$\dot{V}(t,x) := \frac{\partial V(t,x)}{\partial t} + \frac{\partial V(t,x)}{\partial x} f(t,x) \leq -w(|x|)$$

for all $x \in \mathscr{D}$ and $t \geq t_0$, then the origin of (2.1) is uniformly stable. The origin of (2.1) is asymptotically uniformly stable if it is uniformly stable and $w > 0$ for all $x \in \mathscr{D} \setminus \{0\}$. The origin of (2.1) is globally (asymptotically) uniformly stable if it is (asymptotically) uniformly stable stable with $\mathscr{D} = \mathbb{R}^n$ and $u \to \infty$ as $|x| \to \infty$.

Stability of a system can also be examined by the linearisation around an equilibrium point. This approach is mainly used throughout the thesis. The following theory is adapted from Chapter 4 of [96]. Consider a nonlinear system

$$\dot{x} = f(x) \tag{2.2}$$

where $f : \mathscr{D} \to \mathbb{R}^n$ is a continuously differentiable map from a domain $\mathscr{D} \subset \mathbb{R}^n$ into $\mathbb{R}^n$. Suppose the origin $x = 0$ is in $\mathscr{D}$ and is an equilibrium point for system (2.2), that is $f(0) = 0$.
Following [96], since $f(0) = 0$ and $f(x)$ is smooth enough, we can write

$$f(x) = Ax + g(x)$$

where

$$A = \frac{\partial f}{\partial x}(0) \quad \text{and} \tag{2.3}$$

The function $g(x)$ satisfies

$$\frac{||g(x)||}{||x||} \to 0 \quad \text{as} \quad ||x|| \to 0.$$

This suggests that in a small neighbourhood near an equilibrium point the behavior of the nonlinear system can be approximated by it linearization around the origin

$$\dot{x} = Ax,$$

where A is defined in (2.3) and has no eigenvalues with real part equal to zero.
The result above is known as the linearisation theorem or Hartman-Grobman theorem [98].
The following theorem, known as Lyapunov's indirect methods, provides the conditions under which the stability of the origin as an equilibrium point of the nonlinear system can be investigated by means of the stability analysis of its linearisation.

Theorem 2.2 *(Lyapunov's indirect method [96]). Let $x = 0$ be an equilibrium point of the nonlinear system*

$$\dot{x} = f(x)$$

where $f : \mathscr{D} \to \mathbb{R}^n$ is continuously differentiable and $\mathscr{D}$ is a neighbourhood of the origin. Let Jacobian matrix

$$A = \frac{\partial f}{\partial x}(x)\bigg|_{x=0}$$

Then:

i) The origin is asymptotically stable if $Re\lambda_i < 0$ for all eigenvalues of A;

ii) The origin is unstable if $Re\lambda_i > 0$ for one or more eigenvalues of A.

2.3 Passive and semipassive systems

This section introduces the concept of passive and semipassive systems which is used in the thesis. The section deals with the systems that have inputs and outputs. Such open systems systems can be designed and

analysed by means of the framework provided by the theory of dissipative systems. The connection between the mathematical input-output description of a system and physical energy-related phenomena was established by presenting storage functions and supply rates [99][100]. A dissipative system is a system that does not generate energy and dissipates the energy obtained or supplied by its environment. Passive systems are the kind of dissipative systems with a supply rate, which is bilinear product of the input(s) and output(s). Semipassive systems show similar behavior as passive systems, but generate a finite amount of energy. Formal definitions of passivity and semipassivity are given below.

Definition 2.2 *(Passivity and semipassivity, [99][101]). Consider a system*

$$\dot{x}(t) = f(x(t), u(t)), \quad y(t) = h(x(t)), \tag{2.4}$$

where $x \in \mathbb{R}^n$ is the state, $y \in \mathbb{R}^m$ is the output, $u \in \mathscr{L}_\infty(\mathbb{R}, \mathbb{R}^m)$ is the input, which is a bounded and continuous function of time, $f : \mathbb{R}^n \to \mathbb{R}^n$ and $h : \mathbb{R}^n \to \mathbb{R}^m$ are sufficiently smooth functions. Suppose there exists a nonnegative storage function $V \in C^r(\mathbb{R}^n, \mathbb{R}_{\geq 0}), r \geq 0, V(0) = 0$, such that the following dissipation inequality holds

$$V(x(t)) - V(x(t_0)) \leq \int_{t_0}^{t} y^\top(s) u(s) - H(x(s)) ds, \tag{2.5}$$

where $H \in C(\mathbb{R}^n, \mathbb{R})$. The system (2.4) is called

i) C^r-passive if there exists a C^r storage function V and a function H such that (2.5) holds with $H(\cdot) \geq 0$;

ii) strictly C^r-passive if there exists a C^r storage function V and a function H such that (2.5) holds with $H(x) > 0$ and $x \neq 0$;

iii) C^r-semipassive if there exists a C^r storage function V and a function H such that (2.5) holds with $H(\cdot) \geq 0$ outside of a ball $\mathscr{B} = \mathscr{B}(0, R) \subset \mathbb{R}^n$ with radius R centred at 0, i.e.

$$\exists R > 0, \ |x| \geq R \Rightarrow H(x) \geq \sigma(|x|),$$

for some nonnegative continuous function $\sigma(|x|)$ defined for all $|x| \geq R$;

iv) strictly C^r-semipassive if there exists a C^r storage function V and a function H such that (2.5) holds with $H(\cdot) > 0$ outside of a ball $\mathscr{B} = \mathscr{B}(0, R) \subset \mathbb{R}^n$.

Note that if the storage function V belongs to $C^r(\mathbb{R}^n, \mathbb{R}_{\geq 0})$ with $r \geq 1$, inequality (2.5) can be replaced by

$$\dot{V}(x(t)) \leq y^\top(t)u(t) - H(x(t)).$$

Such systems possess some interesting properties from a control theory point of view. For instance, a C^1-passive system with a zero input ($u \equiv 0$) or with a feedback of the form $u = -\psi(y)$, satisfying $y^\top \psi(y) \geq 0$ for all y, is stable in the sense of Lyapunov under some detectability assumptions. Moreover, the zero dynamics ($y \equiv 0$) of a strictly C^1-passive system (2.4) are asymptotically stable, if the storage function is positive definite. Systems with asymptotically stable zero dynamics are also known as minimum phase systems. See [102] and [103] for detailed studies of dissipative and passive systems.

2.4 Retarded functional differential equations

All nodes of the complex networks studied in this thesis, are represented by ordinary differential equations. In some networks in the thesis the coupling between nodes is given by time-delay functions, which makes the closed-loop dynamics be described by a set of delay differential equations. The specific type of delay differential equations that will be used thought out this work are so-called retarded functional differential equations. This section introduces some basic theory about solutions to retarded functional differential equations and their stability properties.

The following theory has been adopted from [104]. Let τ be a non-negative real number and let $\mathbf{C} = C([-\tau, 0], \mathbb{R}^n)$. The norm of an element $\phi \in \mathbf{C}$ is $|\phi| = \sup_{-\tau \leq \theta \leq 0} |\phi(\theta)|$. If $t_0 \in \mathbb{R}$, $T \geq 0$ and $x \in C([t_0 - \tau, t_0 + T])$, for any $t \in [t_0, t_0 + T]$, $x_t(\theta) \in \mathbf{C}$ is defined as $x_t(\theta) = x(t + \theta)$, $-\tau \leq \theta \leq 0$. Let $f : \Omega \to \mathbb{R}^n$ with $\Omega \subset \mathbb{R} \times \mathbf{C}$ is a given functional, then the relation

$$\dot{x}(t) = f(t, x_t), \tag{2.6}$$

is named a retarded functional differential equation on Ω (retarded delay differential equation) and denoted by RFDE (RDDE). If there are $t_0 \in \mathbb{R}$ and $T > 0$ such that $x \in C([t_0 - \tau, t_0 + T], \mathbb{R}^n)$, $(t, x_t) \in \Omega$ and $x(t)$ satisfies (2.6) for all $t \in [t_0 - \tau, t_0 + T)$, then a function x is a solution to (2.6) on the interval $[t_0 - \tau, t_0 + T]$. For given $t_0 \in \mathbb{R}$ and $\phi \in \mathbf{C}$, $x(t; t_0, \phi)$ denotes the solution to (2.6) through (t_0, ϕ), where $x_{t_0} = \phi$. In order to give the

definitions of stability of RFDEs, the following assumptions are imposed. It is assumed that f is completely continuous, in a sense that $f:\Omega\to\mathbb{R}^n$ is continuous and has closed bounded sets of Ω mapped into bounded subsets of $\mathbb{R}^n$. Moreover, it is assumed that f is Lipschitz in ϕ in each compact set in Ω and has a bounded continuous first order derivative with respect to ϕ. Under the imposed assumptions on f there is a guarantee that an absolutely continuous solution $x(t;t_0,\phi)$ does exists and is unique.

The definitions of stability (in the sense of Lyapunov) for ordinary differential equations presented in Section 2.2 are naturally extended to notions of stability for retarded functional differential equations as follows.

Definition 2.3 *(Stability of RFDE, [104][105]). Consider the RFDE*

$$\dot{x}(t)=f(t,x_t), \tag{2.7}$$

and suppose that $f(t,0)=0$ *for all* $t\in\mathbb{R}$. *Then the solution* $x\equiv 0$ *is*

i) stable if for any $t_0\in\mathbb{R}$ *and number* $\epsilon>0$ *there is* $\delta=\delta(t_0,\epsilon)$ *such that* $|\phi|<\delta$ *implies* $|x_t(t_0,\phi)|<\epsilon$ *for all* $t\geq t_0$*;*

ii) uniformly stable if it is stable and the number δ *can be chosen independently of* t_0*;*

iii) asymptotically stable if it is stable and there exists a number $\bar{\delta}=\bar{\delta}(t_0)>0$ *such that* $|\phi|\leq\bar{\delta}$ *implies* $x(t;t_0,\phi)\to 0$ *as* $t\to\infty$*;*

iv) uniformly asymptotically stable if it is uniformly stable and there exists a number $\bar{\delta}=\bar{\delta}(t_0)>0$ *such that for every* $\epsilon>0$ *there is a* $T'=T'(\epsilon)>0$ *such that* $|\phi|\leq\bar{\delta}$ *implies* $|x_t(t_0,\phi)|<\epsilon$ *for all* $t\geq t_0+T'$*;*

v) exponentially stable if there are positive constants m *and* α *such that* $|x(t;t_0,\phi|\leq m\exp(-\alpha(t-t_0))|\phi|$ *for all* $t\geq t_0$.

The stability of an equilibrium of a retarded functional equation can be ensured by constructing a Lyapunov-Krasovskii functional [106]. This can be done using the method of Lyapunov functionals described by the Lyapunov-Krasovskii theorem which is presented below. The following theory is adapted from [107].
Let $V:\mathbb{R}\times C[-\tau,0]\to\mathbb{R}$ be a continuous functional and let $x_\tau(t,\phi)$ be the solution to (2.7) at time $\tau\geq t$ with the initial conditions $x_t=\phi$. The right upper derivative $\dot{V}(t,\phi)$ along (2.7) is defined as follows:

$$\dot{V}(t,\phi)=\lim_{\Delta t\to 0^+}\sup\frac{1}{\Delta t}[V(t+\Delta t,x_{t+\Delta t}(t,\phi))-V(t,\phi)].$$

A non-positive $\dot{V}(t, x_t)$ can be interpreted that x_t does not grow with t, indicating that the system is stable.

Theorem 2.3 *(Lyapunov-Krasovskii Theorem, [108]). Suppose* $f : \mathbb{R} \times C[-\tau, 0] \to \mathbb{R}$ *maps* $\mathbb{R} \times$*(bounded sets in* $C[-\tau, 0]$*) into bounded sets of* $\mathbb{R}^n$ *and that* $u, v, w : \mathbb{R}_+ \to \mathbb{R}_+$ *are continuous nondecreasing functions,* $u(s)$ *and* $v(s)$ *are positive for* $s > 0$*, and* $u(0) = v(0) = 0$*. The trivial solution to (2.7) is uniformly stable if there exists a continuous functional* $V : \mathbb{R} \times C[-\tau, 0] \to \mathbb{R}^+$*, which is positive definite, i.e.*

$$u(|\phi(0)|) \leq V(t, \phi) \leq v(|\phi|),$$

and such that its derivative along (2.7) is non-positive in the sense that

$$\dot{V}(t, \phi) \leq -w(|\phi(0)|).$$

If $w(s) > 0$ *for* $s > 0$*, then the trivial solution is uniformly asymptotically stable. If in addition* $\lim_{s\to\infty} u(s) = \infty$*, then it is globally uniformly asymptotically stable.*

Moreover, sufficient conditions for stability of the RFDE given using the Lyapunov functions instead of functionals (Lyapunov-Razumikhin theorem) can be found in chapter 5.4 (Theorem 4.1 and Theorem 4.2) of [104] and in [107] and references therein.

The RDDE (2.7) is called autonomous when its right hand side does not explicitly depend on time

$$\dot{x}(t) = f(x(t), x(t-\tau)). \tag{2.8}$$

The definitions and stability results, presented above, remain valid, but the initial time can be taken equal to zero, since the solutions to (2.8) are invariant w.r.t. time-shifts.
When the autonomous DDE (2.8) is linear (or can be linearised), in the sense it has the form,

$$\dot{x}(t) = Ax(t) + A_d x(t-\tau), \quad A, A_d \in \mathbb{R}^{n\times n}, \tag{2.9}$$

asymptotic stability is equivalent with the fact that all the eigenvalues, the roots of the characteristic equation,

$$\det(\lambda I - A - A_d \exp(-\lambda\tau)) = 0, \tag{2.10}$$

lie in the open left half plane. Condition (2.10) means that a nonzero vector $q \in \mathbb{C}^{n\times 1}$ such that $(\lambda I - A - A_d \exp(-\lambda\tau))q = 0$ is required to exist. The infinite dimensional nature of the DDE (2.9) means that equation (2.10) is transcendental and has infinitely many solutions. However, the number of eigenvalues to the right of any vertical line in the complex plane $\mathrm{Re}\lambda \geq r,\ r \in \mathbb{R}$ is finite [104].

2.5 Elementary Hopf Bifurcation theory

Throughout this thesis the nodes of the complex networks are represented by globally asymptotically stable dynamical systems when the coupling is absent. They may lose stability under a parameter change in the coupling functions in the sense that the stable network equilibrium dynamics changes to an oscillatory mode. Such change in networks dynamics under parameter variation is related to a Hopf bifurcation. This section introduces some basic theory about the Hopf bifurcations in dynamical systems. The following theory has been adapted from [78] and [109].

Consider a dynamical system in continuous-time that depends on a parameter as follows.

$$\dot{x} = f(x, \alpha), \tag{2.11}$$

where $x \in \mathbb{R}^n$ is the state variable, $\alpha \in \mathbb{R}$ is a parameter and f is a smooth function of both arguments.
Suppose that for all sufficiently small α, the system has a family of equilibria $x_0(\alpha)$ and assume that its Jacobian matrix $J(\alpha) = \frac{\partial f}{\partial x}(x_0(\alpha), \alpha)$ has a pair of complex eigenvalues

$$\lambda_{1,2}(\alpha) = \mu(\alpha) \pm j\omega(\alpha)$$

that become purely imaginary when $\alpha = 0$, i.e., $\mu(0) = 0$ and $\omega(0) = \omega_{bif} > 0$. Generically, as α passes through $\alpha = 0$, the equilibrium changes its stability and a limit cycle emanates or bifurcates from the equilibrium point. This bifurcation is characterized by a single bifurcation condition $\mathrm{Re}\lambda_{1,2} = 0$ and generally can be observed in one-parameter families of smooth ODEs [110].
In order to describe the bifurcation analytically and graphically, system

(2.11) is considered with dimension $n = 2$,

$$\dot{x}_1 = f_1(x_1, x_2, \alpha),$$
$$\dot{x}_2 = f_2(x_1, x_2, \alpha).$$

If the following nondegeneracy conditions hold:

i) $l_1(0) \neq 0$, where $l_1(\alpha)$ is the first Lyapunov coefficient [78];

ii) $\mu'(0) \neq 0$, $'$ is the derivative w.r.t. α.

then the system above can be described near the equilibrium by its normal form, using the coordinate change ($x \mapsto y$ and $\alpha \mapsto \beta$), time rescaling and normalizing ω_{bif} to 1,

$$\dot{y}_1 = \beta y_1 - y_2 + \sigma y_1(y_1^2 + y_2^2),$$
$$\dot{y}_2 = y_1 + \beta y_2 + \sigma y_2(y_1^2 + y_2^2),$$

where $y = (y_1, y_2)^\top \in \mathbb{R}^2$, $\beta \in \mathbb{R}$ is a parameter, and $\sigma = \text{sign} l_1(0) \in \{-1, 1\}$.

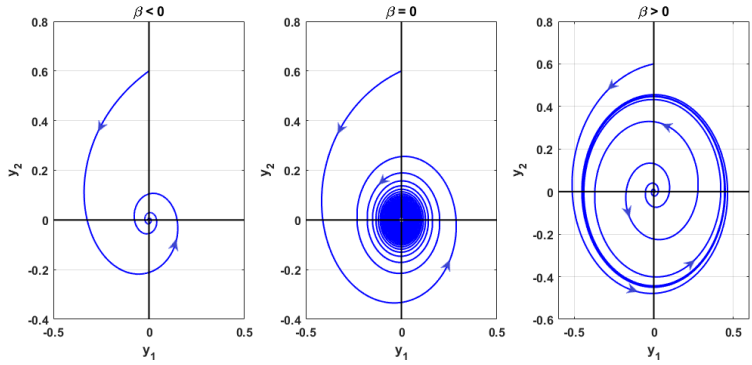


Figure 2.1: Supercritical Hopf bifurcation in the plane. Stable limit cycle for $\sigma = -1$.

If $\sigma = -1$, the normal form has an equilibrium at the origin, which is asymptotically stable for $\beta \leq 0$ (marginally stable at $\beta = 0$) and unstable for $\beta > 0$. Moreover, there exists a stable limit cycle emanating from the equilibrium when $\beta > 0$, which has radius $\sqrt{\beta}$. Such kind of bifurcation is called a supercritical Hopf bifurcation and depicted in Fig. 2.1.

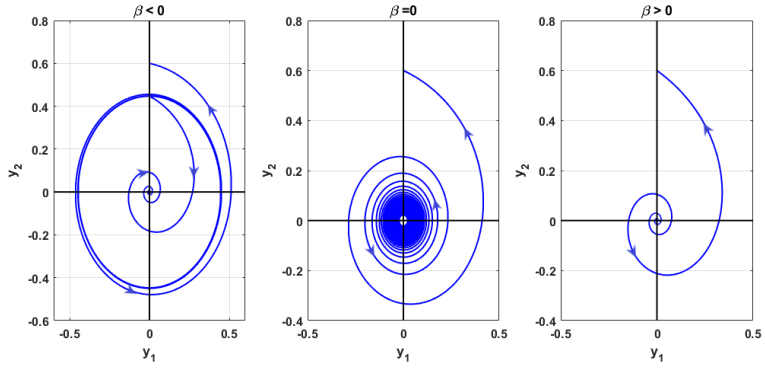


Figure 2.2: Subcritical Hopf bifurcation in the plane. Unstable limit cycle for $\sigma = 1$.

If $\sigma = +1$, the origin of the normal form is asymptotically stable for $\beta < 0$ and unstable for $\beta \geq 0$ (marginally stable at $\beta = 0$) with an unstable limit cycle which exists for $\beta < 0$. This is a subcritical Hopf bifurcation, which is shown in Fig. 2.2.
The Hopf bifurcation theory is also applied for the delay differential equations. The existence of periodic solutions to RDDEs, whose origin is a Hopf bifurcation, is proven in Chapter 11 of [111]. Normal forms for retarded functional differential equations and their application to Hopf bifurcations are presented in [112] and [113].

2.6 Harmonic balance method

In this section the Harmonic Balance method is presented. The method gives an approximation to a periodic solution of ODEs. In order to show how the Harmonic balance equation for a single-input-single-output (SISO) nonlinear system is derived, we consider a system of the Lur'e type:

$$\begin{aligned} \dot{\xi} &= A_L \xi + B_L w, \\ w &= \zeta(\eta), \\ \eta &= C_L \xi, \end{aligned} \tag{2.12}$$

where $\xi \in \mathbb{R}^n$ is the state of the system, $w \in \mathbb{R}^1$ is the input of the system, $\eta \in \mathbb{R}^1$ is the output of the system, $\zeta(\cdot)$ is a scalar nonlinear time-invariant

memoryless C^1 function and A_L, B_L, C_L are constant matrices of appropriate dimension with $C_L B_L > 0$.
The goal of the method is to approximate system's output signal η by a sum of the offset and signal's first harmonic

$$\eta \approx \eta_0 + \eta_1,\ \eta_0 = a_0 = \text{const},\ \eta_1 = a_1 \sin(\omega t + \phi_0 + \phi), \tag{2.13}$$

where a_0 is an offset, a_1 is an amplitude, ϕ is a phase and ϕ_0 is a relative phase, which can be chosen since the system is autonomous. In order to deal with nonlinearity, nonlinear function $\zeta(\eta)$ is approximated by its describing function. The process will be discussed later.
Suppose $\eta(t)$ is periodic with frequency ω and let

$$\eta(t) = \sum_{k=-\infty}^{+\infty} a_k e^{kj\omega t}, \quad a_k = \bar{a}_{-k}. \tag{2.14}$$

Using the Fourier series, the system's input is rewritten as follows

$$w = \zeta(\eta) = \sum_{k=-\infty}^{+\infty} c_k e^{kj\omega t}, \quad c_k = \bar{c}_{-k}. \tag{2.15}$$

We seek for a set of Fourier coefficients a_k, c_k and frequency ω which satisfy the system's equations. Using the orthogonality of the functions $\{\exp(kj\omega t)\}_k$, we find that the Fourier coefficients a_k and c_k must satisfy

$$a_k = W(kj\omega)c_k, \tag{2.16}$$

for all integers k and $W(s) = C_L(sI - A_L)^{-1}B_L$ which is the transfer function representing the linear time-invariant part of system (2.12). Because $W(kj\omega) = \bar{W}(-kj\omega)$, $a_k = \bar{a}_{-k}$, and $c_k = \bar{c}_{-k}$, we only need to look at (2.16) for $k \geq 0$. For many practical relevant cases, most information of the system behavior is contained in the first harmonic ($k = 1$). Moreover, when a nonlinearity is not odd, an offset component related to $k = 0$ appears. According to this, we consider equations for $k = 0, 1$ [96]. Equation (2.16) is reduced to

$$\begin{aligned} &[1 - W(0)K_0(a_0, a_1)]\, a_0 = 0, \\ &\left[1 - W(j\omega)K_1(a_0, a_1)\right] a_1 = 0, \end{aligned} \tag{2.17}$$

where $K_0(a_0, a_1)$ and $K_1(a_0, a_1)$ stand for describing functions which are computed as follows

$$\begin{aligned} K_0(a_0, a_1) &= \frac{c_0}{a_0} = \frac{1}{2a_0\pi}\int_0^{2\pi} \zeta(\eta(\omega t))\mathrm{d}(\omega t), \\ K_1(a_0, a_1) &= \frac{c_1}{a_1} = \frac{1}{a_1\pi}\int_0^{2\pi} \zeta(\eta(\omega t))\sin(\omega t)\mathrm{d}(\omega t). \end{aligned} \tag{2.18}$$

Note that describing functions K_0 and K_1 are real due to the fact that nonlinear function $\zeta(\cdot)$ is time-invariant and memoryless [96].
It is worth mentioning, that the describing function method approximates a nonlinearity by a gain using the first harmonic, which means that the approximation is most accurate when high-order terms are negligibly. In a neighbourhood of a Hopf bifurcation point, oscillations are sinusoidal-like and can be accurately described by the harmonic balance method due to negligible small high order nonlinear terms. A rigorous mathematical justification of this fact is outside the scope of the thesis. For a classical harmonic balance method its mathematical justification is derived in [89], where the accuracy of the method is estimated by the contraction mapping argument. The result in [89] provides a conservative estimate, which is derived under restrictive assumptions, however, these assumptions do not require the amplitude of the oscillations to be small. It would be very interesting but challenging to extend the result from [89] to the case of the multivariable harmonic balance method, studied in Chapter 3 and Chapter 4.

Chapter 3

Pattern Analysis in diffusively coupled Lur'e systems

3.1 Introduction

In recent years, the study of complex networks consisting of coupled nonlinear dynamical systems has been a significant subject in mathematical biology, control theory, applied physics, and interdisciplinary fields. Its relevance is due to several factors: complex networks are prevalent in the world (e.g. neuroscience, heart cells synchronization, social networks, flocks of birds and other kinds of collective behavior); such networks show a rich dynamic behavior and may induce a large number of different applications (see [114], [37] and references therein). In particular, different synchronous regimes and a *pattern formation* in coupled systems are subjects of intensive study.

Numerous activities in nature exhibit oscillatory behavior and can be described by a collection of coupled nonlinear oscillators. Due to complex dynamics and different types of coupling, various phenomena appear in nonlinear networks. An omnipresent form of interaction is a *diffusive coupling* [81], in which the feedback to each (sub)system in the network is a (weighted) sum of differences in each (sub)system's output and those of its neighbours. Networks with diffusive coupling exhibit surprisingly rich phenomena, such as synchronization [115], partial synchronization ([75]), and formation of oscillatory patterns including standing, travelling and rotating waves (see [116] and [90]). Moreover, some of these patterns may co-exist and can be stable for the same set

of parameters [117] [118] [119]. These patterns arise from a *diffusion-driven instability* first discussed by [67]. In that research, the author "suggests that a system of chemical substances reacting together and diffusing through a tissue is adequate to account for the main phenomena of morphogenesis". Several concepts related to the chemical basis of morphogenesis (development of patterns), spatial chemical patterns, and what is now called diffusion-driven instability are introduced. In general, the pattern formation phenomenon refers to the generation of complex organization in space and time.

A nonlinear analysis of Turing instability or the diffusion-driven instability phenomenon is described in [71]. In that paper, an example of two diffusively coupled systems is studied. Each individual system represents a cell which is inert or dead in the sense that it is globally asymptotically stable. However, when the cells are coupled via diffusion, "the cellular system pulses (or expressed perhaps overdramatically, becomes alive!) in the sense that the concentration of enzymes in each cell will oscillate infinitely". The author poses the question of determining conditions under which the diffusive coupling leads to oscillatory behavior in the network of initially globally asymptotically stable systems. Answers to this question are found in [72], [73], and [74], and references therein.

Another related result is presented in [75]. In that work, the authors present conditions under which a network of systems which are globally asymptotically stable by themselves, being diffusively coupled display different synchronous regimes, such as partial synchronous oscillations. In [76] the same phenomenon for a neuron network is described. These conditions are related to the coupling strength between the agents of the network and network topology. When the largest eigenvalue of the coupling matrix exceeds some threshold, the (network) equilibrium loses stability via a *Hopf bifurcation* and oscillatory patterns emerge. The Hopf bifurcation changes the dynamics of the network from a stable equilibrium to oscillatory patterns.

In this chapter, the method for pattern analysis in complex networks is presented. In particular, we consider the problem of *prediction* of oscillatory patterns which appear in (diffusively) coupled Lur'e systems via a Hopf bifurcation. A challenge is that there may be co-existence of different oscillatory patterns, such as an in-phase and an anti-phase synchronization, and clockwise and counterclockwise waves in a ring-like structure. Some of these co-existent patterns may be stable for the same set of parameters (coupling strength), i.e. there is multi-stability. Considering multi-stability, the application of common methods for the analysis of network behavior,

such as the direct Lyapunov method and the analysis of Poincaré maps, becomes highly non-trivial.

To solve these problems, we develop a method based on the *multivariable harmonic balance* (MHB) method, which was firstly introduced in [90] for neuronal circuits called the central pattern generators (CPGs). The method allows to analyse the behavior of the complex network near the bifurcation point and to determine an oscillatory profile that approximates the output of the studied network without simulating ordinary differential equations (ODEs). Despite these advantages, the MHB method cannot be directly applied to a network consisting of diffusively coupled Lur'e systems due to different structure of (sub)systems of the network and in order to achieve the best accuracy of the approximation the coupled systems must be in the neighbourhood of the Hopf bifurcation point. Being inspired by previous results obtained in [75] and [90], we developed a new approach in order to analyze oscillatory behavior and predict the patterns with equal amplitudes for the oscillations in the complex network by means of the multivariable harmonic balance (MHB) method (see [91]). In this chapter, we extend our results and present an approach based on the MHB method aiming at pattern analysis with arbitrary amplitudes of oscillation in networks of (diffusively) coupled identical nonlinear systems.

This chapter is organized as follows. Preliminary results and the problem statement are given in Section 3.2. Pattern analysis using the multivariable harmonic balance is described in Section 3.3. There are four sections in Section 3.3. Section 3.3.1 describes the multivariable harmonic balance method presented in [90]. The MHB equation is derived in Section 3.3.2. Sections 3.3.3 and 3.3.4 introduce the equal amplitude case and the general amplitude case, respectively. Numerical results are given in Section 3.4 and include results for the equal amplitude case and the general amplitude case. In Section 3.5, the conclusions are provided.

3.2 Problem setting

In Section 3.2.1 we introduce dynamical systems and the type of coupling that form networks whose dynamics are analysed in this chapter. In Section 3.2.2, conditions that guarantee the occurrence of oscillatory patterns are provided. Tools being used for the analysis of network behavior are introduced in Section 3.2.3. The formulation of the problem is given in Section 3.2.4.

3.2.1 Networks of interconnected Lur'e systems

In this chapter, a method to analyze the behavior of networks consisting of identical nonlinear dynamical systems is presented. To do so, we consider a network which describes a collection of identical (diffusively) coupled (sub)systems. It is assumed that the network cannot be decomposed into two or more uncoupled networks. To turn the statements above into a mathematical description, we consider a network of N identical systems described by:

$$\begin{aligned} \dot{x}_i &= Ax_i + Bu_i, \\ u_i &= u_{ci} - \psi(z_i), \\ z_i &= Zx_i, \\ y_i &= Cx_i, \end{aligned} \tag{3.1}$$

where $i = 1, ..., N$ stands for the node number, $x_i(t) \in \mathbb{R}^n$ is the state of a i-th (sub)system, $u_i(t) \in \mathbb{R}^1$ is the combined input of a i-th (sub)system which consists of two components: $\psi(\cdot)$ which is a continuously differentiable scalar nonlinear sector-bounded function and $u_{ci} \in \mathbb{R}^1$ which is the input receiving data from the coupling of multiple (sub)systems, $y_i(t) \in \mathbb{R}^1$ is the output of the i-th system used for the coupling, $z_i \in \mathbb{R}^1$ is the argument of the nonlinearity of the i-th (sub)system and A, B, C, Z are constant matrices of appropriate dimension. Taking $u_{ci} = 0$, we have N isolated single input single output systems given in Lur'e form.

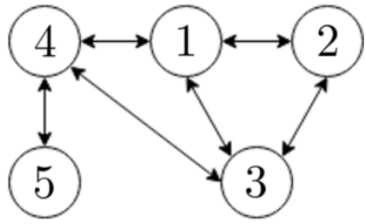


Figure 3.1: An example of the network consisting of dynamical systems.

The (sub)systems are interconnected through linear diffusive output coupling

$$u_{ci} = \gamma(-\gamma_{j1}(y_i - y_1) - \gamma_{i2}(y_i - y_2) - ... - \gamma_{ik}(y_i - y_N)), \tag{3.2}$$

where γ is the positive overall gain which will play the role of bifurcation parameter later on, γ_{il} are non-negative constants and $\gamma_{il} = \gamma_{li}$, $\forall i, l$. Moreover, $\gamma_{il} > 0$ if and only if the i-th and l-th nodes are connected. Graphically, the connection between the nodes i and l is represented by an edge (arrow) between i and l; see Figure 3.1. We assume that the network is connected, i.e. for any two nodes there exists a path (sequence of edges) connects them.
We define the coupling matrix Γ of size $N \times N$ as

$$\Gamma = \gamma \begin{pmatrix} \sum_{l=2}^{N} \gamma_{1i} & -\gamma_{12} & \cdots & -\gamma_{1N} \\ -\gamma_{21} & \sum_{l=1, l\neq 2}^{N} \gamma_{2i} & \cdots & -\gamma_{2N} \\ \vdots & \vdots & \ddots & \vdots \\ -\gamma_{N1} & -\gamma_{N2} & \cdots & \sum_{l=1}^{N-1} \gamma_{Ni} \end{pmatrix}. \tag{3.3}$$

Note that $\Gamma = \Gamma^{\top}$ with all row sums zero and thus all eigenvalues are non-negative [120]. Moreover, since we assumed that the network is connected, the matrix Γ has simple zero eigenvalue.
Using the Laplace transformation, the time-invariant linear part of the network (3.1) is rewritten into the transfer function representation, leading to the following description of the closed loop system (note that s stands for the differential operator)

$$\begin{aligned} y_i &= W_y(s) u_i, \\ z_i &= W_z(s) u_i, \\ u_i &= -\sum_{l=1}^{N} \gamma_{il} y_i - \nu_i, \\ \nu_i &= \psi(z_i), \end{aligned} \tag{3.4}$$

with $W_y(s)$ and $W_z(s)$ defined as

$$W_y(s) = C(sI - A)^{-1} B, \tag{3.5}$$

$$W_z(s) = Z(sI - A)^{-1} B. \tag{3.6}$$

3.2.2 Conditions for oscillatory behavior

The goal of this section is to present conditions that guarantee that the network (3.1)-(3.2) exhibits oscillatory behavior. The system (3.1)-(3.2) is called *Y-oscillatory* if the system's solutions are ultimately bounded and there exist a $i \in \{1, ..., N\}$ such that for *almost all* initial conditions $x(0) \in \mathbb{R}^{Nn}$

$\lim_{t\to+\infty} y_i(t)$ does not exist [121].
Networks of the form (3.1)-(3.2) were considered in [75] and it was shown that individual dynamics of the (sub)systems of the network satisfies some conditions for network synchronization.

Assumption 3.1 *The individual dynamics of system (3.1) and transfer functions (3.5) and (3.6) satisfy the following conditions:*

i) Matrix A is Hurwitz, so there is a positive definite matrix $P = P^\top$, so that $A^\top P + PA = -I$;

ii) Matrix Z satisfies $Z^\top = PB$ with matrix P as in i);

iii) $\psi(\cdot)$ is an odd, strictly increasing C^1-function with the following property $\forall L > 0\ \exists \sigma > 0$ such that $\forall z > \sigma\ \psi(z) > Lz$;

iv) Transfer function $W_y(s)$ is non-degenerate, has an even number of zeros with positive real part and relative degree one, and $W_y(0) > 0$;

v) Transfer function $W_z(s)$ is such that $W_z(0) > 0$.

The following theorem from [75] provides a condition under which a network that satisfies Assumption 3.1, exhibits oscillatory behavior.

Theorem 3.1 *Consider a network of diffusively coupled systems of the form (3.4) that satisfy Assumption 3.1 with a symmetric coupling matrix Γ as in (4.3).*
There is a number $\bar{\lambda} > 0$ such that if the largest non-zero eigenvalue λ_{max} of Γ exceeds $\bar{\lambda}$ then the network is Y-oscillatory.

The proof of the theorem captures three points:

i) The origin is the unique equilibrium point of the closed loop system;

ii) The system is uniformly ultimately bounded (see [96]);

iii) The origin is hyperbolically unstable if $\lambda_{max} > \bar{\lambda}$, where λ_{max} is the largest eigenvalue of Γ.

Depending on the value of the parameter γ, the dynamics of a network has at least two different modes (a globally asymptotically stable mode and a Y-oscillatory mode). In this chapter, we consider the case when the oscillatory behavior is caused by a Hopf bifurcation in the network at the point $\lambda_{max} = \bar{\lambda}$. Therefore, γ is chosen to be the bifurcation parameter. The

Hopf bifurcation point can be easily computed for any network consisting of nonlinear dynamical systems of the form (3.4). The Hopf bifurcation of an equilibrium is characterized by one bifurcation condition which is the presence of a purely imaginary pair of eigenvalues of the Jacobian matrix evaluated at this equilibrium [78]. For some networks the largest eigenvalue λ_{max} of the coupling matrix Γ has algebraic and geometric multiplicity larger than one (see Section 3.3) which corresponds to the occurrence of an *equivariant Hopf* bifurcation [122]. Assuming that $\psi'(0) = 0$, the Hopf bifurcation (equivariant Hopf bifurcation) occurs when the matrix $A - BC\bar{\lambda}$ has a pair of purely imaginary eigenvalues with algebraic and geometric multiplicity one (larger than one) and the other eigenvalues have negative real part. We also compute the bifurcation frequency ω_{bif} which will be required later on.
According to normal form theory (see [77] and references therein), the oscillations are sinusoidal-like near the bifurcation point. It justifies using the describing function method to replace the nonlinearity by its linear approximation and then to analyze the system of linear equations by means of the harmonic balance method which is presented in Section 2.6.

3.2.3 Describing Function Approximation

The harmonic balance method provides an analytical approximation of periodic solution(s) of an ODE and is applicable to nonlinear systems. In order to apply this method we approximate the nonlinearity $\psi(\cdot)$ of (sub)system (3.1) with its describing function. Suppose a (sub)system of the Y-oscillatory network has a periodic solution $z_i(t)$. Then, by Fourier series expansion, we obtain

$$z_i(t) = \sum_{m=0}^{\infty} a_{im} \sin(\omega m t) + b_{im} \cos(\omega m t)$$

for real vectors a_{im} and b_{im} and frequency ω. In the neighbourhood of a bifurcation point the solution can be approximated by its first harmonics

$$z_i(t) \cong \alpha_i \sin(\omega t + \phi_0 + \phi_i), \tag{3.7}$$

where α_i is the amplitude, ω is the frequency, ϕ_0 is the relative phase and ϕ_i is the phase for the i-th (sub)system of the network. For an autonomous system we can take $\phi_0 = 0$ without loss of generality. In order to approximate the nonlinearity $\psi(\cdot)$, which is assumed to be odd function, by its describing function k, we first compute the describing function which

stands for the gain and then replace the nonlinearity with the linear gain as follows:

$$\psi(z_i) \cong k(\alpha_i) z_i, \tag{3.8}$$

where

$$k(\alpha_i) := \frac{2}{\pi \alpha_i} \int_0^{\pi} \psi(\alpha_i \sin\theta) \sin\theta \mathrm{d}\theta, \tag{3.9}$$

is the describing function of $\psi(\cdot)$.
The describing function $k(\alpha_i)$ stands for the average gain of the nonlinearity $\psi(\cdot)$ when the input of the nonlinearity is a sinusoidal signal of amplitude α_i [96].

3.2.4 Problem formulation

Networks of the form (3.1)-(3.2), whose (sub)system's individual dynamics satisfy Assumption 3.1, exhibit oscillatory behavior if the coupling between network agents is strong enough. For coupling strength slightly larger then the bifurcation point, these oscillatory patterns are characterized by a set of parameters (oscillatory profiles); amplitudes α_i, phases ϕ_i and frequency ω. Some of these patterns can co-exist and can be locally stable, which implies the multi-stability of the network dynamics. Since we consider the case when oscillations appear via a Hopf bifurcation (equivariant Hopf bifurcation), the use of an approach based on the harmonic balance method is justified at least for γ close to the bifurcation point. The harmonic balance method helps to avoid a classical analysis, e.g., by means of the direct Lyapunov method, which is cumbersome when we deal with multi-stability. Moreover, the harmonic balance method is numerically efficient. In this chapter, we consider the problem of computing approximations (3.7) of all patterns of oscillations in a given network.

3.3 Pattern Prediction by Multivariable Harmonic Balance

In this section, we review the multivariable harmonic balance (MHB) method which we develop for networked Lur'e systems in order to analyze the behavior of networks of the form (3.4) when pattern formation occurs.

The harmonic balance method for networks of CPGs (Central Pattern Generators) [see Section 3.3.1 for details], called the Multivariable Harmonic Balance (MHB), was described in [90]. The MHB method approximates the behavior of a network consisting of nonlinear systems and determines an oscillatory profile (frequency ω, amplitudes α_i, phases ϕ_i) as a solution to an eigenvalue problem. In Section 3.3.1, the Multivariable Harmonic Balance described in [90] is introduced. In Section 3.3.2, we show how the MHB method is applied to the network (3.1),(3.2). There are two cases to discuss namely the equal amplitude case and the general amplitude case which are described in Sections 3.3.3 and 3.3.4, respectively.

3.3.1 Multivariable Harmonic Balance

The Multivariable Harmonic Balance (MHB) developed in [90] considers networks of identical interconnected (sub)systems described by a dynamical mapping from input u_i to output z_i:

$$z_i(s) = f(s)u_i(s), \qquad u_i(s) = \sum_{l=1}^{N} \mu_{il}(s)v_i, \qquad v_i = \psi(z_i),$$

where $f(s)$ is a rational transfer function of variable s, which represents the linear time-invariant part of each (sub)system, $\psi(z_i)$ is a continuously differentiable odd static nonlinear function, $z_i(s)$ is the i-th (sub)system output and $\mu_{iN}(s)$ is a transfer function representing the connection from N-th system to j-th system. In vector form, these dynamics can be written as

$$z = F(s)u, \qquad u = M(s)v, \qquad v = \Psi(z), \tag{3.10}$$

where $\Psi(z) := \text{col}[\psi(z_1),...,\psi(z_N)]$, $z := \text{col}[z_1,...,z_N]$, $F(s) := f(s)I_N$ and $M(s)$ is the transfer matrix of the coupling whose (i,N) entry is $\mu_{iN}(s)$. Using equations (3.7)-(3.9), the dynamic equations are approximated by the MHB equation

$$(\mathscr{M}(s)\mathscr{K}(\alpha) - I_N)q = 0, \quad q_i := \alpha_i e^{j\phi_i}, \quad q \in \mathbb{C}^N, \tag{3.11}$$

where $\mathscr{M}(s) = F(s)M(s)$, $\mathscr{K}(\alpha) := k(\alpha_i)I_N$ is a diagonal matrix and q is a solution to the eigenvalue problem. The MHB equation characterizes the oscillatory profiles for (3.10) as follows. In order to obtain approximations of oscillatory solutions, we substitute a sample solution of the form $q_i = \alpha_i \exp(j\phi_i)$. All three components ($\alpha$, ϕ, ω) of the pattern are computed

and the oscillatory profile is reconstructed using (3.7).
In general, the MHB equation is nonlinear in α and might have multiple solutions and the goal is to determine the stable oscillations. In order to examine stability of such oscillatory solution, we use an approximate method from [123] commonly accepted in the engineering literature. Based on (3.8), we consider the linear systems obtained by replacing the nonlinearity Ψ with constant gain $\mathscr{K}(\alpha)$ as follows.

$$L_K := \begin{cases} z = \mathscr{M}(s)v, \\ v = \mathscr{K}(\alpha)z. \end{cases} \tag{3.12}$$

The block scheme representation of the linear system L_K is illustrated in Figure 3.2. From the perspective of the describing function method, the linear system L_K contains some information on the network behavior when its oscillations are sinusoidal-like with a set of amplitudes α. According to the approximate method from [123], the oscillation with certain ω, α, ϕ is stable if the linear approximation L_K is marginally stable, which is equivalent (if linear system has pure imaginary eigenvalues) to the boundedness of all solutions of (3.12).

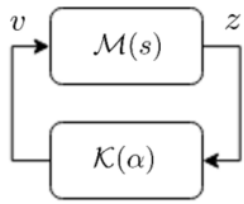


Figure 3.2: Linear system L_K.

From the above, the key ideas of the MHB analysis are summarised as follows:

- The oscillatory profile can be obtained by solving equation (3.11) for frequency ω and eigenvector z containing encoded amplitudes and phases.
- The predicted oscillatory pattern is stable if the corresponding linear system L_K given in (3.12) with $K := \mathscr{K}(\alpha)$ is marginally stable with a pair (pairs) characteristic roots at $s = \pm j\omega$ on the imaginary axis and with the rest characteristic roots located in the open left half plane.

3.3.2 Deriving the MHB equation

It is shown that the MHB method turns the problem of determining oscillatory profiles into an eigenvalue problem. System (3.4) does not belong to the class of systems considered in [90], so the previously described MHB method cannot be directly applied. In [90], it was considered the case of linear system dynamics with nonlinear coupling and we deal with nonlinear system dynamics with diffusive linear coupling. In order to apply the MHB analysis, a loop transformation is performed. Figure 3.3 displays how the loop transformation reorders the structure of the network. The left and right blocks describe the networks (3.4) and (3.10), respectively.

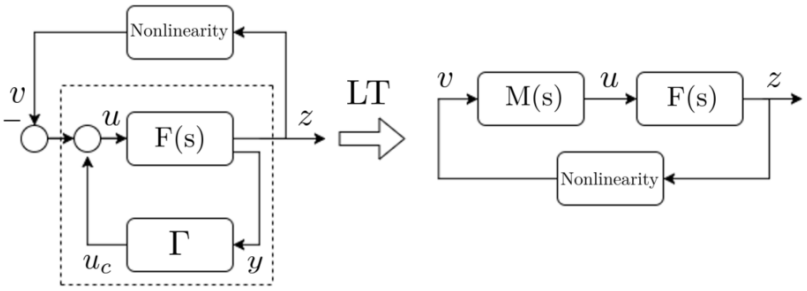


Figure 3.3: Loop Transformation reorders the structure of the network in order to apply the MHB method.

The following manipulations are performed to turn system (3.4) into the form of (3.10). Recall System (3.4) and rewrite the input u in vector form as

$$u = -W_y(s)\Gamma u - v,$$
$$W_y(s)\left[\frac{1}{W_y(s)} I_N + \Gamma\right] u = -v,$$

with matrix Γ defined in (4.3). Defining the resolvent $R(\frac{1}{W_y(s)}) = [\frac{1}{W_y(s)} I_N + \Gamma]^{-1}$, we obtain

$$u = -\frac{1}{W_y(s)} R\left(\frac{1}{W_y(s)}\right) v.$$

The network now takes the form of (3.10) with

$$\begin{aligned} F(s) &= W_z(s) I_N, \\ M(s) &= -\frac{1}{W_y(s)} \left[\frac{1}{W_y(s)} I_N + \Gamma \right]^{-1}. \end{aligned} \tag{3.13}$$

Combining the second equation from (3.10) with (3.13) and replacing s by $j\omega$, we arrive at the following equation

$$\mathscr{M}(j\omega) = -\frac{F(j\omega)}{W_y(j\omega)} \left(\frac{1}{W_y(j\omega)} I_N + \Gamma \right)^{-1}.$$

Define the diagonal matrix

$$H(j\omega) := \frac{F(j\omega)}{W_y(j\omega)} = \left(\frac{W_z(j\omega)}{W_y(j\omega)} \right) I_N$$

and substitute it in the previous equation in order to obtain

$$\mathscr{M}(j\omega) = -H(j\omega) \left(\frac{1}{W_y(j\omega)} I_N + \Gamma \right)^{-1}.$$

Subsequently, we rewrite the MHB equation (3.11) as follows

$$\mathscr{M}(j\omega)(\mathscr{K}(\alpha) - \mathscr{M}^{-1}(j\omega))q = 0,$$

where $\mathscr{M}^{-1}(j\omega) = -((1/W_y(j\omega))I_N + \Gamma)H(j\omega)^{-1}$ and expand it in order to obtain

$$\mathscr{M}(j\omega) \left(\frac{W_z(j\omega)}{W_y(j\omega)} \right) \left[\mathscr{K}(\alpha) \left(\frac{W_z(j\omega)}{W_y(j\omega)} \right) + \frac{1}{W_y(j\omega)} I_N + \Gamma \right] q = 0.$$

Since $\mathscr{M}(j\omega)(W_z(j\omega)/W_y(j\omega))$ is non-singular for $\omega > 0$, we obtain

$$J(\alpha,\omega)q := \left[\mathscr{K}(\alpha) \left(\frac{W_z(j\omega)}{W_y(j\omega)} \right) + \frac{1}{W_y(j\omega)} I_N + \Gamma \right] q = 0, \quad q_i := \alpha_i e^{j\phi_i} \tag{3.14}$$

which is the multivariable harmonic balance equation for the networks of identical Lur'e systems. We focus on determining patterns that appear in such networks. We consider both the equal amplitude case with $\alpha_i = \alpha_e \ \forall i$, and some $\alpha_e \in \mathbb{R}^+$, and the general amplitude case with possibly (all) different $\alpha_i \in \mathbb{R}^+$, $i = 1, ..., N$.

3.3.3 Equal amplitude case

In this section we review the equal amplitude case to gain some insight into the method. This special case is derived for networks exhibiting oscillations with equal amplitudes $\alpha_i = \alpha_e \ \forall i$. In particular, we consider ring-like networks with three and four nodes (Fig.3.4). Each (sub)system of these networks is a dynamical system that satisfies Assumption 3.1 and whose dynamics are presented in Section 3.4. The network topology is represented by a symmetric unweighted graph with the overall coupling gain, which means that $\gamma_{il} = 1$ if there is the connection between the jth and lth nodes and $\gamma_{il} = 0$ otherwise. The nodes are interconnected with neighbours via diffusive coupling. According to this, considered networks are regular in the following sense: Networks are referred to as regular if each node has exactly the same number of links [124]. Regularity favours the occurrence of stable oscillations with equal amplitudes. Since we look for $\alpha_i = \alpha_e \ \forall i$, the analysis of the network behavior can be substantially simplified using the structural properties of the network. In this section, it is shown how the oscillatory profile is determined by the MHB method for the equal amplitude case.

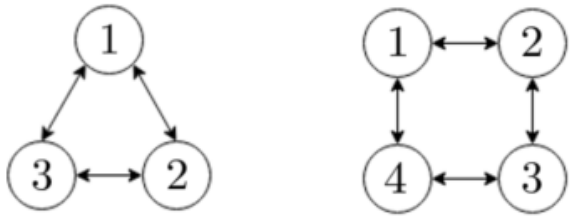


Figure 3.4: Ring-like networks of diffusively coupled systems displaying oscillations with equal amplitudes

Fig. 3.5 reflects the oscillatory patterns that can be observed in the networks shown in Fig.3.4. Oscillatory profiles are obtained by direct simulation of ordinary differential equations (ODEs) of network (3.1). For presentation purposes, components of $z_i(t)$ are shifted to $z_i(t) + (N + 1 - i)$. The oscillatory pattern has equal amplitudes with a phase shift of 120 degrees for the three-node configuration which is a rotating wave. A standing wave is observed for the four-node configuration. There are two synchronized groups of nodes which are in antiphase with each other.

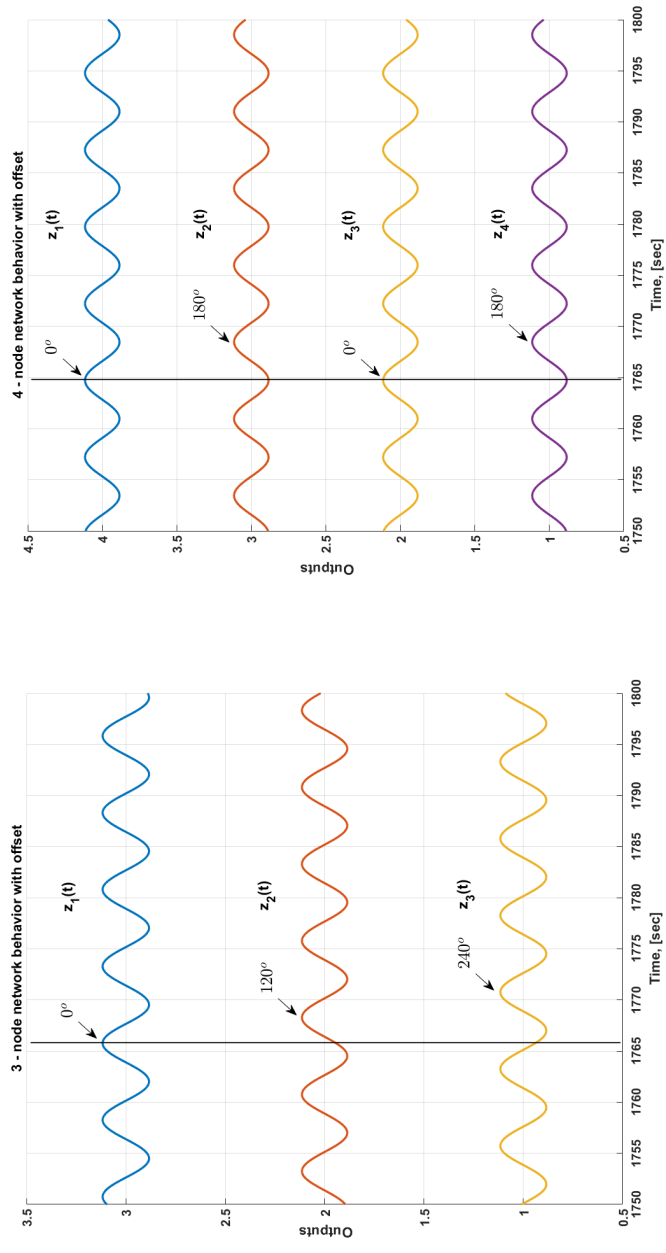


Figure 3.5: Oscillatory patterns with equal amplitudes in ring-like networks (left fig.: 3-node network, right fig.: 4-node network). Network dynamics is given in Section 3.4.

Since we look for equal amplitudes $\alpha_i = \alpha_e \ \forall i$, the describing function matrix $\mathcal{K}(\alpha) = k(\alpha_e) I_N$ and equation (3.14) reduces to

$$\left[\frac{k(\alpha_e) W_z(j\omega) + 1}{W_y(j\omega)} I_N + \Gamma \right] q = 0, \quad q_i := \alpha_e e^{j\phi_i}, \tag{3.15}$$

where q is the solution to the eigenvalue problem. One can see that equation (4.18) has several solutions. The trivial solution $q = 0$ corresponds to the equilibrium and is not point of interest. Therefore, we solve

$$\det \left[\frac{k(\alpha_e) W_z(j\omega) + 1}{W_y(j\omega)} I_N + \Gamma \right] = 0.$$

After diagonalizing the coupling matrix Γ via a similarity transformation, which is possible due to $\Gamma = \Gamma^\top$, and using the property of the determinant product, we arrive at

$$\frac{k(\alpha_e) W_z(j\omega) + 1}{W_y(j\omega)} + \lambda_i = 0, \tag{3.16}$$

where λ_i is an eigenvalue of the coupling matrix Γ.
The described procedure implies that different oscillatory patterns may appear based on each eigenpair (an eigenvalue and its corresponding eigenvector) of the matrix $\left[\frac{k(\alpha_e) W_z(j\omega)+1}{W_y(j\omega)} I_N + \Gamma \right]$. Nonetheless, from Theorem 3.1, it is known that if λ_{max} exceeds some threshold the network is Y-oscillatory. It was mentioned above that an oscillation is expected to be stable if the linear approximation (3.12) is marginally stable. Since $\Gamma = \Gamma^\top$, the eigenvalues located on the imaginary axis, have linearly independent eigenvectors which are eigenvectors of the coupling matrix Γ. The eigenvalue with the largest real part λ_{max} of the coupling matrix Γ characterizes the Hopf bifurcation (equivariant Hopf bifurcation) point in the network. We now consider equation (3.16) for λ_{max}

$$\frac{k(\alpha_e) W_z(j\omega) + 1}{W_y(j\omega)} + \lambda_{max} = 0. \tag{3.17}$$

Substituting (3.5) and (3.6) into (3.17), we obtain

$$\begin{aligned} k(\alpha_e) Z (j\omega I_n - A)^{-1} B + 1 + \lambda_{max} C (j\omega I_n - A)^{-1} B = 0, \\ 1 + (k(\alpha_e) Z + \lambda_{max} C)(j\omega I_n - A)^{-1} B = 0. \end{aligned}$$

Since the isolated system is exponentially stable, $\det(j\omega I_n - A) \neq 0$ for all ω, we have

$$(j\omega I_n - A)[1 + (k(\alpha_e)Z + \lambda_{max}C)(j\omega I_n - A)^{-1}B] = 0.$$

Using Schur's Lemma (see [125]), we arrive at

$$\det[j\omega I_n - A + B(k(\alpha_e)Z + \lambda_{max}C)] = 0.$$

Thus the matrix $A - B(k(\alpha_e)Z + \lambda_{max}C)$ has a pair of pure imaginary eigenvalues with algebraic and geometric multiplicity one for Hopf bifurcation (larger than one for equivariant Hopf bifurcation) for $\pm j\omega$, where ω stands for frequency of the oscillations and the other eigenvalues are in the open left-half complex plane

$$\mathrm{Re}(\lambda_{1,2}(A - B(k(\alpha_e)Z + \lambda_{max}C))) = 0. \tag{3.18}$$

In other words, $k(\alpha_e)$ and ω can be derived from the Hopf bifurcation condition. Now two components of the oscillatory profile are obtained: α_e using (3.9) and ω. The phases ϕ_j are encoded in the eigenvector that corresponds to the largest eigenvalue λ_{max} of the coupling matrix Γ. Substituting $(k(\alpha_e)W_z(j\omega) + 1)/W_y(j\omega) = -\lambda_{max}$ in (4.18), we obtain

$$[\Gamma - \lambda_{max}I_N]q = 0. \tag{3.19}$$

Since we look for equal amplitudes, we need such eigenvector q with the entries represented as $q_i = \alpha_i \exp(j\phi_i)$ that all elements of q_i have the same modulus α_e. In order to determine the phases from the eigenvector the following equation is used

$$\phi_i = \arg(q_i). \tag{3.20}$$

Having all components of the oscillatory profile computed, the approximation of the oscillatory pattern of the given network using the equation (3.7) can be constructed.

It was mentioned above that multiple oscillatory patterns occurring in such networks may co-exist. Co-existence implies that there simultaneously exist at least two stable solutions in ring-like structured networks, such as clockwise and counter-clockwise rotating waves. This happens when the largest eigenvalue λ_{max} of the coupling matrix Γ has algebraic and geometric multiplicity two which implies the existence of two linearly independent eigenvectors corresponding to this eigenvalue or, in other words, an equivariant Hopf bifurcation occurs [122]. The phases of clockwise and counter-clockwise rotating waves are encoded in these eigenvectors and be determined using (3.20).

3.3.4 General amplitude case

In this section a method for estimating the profile of oscillations with arbitrary amplitudes is presented. Networks exhibiting oscillatory patterns with different amplitudes can be easily obtained by attaching additional nodes to the networks presented in Fig.3.4 as shown in Fig.3.6. These networks consist of identical dynamical systems, whose individual dynamics is given in Section 3.4 and [75], that satisfy Assumption 3.1. As in the equal amplitude case, we consider networks whose topology is described by a symmetric unweighted graph with the overall coupling gain. Unlike the equal amplitude case, these networks are not regular.

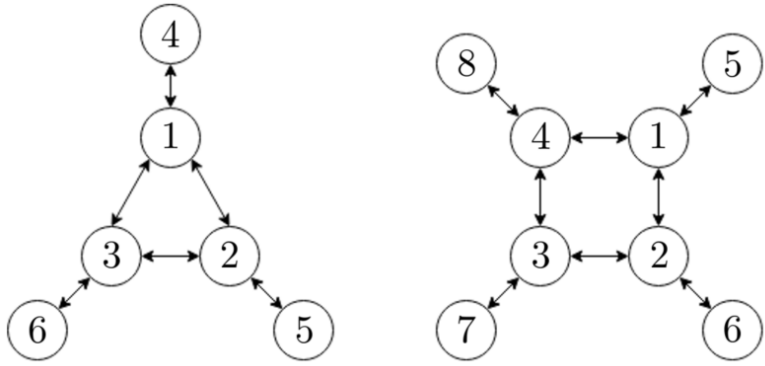


Figure 3.6: Networks of identical diffusively coupled systems displaying oscillations with unequal amplitudes.

Such networks are perfect candidates to illustrate and study the general amplitude case due to their structure and behavior. Fig. 3.7 reflects the oscillatory patterns that can be observed in the networks shown in Fig. 3.6. Results are obtained by the direct simulation. For presentation purposes, components of $z_i(t)$ are shifted to $z_i(t)+(N+1-i)$. Two groups of nodes with equal amplitudes are observed. The first group corresponds to the core ring which is the subnetwork of nodes with more than one neighbour. Core rings of the networks from Fig. 3.6 belong to the first group and the attached nodes belong to the second group.

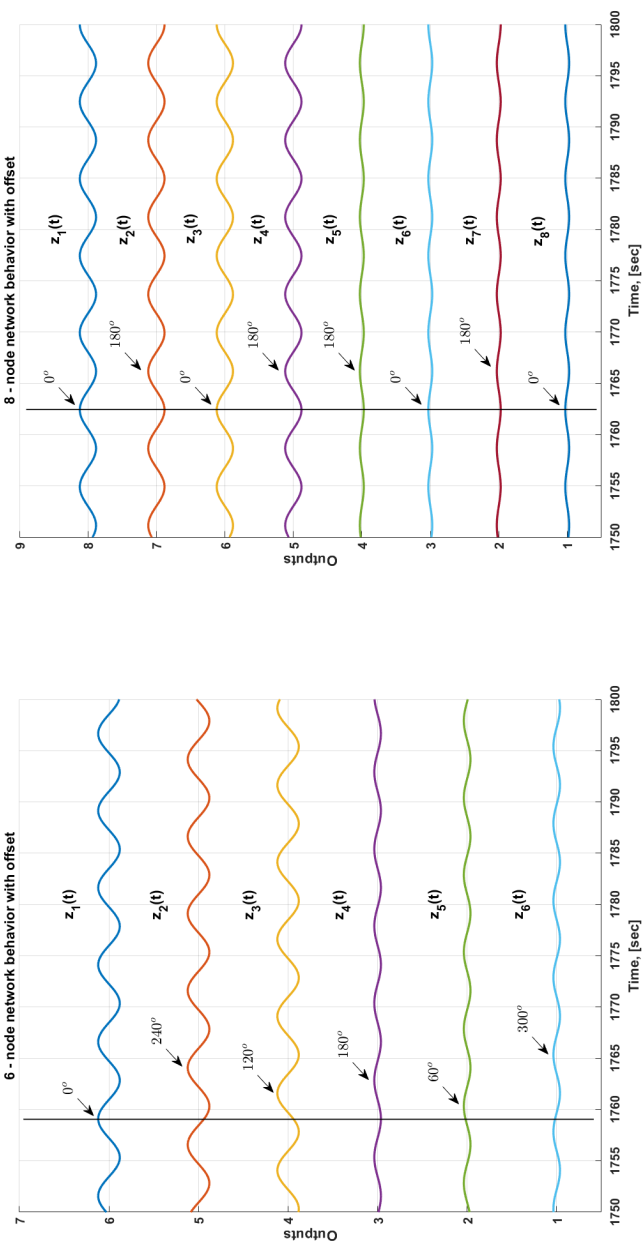


Figure 3.7: Oscillatory patterns with unequal amplitudes (left fig.: 6-node network, right fig.: 8-node network). Network dynamics is given in Section 3.4.

Recall equation (3.14),

$$J(\alpha,\omega)q := \left[\mathscr{K}(\alpha)\left(\frac{W_z(j\omega)}{W_y(j\omega)}\right) + \frac{1}{W_y(j\omega)} I_N + \Gamma\right] q = 0.$$

To solve the equation above, it is represented as an optimization problem. Since the trivial solution $q = 0$ is not a point of interest, we look for a set of phases ϕ_i, amplitudes α_i and frequency ω which solves the nonlinear equation (3.14). Define the objective function to minimize as

$$F(g) := Q'Q + p^\top p, \tag{3.21}$$

where

$$g := [\phi;\alpha;\omega] \in \mathbb{R}^{2N+1}, \quad Q := J(\alpha,\omega)q \in \mathbb{C}^N, \quad p := \alpha - |q| \in \mathbb{R}^N,$$

where $|q| = [|q_1|,|q_2|,...,|q_k|]^\top$.
The vector g contains unknown phases, amplitudes and frequency, the component p represents the second equation of (3.14). To simplify the problem the phase of the first node is fixed at $\phi_1 = 0$ and boundaries are chosen as: $\phi_i \in [0,2\pi] \quad \forall i \neq 1$, $\alpha_i \in [0,\beta] \quad \forall i$, $\omega \in [0,2\omega_{bif}]$, where β is a heuristically chosen number. A smart choice of β allows a substantial reduction in convergence time.
Solutions to the nonlinear equation (3.14) are found by minimizing the squared residual norm of the objective function (4.35). The local solver `fmincon` included in `MATLAB` environment [126] is used. The solver uses the *interior-point* algorithm [127] in order to find a minimum of constrained nonlinear multivariable function in the defined feasible region. Since equations (3.14) are nonlinear and multiple solutions exist, the solutions heavily depend on the initial conditions. Multiple values of the initial conditions are generated by the `MultiStart` algorithm [128].
A big advantage of the `MultiStart` method is that start points for the minimization procedure are not needed to be specified. A set of random points is used as initial conditions. The key point in the procedure is to choose the correct boundaries for the start points and the unknown variables, which can be easily done on our case.
The procedure has the following steps:

1. Define the objective function to minimize;
2. Define the constraints for start points and unknowns;
3. Set start points for the solver (random or custom);

4. Run the solver.

Moreover, the `MultiStart` algorithm can deal with multi-stability. For example, stable clockwise and counter-clockwise wave-like solutions can be simultaneously found.

3.4 Numerical examples

In this section, it is shown how the multivariable harmonic balance method is applicable to networks consisting of dynamical systems of Lur'e form whose structures given in the Figures 3.4 and 3.6. These networks are perfect candidates to demonstrate the performance of the method. The networks exhibit different oscillatory patterns, such as patterns with equal and unequal amplitudes, patterns with a simple phase shift (180 degrees) and with non-trivial phase shift (e.g. 120 degrees), and co-existing clockwise and counter-clockwise wave-like patterns. The individual dynamics of the nodes, as in [75], is given in (3.1) with

$$A = \begin{pmatrix} 1 & -1 & 1 \\ 1 & 0 & 0 \\ -4 & 2 & -3 \end{pmatrix}$$

$$B = \begin{pmatrix} 0 & 0 & 1 \end{pmatrix}^\top, \; C = \begin{pmatrix} 0 & 0 & 1 \end{pmatrix}, \; Z = B^\top P,$$

where P is the solution to the Lyapunov equation

$$A^\top P + PA = -I_3.$$

The nonlinear function $\psi(\cdot)$ is given as follows

$$\psi(z_i) = z_i^3;$$

and computing the describing function by (3.9), we obtain

$$k(\alpha_i) = \frac{3}{4}\alpha_i^2.$$

The presented setting satisfies the conditions from Assumption 3.1. Since numerical methods are employed, it implies that a computational error exists which is given as residual of Eq.(3.14). In order to show, that the MHB method accurately predicts oscillatory patterns, the reconstructed oscillations and the output of a direct simulation are compared. The direct

simulation results are obtained using a nonstiff differential equation solver of medium order `ode45` included in `MATLAB` environment [129]. In order to measure the accuracy of the method we provide residual norm of the MHB equation and compare amplitudes and frequency with the ones that are extracted from ODE simulation as follows.

$$\Delta\alpha = 100||\alpha - \alpha_s||/||\alpha_s||;$$
$$\Delta\omega = 100(\omega - \omega_s)/\omega_s,$$

where α_s and ω_s are taken from the simulation. In the following two sections, we will present results of the analytical approach for the equal amplitude case and the numerical approach for the general amplitude case.

3.4.1 Results for the equal amplitude case

In this section, we show that it is possible to predict patterns occurring in regular networks with certain symmetry and that oscillatory patterns possess equal amplitudes. An example of such networks is given in the Figure 3.4. It is shown how to refine an oscillatory profile of the given network by means of the analytical approach presented above. This approach is applicable only for networks exhibiting patterns with equal amplitudes.
The coupling topology of the networks are given by matrices Γ_3 and Γ_4 where a subscript denotes the number of nodes in the network

$$\Gamma_3 = \gamma_3 \begin{pmatrix} 2 & -1 & -1 \\ -1 & 2 & -1 \\ -1 & -1 & 2 \end{pmatrix}, \quad \Gamma_4 = \gamma_4 \begin{pmatrix} 2 & -1 & 0 & -1 \\ -1 & 2 & -1 & 0 \\ 0 & -1 & 2 & -1 \\ -1 & 0 & -1 & 2 \end{pmatrix},$$

where $\gamma_{3,4}$ are bifurcation parameters. In the Section 3.2, it is shown that the Hopf bifurcation (equivariant Hopf bifurcation) occurs in the network when the largest eigenvalue λ_{max} with algebraic and geometric multiplicity one (larger than one) of the coupling matrix parametrized by bifurcation parameter γ exceeds some threshold $\bar{\lambda}$. Parameters $\bar{\lambda}_3$, $\bar{\lambda}_4$ can be calculated from the Hopf bifurcation (equivariant Hopf bifurcation) condition $A - BC\bar{\lambda}$ described in Section 3.2.2 and for the given networks these are: $\bar{\lambda}_3 = 0.43426$ and $\bar{\lambda}_4 = 0.32569$.
For the three node network, two stable wave-like oscillatory patterns (clockwise and counter-clockwise waves) are found and the oscillation

parameters are successfully determined. The accuracy of the MHB method and the derived oscillatory profiles for the coupling strength $\gamma_3 = 1.01$ are presented in Table 3.1 and Table 3.2.

Wave	ω	α_e	ϕ_1	ϕ_2	ϕ_3
Clockwise	0.8365	0.1296	0	240	120
Counterclockwise	0.8365	0.1296	0	120	240

Table 3.1: Multi-stable oscillatory profiles of the network represented by matrix Γ_3.

For the four node network, one wave-like solution is predicted. The

Wave	Residual	$\Delta\alpha$ in %	$\Delta\omega$ in %
Clockwise	9.9256e-07	0.5781	0.0371
Counterclockwise	9.9256e-07	0.5781	0.0371

Table 3.2: Comparison of the MHB method and ODE simulation of the network represented by matrix Γ_3.

Residual	$\Delta\alpha$ in %	$\Delta\omega$ in %	ω	α_e	$\phi_{1,3}$	$\phi_{2,4}$
1.0171e-06	1.0793	0.0521	0.8362	0.1159	0	180

Table 3.3: Oscillatory profile and comparison of the MHB method and ODE simulation of the network represented by matrix Γ_4.

predicted solution corresponds to a partial synchronization regime. We can observe synchronous behavior between two pairs of nodes, namely between the 1st and the 3rd, and between the 2nd and the 4th. Moreover,

these pairs are in anti-phase synchronization with respect to each other. The accuracy of the MHB method and the predicted oscillatory profile for the coupling strength $\gamma_4 = 1.01$ are provided in Table 3.3.
In the case of the four node network, the MHB method predicts the result which was previously obtained by means of the direct Lyapunov method in [75]. For the three node case, the analysis by means of the direct Lyapunov method is cumbersome due to the co-existence of two stable solutions.
Figure 3.8 shows that in the initial period of time the oscillations computed by the simulation and the output of the MHB method do not match because of transient effects. When the transients have sufficiently decayed the outputs are almost identical which implies that the MHB method accurately describes the patterns occurring in the networks. The vertical axis stands for the mismatch between outputs of the simulation and the MHB method and the mismatch is computed as $e(t) = z(t) - q(t)$. For some initial conditions, oscillations computed by the MHB method have different initial phases compared to the simulation ones. In order to compensate for this difference, an initial phase offset ϕ_0 can be applied to the MHB output vector as shown in (3.7).

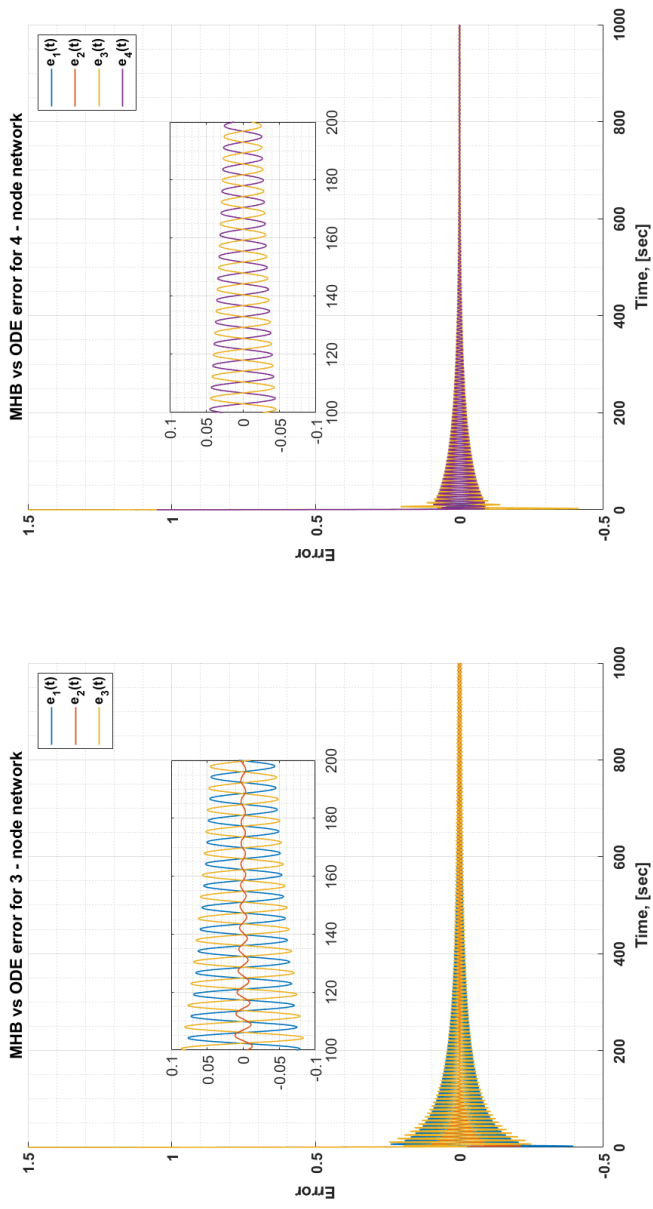


Figure 3.8: Error between the MHB method and ODE simulations for three- and four-node networks for $\gamma_{3,4} = 1.01\bar{\lambda}_{3,4}$. Inner plots represent zoomed-in sections for the presentation purposes.

3.4.2 Results for the general amplitude case

In this section, the results obtained by means of the optimization tools are presented. The numerical approach seeks for the set of the phases, amplitudes, and frequency that solves equation (3.14). This optimization method can also be applied to the equal amplitude case, at the cost of higher computation time. In the equal amplitude case the structure of the network can be exploited in such a way that one ends up with an eigenvalue problem of size n instead of nN.
Here we present the analysis of the networks which are given in Figure 3.6 and whose structure is described by matrices Γ_6 and Γ_8 where a subscript denotes the number of nodes in the network:

$$\Gamma_6 = \gamma_6 \begin{pmatrix} 3 & -1 & -1 & -1 & 0 & 0 \\ -1 & 3 & -1 & 0 & -1 & 0 \\ -1 & -1 & 3 & 0 & 0 & -1 \\ -1 & 0 & 0 & 1 & 0 & 0 \\ 0 & -1 & 0 & 0 & 1 & 0 \\ 0 & 0 & -1 & 0 & 0 & 1 \end{pmatrix},$$

$$\Gamma_8 = \gamma_8 \begin{pmatrix} 3 & -1 & 0 & -1 & -1 & 0 & 0 & 0 \\ -1 & 3 & -1 & 0 & 0 & -1 & 0 & 0 \\ 0 & -1 & 3 & -1 & 0 & 0 & -1 & 0 \\ -1 & 0 & -1 & 3 & 0 & 0 & 0 & -1 \\ -1 & 0 & 0 & 0 & 1 & 0 & 0 & 0 \\ 0 & -1 & 0 & 0 & 0 & 1 & 0 & 0 \\ 0 & 0 & -1 & 0 & 0 & 0 & 1 & 0 \\ 0 & 0 & 0 & -1 & 0 & 0 & 0 & 1 \end{pmatrix},$$

where $\gamma_{6,8}$ are bifurcation parameters. The Hopf bifurcation (equivariant Hopf bifurcation) occurs in these networks when the largest eigenvalue of matrix $\Gamma_{6,8}$ exceeds $\bar{\lambda}_6 = 0.30278$ and $\bar{\lambda}_8 = 0.24881$ for the six node network and the eight node network, respectively.
We use the `MultiStart` optimization framework in order to predict patterns that appear in the given networks. The objective function is given in (4.35), without loss of generality, we set the first phase $\phi_1 = 0$ in order to simplify the problem , and boundaries are chosen to be $\phi_i \in [0, 2\pi] \quad \forall i \neq 1,\ \alpha_i \in [0, \beta] \quad \forall i,\ \omega \in [0, 2\omega_{bif}]$, where $\omega_{bif\ 6,8} = 0.8350$ derived from the bifurcation condition and $\beta = 0.2$ is heuristically chosen. In order to show the accuracy of the MHB method for the general amplitude case, an error analysis is performed. First, we present the results for the network of

six nodes and the coupling strength parameter $\gamma_6 = 1.01$. The procedure starts from ten random points within the chosen domain and two distinct solutions are found that represent the clockwise and counter-clockwise waves. Existence of these waves implies the multi-stability of the network dynamics. The frequency, amplitudes, and phases of determined oscillatory patterns are given in Table 3.4 and Table 3.5, respectively. The accuracy of the method is given in Table 3.7.

Wave	ω	α_1	$\alpha_{2,3}$	α_4	$\alpha_{5,6}$
CW	0.8364	0.1226	0.1242	0.0375	0.0380
CCW	0.8364	0.1226	0.1242	0.0375	0.0380

Table 3.4: Amplitudes and frequency of oscillatory profiles of the network represented by matrix Γ_6. Multi-stability.

Wave	ϕ_1	ϕ_2	ϕ_3	ϕ_4	ϕ_5	ϕ_6
CW	0	240	120	180	60	300
CCW	0	120	240	180	300	60

Table 3.5: Phases of oscillatory profiles of the network represented by matrix Γ_6. Multi-stability.

Wave	Residual	$\Delta\alpha$ in %	$\Delta\omega$ in %
CW	0.00016	2.5387	0.0499
CCW	0.00016	2.5080	0.0230

Table 3.6: Comparison of the MHB method and ODE simulation applied to the network represented by matrix Γ_6. Multi-stability.

One can see that the multivariable harmonic balance method accurately

predicts the oscillatory patterns which appear in such networks, even for co-existing patterns.

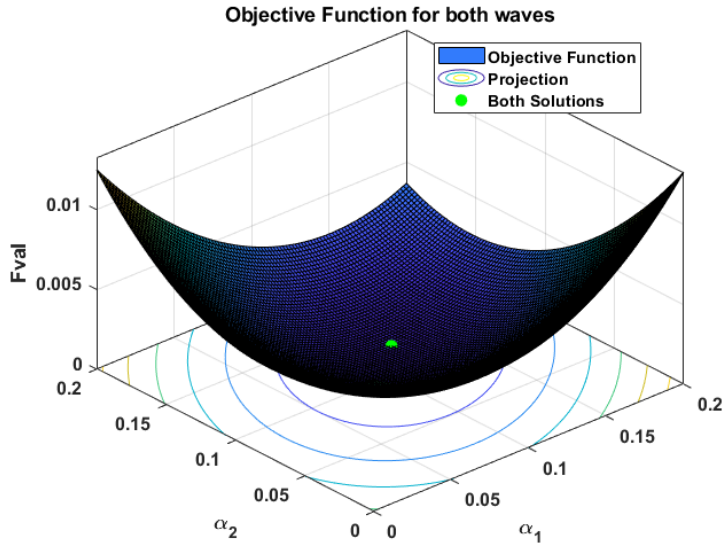


Figure 3.9: Objective Function cross-section of α_1 and α_2 for clockwise and counterclockwise waves. Since both wave-like solutions has equal amplitudes α_1 and α_2, they are shown as a single point. Fval is the objective function value.

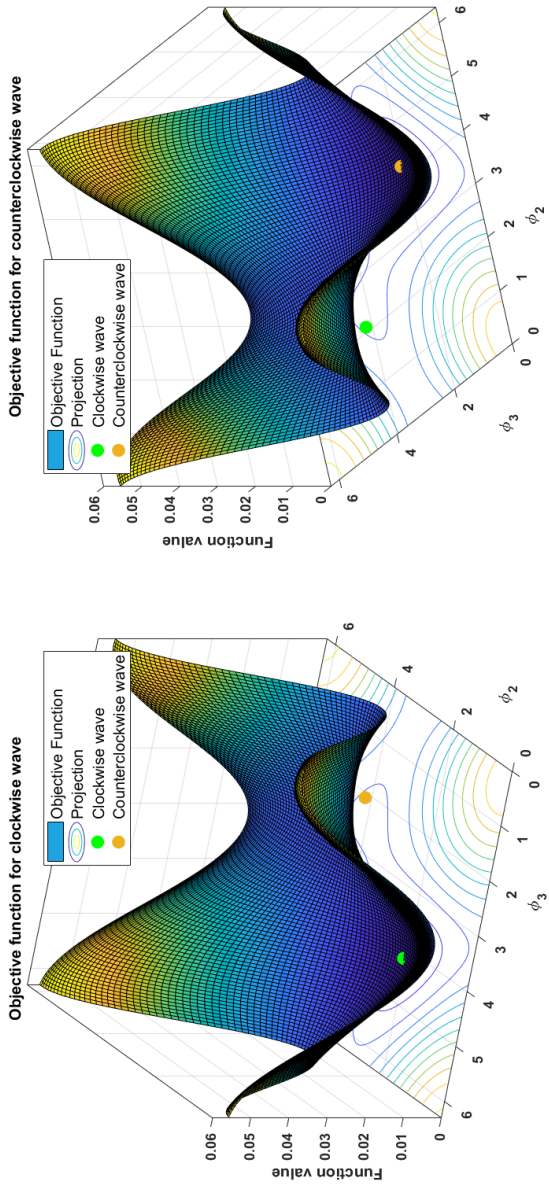


Figure 3.10: Objective Function cross-section of ϕ_2 and ϕ_3 for both solutions.

The objective function (4.35) has the argument $g \in \mathbb{R}^{2N+1}$. It is not possible to visualize a function of this dimension in 3D and that is why we provide cross-sections of the objective function. We change two (out of the $2N+1$) variables within some range and fix the remaining variables. Figures 3.9 and 3.10 show cross-sections in order to display that the computed solutions correspond to local minima. Figure 3.10 shows that there exist local minima for the clockwise and counter-clockwise wave-like solutions which implies multi-stability of the network.
We have the same setting (ten random points within the chosen boundaries) for the eight node network whose structure is represented by coupling matrix Γ_8. Multi-stability is not observed in this network. The coupling strength parameter is chosen to be $\gamma_8 = 1.01$. The determined oscillatory pattern is provided in Table 3.7 and the accuracy of the method is given in Table 3.8.

ω	$\alpha_{1,2,3,4}$	$\alpha_{5,6,7,8}$	$\phi_{1,3,6,8}$	$\phi_{2,4,5,7}$
0.8363	0.1209	0.0289	0	180

Table 3.7: Oscillatory profile of the network represented by matrix Γ_8.

Residual	$\Delta\alpha$ in %	$\Delta\omega$ in %
0.00056	2.4267	0.0367

Table 3.8: Comparison of the MHB method and ODE simulation applied to the network represented by matrix Γ_8.

In a network of an even number of nodes in a "core" ring, we observe a partial synchronization mode and a simple phase shift of 180 degrees. As it was mentioned above, the MHB method approximates a nonlinearity by a linear gain. Theoretically, the accuracy of the approximation becomes better as the network moves closer to a bifurcation point. We show how the accuracy changes when we increase the coupling strength. The example of eight nodes is used to illustrate this dependence and the results are

presented in Table 3.9 and Figure 3.11.
We run the method for the eight node network but for different coupling strength parameter γ_8. We performed six runs increasing γ_8 from 1.01 till 1.5.

Run	1	2	3	4	5	6
γ	1.01	1.1	1.2	1.3	1.4	1.5
Residual	0.0005	0.0003	0.0003	0.0003	0.0003	0.0568
$\Delta\omega$ in %	0.0127	0.0242	0.0798	0.1135	0.2266	0.3262
$\Delta\alpha$ in %	0.7264	0.7905	0.8440	0.9247	1.1635	1.2844

Table 3.9: Comparison of the MHB method and ODE simulation for 8-node network vs. coupling strength.

The numbers in Table 3.9 and Figure 3.11 illustrate that the accuracy changes as it was expected and the mismatch increases when the system goes away from the Hopf bifurcation point. This data shows that the MHB method can accurately predict oscillatory patterns even if the system is "far" from the bifurcation point.

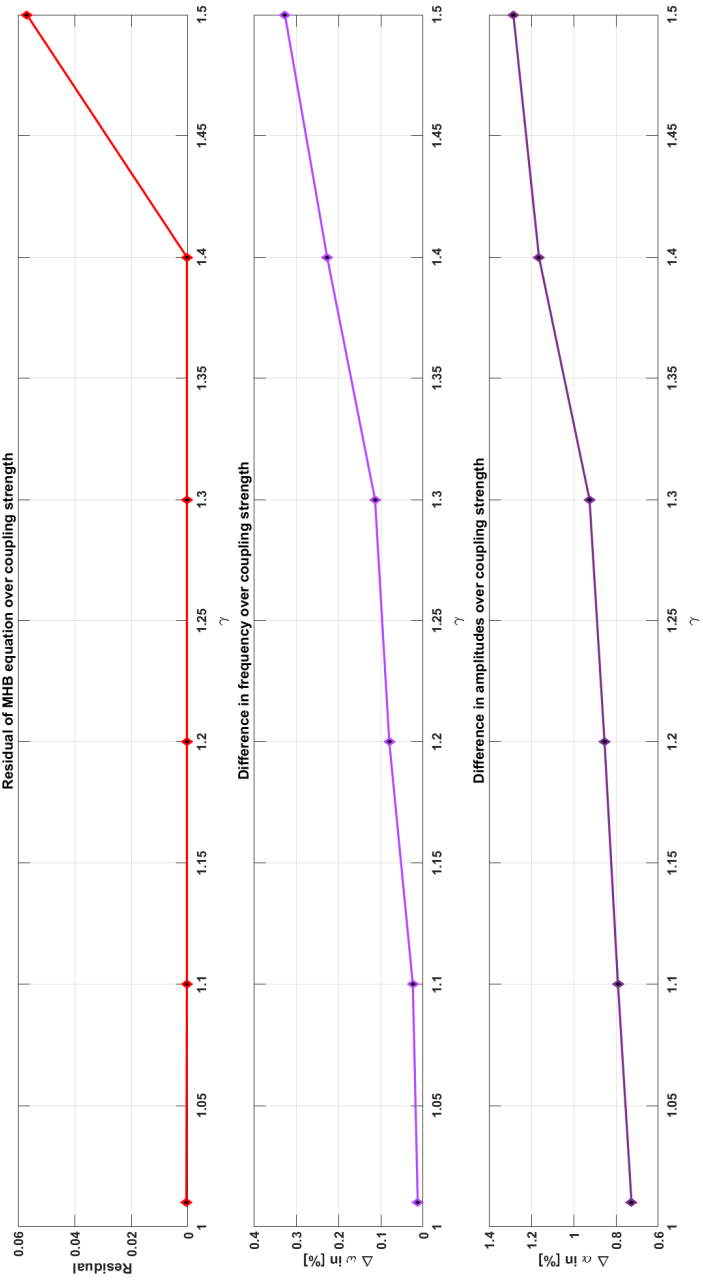


Figure 3.11: Comparison of the MHB method and ODE simulation for network represented by Γ_8 for different coupling strength.

3.5 Concluding remarks

This chapter addresses the problem of predicting patterned oscillations of arbitrary amplitudes in networks of identical nonlinear dynamical systems of Lur'e form. The patterns are characterized by a set of parameters consisting of frequency ω, amplitudes α_i and phases ϕ_i. In this chapter, we consider the case when the Hopf bifurcation (equivariant Hopf bifurcation) is the origin of oscillations and the oscillations are sinusoidal-like in the neighbourhood of the bifurcation point. According to this the nonlinearity can be approximated by its describing function and the network behavior can be analyzed by means of the harmonic balance method. Moreover, these patterns may co-exist which implies multi-stability. Multi-stability makes the usage of common tools, such as the direct Lyapunov method, highly involved. The multivariable harmonic balance (MHB) method for coupled systems of specific class was presented in [90]. The method is able to determine the oscillatory profile of patterns that occur in the network of specific structure and deals with multi-stability. The MHB method is not directly applicable to the networks of interest and in this chapter, we present the MHB method for the networks consisting of the Lur'e systems coupled via diffusion. The multivariable harmonic balance equation for networks of Lur'e systems is derived and it is shown that the method can accurately predict patterns that are formed in the networks of diffusively coupled Lur'e systems. For this, two cases are considered the equal amplitude case and the general amplitude case. The equal amplitude case can be easily solved using structural properties of the network. The general amplitude case requires numerical analysis. A numerical optimization routine has been developed which determines optimal solutions to the MHB equation and therewith predicts all possible stable patterns of oscillations. The MHB method, presented in this chapter, is tested on an artificial toy example, but it can be applied to problems, appearing in many scientific fields, ranging from biology, control engineering, neuroscience, physics, chemistry, to social sciences, and beyond.

Chapter 4

Delay Coupled Systems: Bifurcation and Pattern analysis

4.1 Introduction

Complex networks are prevalent in the world and can be used to describe the behavior of neuronal systems, heart cells synchronization, social networks, flocks of birds and other kinds of collective behavior [37], [114]. Complex networks exhibit rich dynamical behavior, with synchronized or partially synchronized motion being only few out of many possibilities. To explore the complex behavior that can occur, bifurcation analysis is essential, as it allows to characterize the behavior that appears due to parameter variations [78]. As such, it brings an insight in complex behavior that may occur near well-understood dynamical regimes, such as the synchronized state. A second motivation to investigate bifurcations in networked systems is to assess the robustness of a regime to parameter variations and to identify structurally possible regimes which are defined by a network topology. While a well-developed theory for bifurcations of nonlinear dynamical systems with delays exists [111], [113], these results are restricted to low-dimensional systems, and do not exploit the network structure. About one decade later, theoretical bifurcation results were pursued that take into account the structure in the networks [130]. It is possible to exploit the theoretical results for the development of numerically efficient software to assess the emergent behavior of complex systems, and explore different oscillatory regimes occurring in such systems.

Historically, the problem of emergence of oscillations in coupled systems (systems which are globally asymptotically stable when the coupling is absent) arises from the Turing's work on morphogenesis [67]. About two decades later, a nonlinear analysis of Turing instability or diffusion-driven instability was performed by Smale [71]. An example of two identical diffusively coupled fourth order systems is studied. Each individual system takes the role of a cell which is inert or "dead" in the sense that it is globally asymptotically stable in isolation. However, when the cells are interconnected via diffusive coupling, "the cellular system pulses (or expressed perhaps overdramatically, becomes alive!) in the sense that the concentration of enzymes in each cell will oscillate infinitely". The author posed the question of determining conditions under which an oscillatory behavior in networks of initially globally asymptotically stable systems, can be caused by diffusive coupling. A partial answer to this question was given in [73]. The authors studied the dynamics of two diffusively coupled Lur'e systems using frequency domain methods and showed that diffusion-driven oscillations are possible with third-order systems. In [74], it was proven that the emergence of diffusion-driven oscillations from a unique equilibria, as a result of the first bifurcation, is not possible in systems of order lower than three. Moreover, in that same paper, conditions for the emergence of diffusion-driven oscillations were presented. Results for different synchronous regimes, such as synchronization [115], [131], partial synchronization [75], [132], and pattern formation including standing, travelling and rotating waves [116], [90], [92], are found in given references.

The above-mentioned studies all consider diffusive coupling [81], which is (usually) symmetric and delay-free. In this chapter, we focus on pattern analysis of delay-coupled systems and study networks of Lur'e systems interconnected via linear time-delayed coupling functions. More precisely, the coupling function for a single system in a network is defined to be the weighted difference of the time-delayed output of its neighbours and its own non-delayed output. Physically, the adopted delay model represents the time that a signal takes to propagate from its source to its destination, and therefore the systems have access to their own outputs immediately. Such time-delay coupling functions appear, among others, in network of neurons [83], electrical circuits [84], and networked control systems [85]. As a starting point for this research, the work of [82] is used. The authors derived conditions under which a network of nonlinear dynamical systems which are globally asymptotically stable by themselves, being

interconnected via linear time-delay coupling functions, display oscillatory behavior and different patterns can emerge, such as partially synchronous oscillations and rotating waves. The (network) equilibrium loses its stability via a Hopf bifurcation which leads to pattern formation. The Hopf bifurcation changes the dynamics of the network from a stable equilibrium to oscillatory patterns. As a corollary to these results, the authors have shown that a network of inert systems with time-delay coupling can be globally oscillatory (considering case of a subcritical Hopf bifurcation) only if the systems are at least of second order.

In this chapter, we develop a numerically efficient method aiming at detecting co-existing oscillatory modes (patterns) even if some of them are unstable, in networks of nonlinear systems of Lur'e form interconnected via linear time-delayed coupling functions. Lur'e models are widely used in many fields (e.g. computational biology, control theory and etc.) and simplify the analysis by means of the harmonic linearization due to a scalar nonlinearity. The harmonic function approximation is characterized by offset components, amplitudes, phases and a frequency of oscillations. We consider the case where a Hopf bifurcation of both types (subcritical and supercritical) causes the instability of the network dynamics. The coupling strength and time-delay term take the role of bifurcation parameters. A challenge is that there may be co-existence of different oscillatory patterns for the same parameters (coupling strength and time delay), e.g. stable relaxation oscillations and unstable harmonic oscillations. Due to the co-existence of different modes, the application of common methods for the analysis of delay-coupled system behavior, such as the Lyapunov-Krasovskii method and the analysis of Poincaré maps, becomes highly non-trivial.

To solve these problems, we present an extension of the multivariable harmonic balance (MHB) method for delay-coupled systems and elaborate it by a tool for bifurcation analysis called `ddebiftool`. The method allows to analyse the behavior of the complex network and to determine an oscillatory profile that approximates the output of the studied network without simulating delay differential equations (DDEs), which is time-consuming for networks of many agents. The method presented in this chapter extends the approach presented in [92] towards networks with a time-delay coupling and shows additional possibilities of the Multivariable Harmonic Balance method, such as the simultaneous detection of stable and unstable coexisting periodic solutions. The MHB approach is numerically efficient and scalable due to the exploitation of a network structure and allows to

compute all co-existing regimes, even if some of them are unstable. The results of the MHB analysis can be also used as an input for continuation tools (e.g. DDE-BIFTOOL, AUTO-07P, MATHCONT), since them require accurate initial conditions.

It is worth mentioning, that the conventional Harmonic Balance method is sometimes considered as a rather empirical approach. This issue is overcome at least for scalar nonlinearities by the mathematical analysis in [96][89] [133]. The extension of these results to the MHB method, which facilitate the study of the oscillatory networks, is an open and interesting problem, which lies outside the scope of this chapter. This chapter focuses on numerical efficiency of the MHB method. In addition, we provide numerical evidences that the MHB method can accurately predict the oscillation profiles.

This chapter is organized as follows. Preliminary results and the problem statement are given in Section 4.4.2. More precisely, in Section 4.2.1, networks of Lur'e systems with time delay coupling are introduced. Conditions for the occurrence of oscillations are presented in Section 4.2.2. We give some details about two types (subcrtical and supercritical) of a Hopf bifurcation and show how to compute analytically critical values of the time-delay component in Section 4.2.3. In Section 4.2.4, the harmonic balance method is introduced. The problem is stated in Section 4.2.5. In Section 4.4.3, the MHB equation for delay-coupled systems is derived, including Equal Amplitude (EAC) case. Numerical examples are provided in Section 4.4.4. The latter includes results for both the supercritical Hopf bifurcation case and the subcritical Hopf bifurcation case. In Section 4.4.5, the conclusions are given.

4.2 Problem setting

4.2.1 Networks of delay coupled Lur'e systems

We consider a network of identical delay-coupled systems. N single-input-single-output (SISO) nonlinear systems of Lur'e type are and described by

following equations:

$$\begin{aligned} \dot{x}_i &= Ax_i + Bu_i, \\ y_i &= Cx_i, \\ u_i &= u_{ci} + \psi(y_i), \end{aligned} \tag{4.1}$$

where $i \in 1,\dots,N$ stands for the system index, $x_i \in \mathbb{R}^n$ is the state of i-th system, $u_i \in \mathbb{R}$ is the combined input of the i-th system which consists of two components: $\psi(\cdot)$, which is a C^1 scalar nonlinear time-invariant memoryless function, and $u_{ci} \in \mathbb{R}$, which is the input receiving data from the coupling of multiple systems. $y_i \in \mathbb{R}$ is the output of the i-th system used for the coupling and A, B, C are constant matrices of appropriate dimension with CB being a positive constant. In addition, we make the following assumption.

Assumption 4.1 *The isolated ($u_{ci} \equiv 0$) system (4.1), described by $\dot{x}_i := f(x_i) := Ax_i + B\psi(Cx_i)$, has a unique equilibrium point x_{i0}, which is globally asymptotically stable and locally exponentially stable.*

We remark that local exponential stability of the equilibrium is equivalent to the Jacobian matrix $J_0 = J(x_{i0}) = \frac{\partial f}{\partial x_i}(x_{i0})$ at x_{i0} being Hurwitz, i.e., all eigenvalues of J_0 have negative real parts.
The N systems (4.1) are interconnected via linear time-delay coupling functions of the form

$$u_{ci}(t) = \gamma \sum_l \gamma_{il}[y_l(t-\tau) - y_i(t)], \tag{4.2}$$

where positive constant γ stands for the coupling strength, positive constant τ stands for the time delay, and nonnegative constants $\gamma_{il} \in [0,1]$ are the interconnection weights. We remark that γ_{il} is positive if and only if there is a connection from system l to system i. Graphically, the connection between the nodes l and i is represented by an edge (arrow) between l and i; see Fig. 4.1. Positive constants γ and τ will be used as bifurcation parameters later on.
In order to specify the interaction structure of the network, we define the (weighted) adjacency matrix of the graph $\Gamma = (\gamma_{il}) \in \mathbb{R}^{N\times N}$ as

$$\Gamma = \begin{pmatrix} 0 & \gamma_{12} & \cdots & \gamma_{1k} \\ \gamma_{21} & 0 & \cdots & \gamma_{2k} \\ \vdots & \vdots & \ddots & \vdots \\ \gamma_{k1} & \gamma_{k2} & \cdots & 0 \end{pmatrix}. \tag{4.3}$$

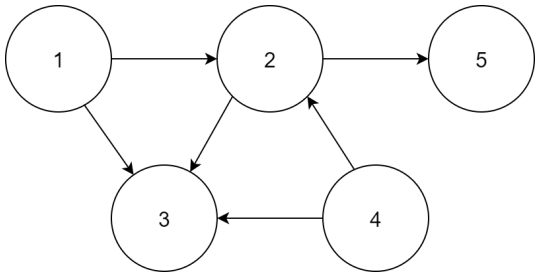


Figure 4.1: An example of the directed network consisting of dynamical systems.

We allow the graph to be directed in sense that all the edges are directed from one node to another. The graph is assumed to be simple in the sense that self-connections and multi[al edges joining the same pair of nodes are forbidden. Moreover, we assume that every pair of systems can be joined by a sequence of directed edges, which is equivalent to strong connectivity of the graph. In addition, the following assumption is made.

Assumption 4.2 *The sum of each row of the matrix* Γ *equals* 1.

Previously this assumption was used for the delay-coupled nonlinear system analysis in [134], [135] and it was used to ensure that a synchronous (oscillatory) state exists in such networks. Moreover, according to the Gershgorin Disc Theorem [120], Assumption 4.2 implies that all eigenvalues of Γ are located in the closed unit disc in $\mathbb{C}$.

4.2.2 Conditions for oscillations

The goal of this section is to present conditions that guarantee that the network (4.1)-(4.2) exhibits oscillatory behavior. Let $\sigma \in \mathscr{C}([0,\infty],\mathbb{R})$ be uniformly bounded. Such a function is oscillatory (in the sense of Yakubovich) if $\lim_{t\to+\infty} \sigma(t)$ does not exist [121]. Likewise we say that a system is oscillatory if it admits the following properties:

- All its solutions are uniformly (ultimately) bounded on $[0,\infty)$;
- The system has a finite number of hyperbolically unstable equilibria.

Note, that nonlinear systems (4.1) connected via coupling (4.2) are described by Delay Differential Equations (DDEs). An equilibrium solution of

a DDE is called hyperbolic if the roots of its characteristic equation have nonzero real part [104].
Since the goal of this chapter is to analyse oscillatory patterns in the networks, following [82] we establish conditions for oscillatory behavior of the network (4.1)-(4.2). Suppose Assumption 4.1 and Assumption 4.2 hold true and

- the solutions of the network (4.1)-(4.2) are uniformly bounded and uniformly ultimately bounded [136];
- the network (4.1)-(4.2) has a unique but hyperbolically unstable equilibrium at $x_0 = \mathbf{1}_N \otimes x_{10}$.

Under these conditions, the coupled systems will exhibit oscillatory behavior. Uniqueness of the equilibrium is not necessary for the existence of oscillations. However, the stability analysis of additional equilibria could be cumbersome as the locations of these equilibria heavily depend on the overall coupling strength γ. In addition, for a unique equilibrium the coupled systems can be oscillatory only if one of outputs is an oscillatory function of time. In case none of the outputs is an oscillatory function, the value of each coupling function converges to zero and the system cannot be oscillatory by Assumption 4.1.

We now discuss conditions under which the solutions are bounded. We consider a single system (4.1) and let $u_i(\cdot)$ be a piece-wise continuous input function defined on $[0, T)$, $T \in \mathbb{R}_+$, and taking values in a compact set $\mathcal{U} \subset \mathbb{R}$. Let $x_i(\cdot) = x_i(\cdot, x_{i0}, u_i[0, T))$ be the solution of system (4.1) corresponding to input $u_{ci}(\cdot)$ and initial conditions x_{i0} and $t = 0$. Then a (strictly) $\mathscr{C}^r$-semipassive system is defined as follows.

Definition 4.1 *Assume that there is storage function $S \in \mathscr{C}^r(\mathbb{R}^n, \mathbb{R}_+ \cup \{0\})$, such that*

$$S(x_i(t)) - S(x_i(0)) \leq \int_0^t [(y_i u_i(s)) - H(x_i(s))]ds \tag{4.4}$$

with $H \in \mathscr{C}(\mathbb{R}^n, \mathbb{R})$ and $t \in (0, T]$. If there is a constant $R > 0$ and a nonnegative nondecreasing function $h : \mathbb{R}_+ \cup \{0\} \to \mathbb{R}_+ \cup \{0\}$ such that

$$H(s) \geq h(|s|), \ \forall |s| \geq R, \tag{4.5}$$

then system (4.1) is called $\mathscr{C}^r$-semipassive. If (4.5) holds for all $|s| \geq R$ and function h is strictly increasing and such that $h(s) \to \infty$ as $s \to \infty$, then system (4.1) is strictly $\mathscr{C}^r$-semipassive.

Lemma 4.1 *(Boundedness) Let* $w_0,\ w_1 : [0,\infty) \to [0,\infty)$ *be strictly increasing functions, which satisfy* $w_0(0) = w_1(0) = 0$ *and* $w_0(s), w_1(s) \to \infty$ *as* $s \to \infty$. *Suppose that each system (4.1) is strictly* $\mathscr{C}^1$*-semipassive with storage function* S *that satisfies*

$$w_0(|x_i(t)|) \leq S(x_i(t)) \leq w_1(|x_i(t)|).$$

Then for each fixed γ *and* τ *the solutions of the coupled systems (4.1)-(4.2) are uniformly bounded and uniformly ultimately bounded.*

The proof of Lemma 4.1 can be found in [137]. Note that, unlike in the Ordinary Differential Equation (ODE) (finite dimensional) case, uniform ultimately boundedness does not imply uniform boundedness in the DDE case [138].

In order to verify the second condition, it is needed to show that the equilibrium point x_0 is unique and unstable. Using Assumption 4.2, we can write the network dynamics as

$$\dot{x}(t) = F(x(t)) + \gamma[(\Gamma \otimes BC)x(t-\tau) - (I_N \otimes BC)x(t)]. \tag{4.6}$$

The linearization of (4.6) around the network equilibrium x_0 results in

$$\dot{\hat{x}}(t) = [I_N \otimes (J_0 - \gamma BC)]\hat{x}(t) + (\gamma\Gamma \otimes BC)\hat{x}(t-\tau). \tag{4.7}$$

It is well known that the zero solution of the linear system (4.7) is unstable for some γ and τ if its associated characteristic equation

$$\Delta(\lambda;\gamma,\tau) = 0 \tag{4.8}$$

with

$$\Delta(\lambda;\gamma,\tau) := \det(\lambda I_{Nn} - I_N \otimes (J_0 - \gamma BC) - (\gamma\Gamma \otimes BC)e^{-\lambda\tau})$$

has a root in $\mathbb{C}_+$ [139]. However, computing the roots of the characteristic equation in the (γ,τ)-parameter space is cumbersome for large N. To address this issue, we use sufficient conditions for instability of the network equilibrium presented in [82]. In order to do so, we denote by

$$\mathscr{H}(s) := C(sI_n - J_0)^{-1}B = \frac{p(s)}{q(s)},$$

the transfer function from u_{ci} to y_i of system (4.1), linearised around its equilibrium. Here p and q are polynomials of degree $n-1$ and n, respectively, because system (4.1) has relative degree one ($CB > 0$). The following two lemmas are reported in [82]:

Lemma 4.2 *(Instability) Suppose that Assumption 4.2 holds true. Let*

$$\nu := \inf_{\omega>0} \mathscr{R}(\mathscr{H}(j\omega)).$$

If $\nu < 0$, then for each $\gamma \geq \frac{-1}{2\nu}$ there exists a $\tau > 0$ such that the characteristic equation (4.8) has a root in $\mathbb{C}_+$.

Note that using Lemma 4.2 a value of $\gamma_{min} := \frac{-1}{2\nu}$ can be computed. It is important to mention that the condition for instability is delay-dependent. We continue with conditions for uniqueness of the network equilibrium.

Lemma 4.3 *(Uniqueness of the network equilibrium) Let Assumption 4.1 hold true and denote the eigenvalues of Γ by λ_i^Γ, $i = 1, ..., N$. Let λ^* be the smallest real-valued eigenvalue of Γ. Choose $\bar{\gamma} \in (0, \infty]$ as the largest number for which matrix*

$$J(\chi) - \gamma(1-\lambda^*)BC$$

is nonsingular for all $\chi \in \mathbb{R}^n$ and all $\gamma \in [0, \bar{\gamma})$ with the Jacobian matrix $J(\chi) = \frac{\partial f}{\partial x_i}(\chi)$. Then the network equilibrium solution $x_0 = 1_N \otimes x_{10}$ is the unique equilibrium solution of (4.6) for $\gamma \in [0, \bar{\gamma})$.

Using the conditions presented in Lemmas 4.2 and 4.3, one can easily determine a range of coupling strengths $\gamma \in [\gamma_{min}, \bar{\gamma})$ for which there exists delay values such that oscillations are present.

4.2.3 Critical values of time delay

In this section we discuss two types of Hopf bifurcations which cause the instability of the network equilibria and may lead to pattern formation in oscillatory networks and show how to to compute critical time-delays. It will be shown how to detect Hopf bifurcation in such networks for the bifurcation parameter space (coupling strength γ and time delay τ). Networks (4.1)-(4.2) are described by DDEs of retarded type. We remark that for the considered class of delay systems, even though they are

infinite-dimensional, the Hopf bifurcation theorem holds, and the center manifold corresponding to a Hopf bifurcation is finite-dimensional [104]. Accordingly, when a linearized equilibrium becomes unstable, the number of unstable modes is always finite. This allows a direct extension of tools for finite-dimensional systems to detect/compute bifurcations and periodic solutions nearby [104].
The Hopf bifurcation results in the birth of a limit cycle from an equilibrium in dynamical systems. For ODEs and DDEs the Hopf bifurcation is characterized by eigenvalues crossing the imaginary axis. The bifurcation can be supercritical or subcritical, resulting in stable or unstable limit cycle, respectively. According to normal form theory (see [77] and references therein), oscillations are sinusoidal-like near the bifurcation point. It justifies using the describing function method to replace the nonlinearity by its gain approximation and then to analyze the system of nonlinear (die to nonlinear dependence of the gain on the offset and amplitudes) equations by means of the harmonic balance method.

In order to determine bifurcation points, we need to compute critical values of τ_c for γ_{min}. In our approach we fix γ first and then compute critical values of the delay parameter, values for which the linearised system has imaginary axis eigenvalues. The critical delays of a DDE can be computed by solving a nonlinear two-parameter eigenvalue problem [140]. The solution to this two-parameter problem can be translated into solving a generalized eigenvalue problem by reducing number of parameters.
This method uses a property of Kronecker summation of two matrices. In matrix algebra [141], the Kronecker sum of two square matrices $M_1 \in \mathbb{R}^{n_1 \times n_1}$ and $M_2 \in \mathbb{R}^{n_2 \times n_2}$ is represented as follows

$$M_1 \oplus M_2 = M_1 \otimes I_{n_2} + I_{n_1} \otimes M_2$$

The most crucial feature of the Kronecker summation is that the new square matrix

$$M_1 \oplus M_2 \in \mathbb{R}^{(n_1 \cdot n_2) \times (n_1 \cdot n_2)}$$

has $n_1 \cdot n_2$ eigenvalues which are pairwise combinatoric summations of the n_1 eigenvalues of M_1 and n_2 eigenvalues of M_2. So the Kronecker sum operation induces the "eigenvalue addition" property to the matrices and we take advantage of this feature.
Recall the characteristic equation (4.8). In order to compute critical delays which are required to find bifurcation points, γ is fixed at $\gamma = \gamma_{min}$, which

is computed using Lemma 4.2. One substitutes λ by $j\omega$, with $\omega \geq 0$. Define the time-delay component as follows

$$\mathscr{P} := \exp(-j\omega\tau_c). \tag{4.9}$$

Since we look for bifurcation points, the following equation is considered.

$$\det[j\omega I_{nn} - \mathscr{A} - \mathscr{B}\exp(-j\omega\tau_c)] = 0, \tag{4.10}$$

where $\mathscr{A} = I_n \otimes (J_0 - \gamma_{min}BC)$ and $\mathscr{B} = (\gamma_{min}\Gamma) \otimes (BC)$. It can be interpreted as $j\omega$ is an eigenvalue of matrix $\mathscr{A} + \mathscr{B}\mathscr{P}$ with scalar $\mathscr{P} := \exp(-j\omega\tau_c)$. The transposed matrix $\mathscr{A}^\top + \mathscr{B}^\top\bar{\mathscr{P}}$ with $\bar{\mathscr{P}} = 1/\mathscr{P}$, by analogue, has eigenvalue $-j\omega$.
Following [142], we define and solve the auxiliary characteristic equation (ACE) of the network (4.1) and (4.2), with $\mathscr{P} := \exp(-j\omega\tau_c)$

$$ACE(\mathscr{P}) := \det[(\mathscr{A} + \mathscr{B}\mathscr{P}) \oplus (\mathscr{A}^\top + \mathscr{B}^\top\bar{\mathscr{P}})] = 0, \tag{4.11}$$

and look for the eigenvalues on the unit circle. For each such eigenvalue $\mathscr{P}$, we compute the imaginary axis eigenvalues of $\mathscr{A} + \mathscr{B}\mathscr{P}$. Next, the delay values τ_c are derived from (4.9) for each pair $(\mathscr{P}, \omega)$. Note that there are infinitely many values, separated by $2\pi/\omega$. The key of this approach is that we do not need to compute roots of the characteristic equation of a delay system, only of matrices. In addition, with this approach the direction of eigenvalues can be computed.

Each pair (γ_{min}, τ_c) is a Hopf bifurcation point. Since we have a parameter space of dimension two (coupling strength γ and time delay τ), it is convenient to combine the presented above approach with the numerical computation of bifurcation curves. In order to compute bifurcations curves, it is necessary to employ a numerical bifurcation analysis tool for delay systems such as `ddebiftool` [143].

4.2.4 Problem of pattern analysis in delay-coupled systems

Networks, whose individual dynamics and coupling functions are represented by (4.1) and (4.2), respectively, exhibit oscillatory behavior with a certain pattern and this pattern is a function of the parameters γ and τ. Such oscillatory patterns are characterized by a set of parameters (oscillatory profiles): offsets α_0, amplitudes α, phases ϕ and frequency ω. It is worth mentioning, that offsets can be present, because the nonlinearity is

not assumed to be odd like in Chapter 3. These patterns, either stable or unstable, may co-exist for the same values of parameters γ and τ. Since we consider the case where oscillations appear via Hopf bifurcation, either subcritical, or supercritical, the use of an approach based on the harmonic balance method is justified. The harmonic balance method helps to avoid the direct Lyapunov method, which is cumbersome when we deal with co-existing periodic solutions. Using the harmonic balance method, it is possible to compute the oscillatory profile and approximate oscillations by

$$y(t) \cong \alpha_0 + \alpha \sin(\omega t + \phi_0 + \phi). \tag{4.12}$$

Moreover, the harmonic balance method is numerically efficient, it can be used as additional tool in terms of bifurcation analysis, and it provides good oscillatory profiles for continuation procedures. In this chapter, we consider the problem of deriving oscillatory profiles and computing approximations (4.12) of all patterns of oscillations in a given network.

4.3 Multivariable Harmonic Balance for delay coupled systems

Our goal is to study a network behavior. The harmonic balance method extended for networks is called Multivariable Harmonic Balance (MHB). We are now going to apply the MHB method to coupled systems (4.1)-(4.2). The idea of the method is to turn the problem of determining an approximate periodic solution in the form of a harmonic signal, characterized by offsets α_0, amplitudes α, phases ϕ and frequency ω, into an eigenvalue problem. By means of the Laplace transformation, the time-invariant linear part of coupled systems (4.1)-(4.2) is rewritten into the transfer function representation, leading to the following description of the closed loop system:

$$\begin{aligned} y &= W(s) I_N u, \\ u &= M(\Delta_\tau) y + v, \\ v &= \Psi(y), \end{aligned} \tag{4.13}$$

where y, u and v are of dimension $N \times 1$, $I_N \in \mathbb{R}^{N\times N}$ is an identity matrix, $W(s) = C(sI - A)^{-1}B$, $M(\Delta_\tau) = \gamma\Delta_\tau\Gamma - \gamma I_N$ represents the coupling structure, Δ_τ is the delay operator ($\Delta_\tau f(t) = f(t-\tau)$) and $\Psi(y) \in \mathbb{R}^N$ is a column vector of nonlinearities. We remark that s stands for the differentiation

operator.
Recall (4.13) and rewrite the coupled system's input u as

$$u = M(\Delta_\tau)W(s)I_N u + v, \tag{4.14}$$

$$W(s)\left[\frac{1}{W(s)}I_N - M(\Delta_\tau)\right]u = v. \tag{4.15}$$

Defining $R(s,\Delta_\tau) = \left[\frac{1}{W(s)}I_N - M(\Delta_\tau)\right]^{-1}$, the input u takes the form

$$u = \frac{1}{W(s)}R(s,\Delta_\tau)v. \tag{4.16}$$

Substituting (4.16) in (4.13), we obtain

$$y - R(s,\Delta_\tau)\Psi(y) = 0. \tag{4.17}$$

Premultiplying (4.17) by $R(s,\Delta_\tau)^{-1}$, we derive

$$\left[\frac{1}{W(s)}I_N - M(\Delta_\tau)\right]y - \Psi(y) = 0. \tag{4.18}$$

The nonlinearities $\Psi(y)$ are approximated by their describing functions, whose components can be computed using (2.18). The network output signal y is approximated by a sum of the offsets and signal's first harmonic

$$y \cong q_0 + q_1,\ q_0 = \alpha_0 = \text{const},\ q_1 = \alpha\sin(\omega t + \phi_0 + \phi), \tag{4.19}$$

where $\alpha_0 = [\alpha_{01}, \alpha_{02}, ..., \alpha_{0N}]^\top$, $\alpha = [\alpha_1, \alpha_2, ..., \alpha_N]^\top$, and $\phi = [\phi_1, \phi_2, ..., \phi_N]^\top$. The objective is to determine an oscillatory profile consisting of the following parameters: α_0 is a constant offset vector, α is a vector of amplitudes, ϕ is a vector of phases and ω stands for the frequency of oscillations.
Using (4.18) and recalling the Fourier expansion and substituting s by $kj\omega$, Δ_τ by $\exp(-kj\omega\tau)$, and $\Psi(y) \approx K_0(\alpha_0,\alpha_1) + K_1(\alpha_0,\alpha_i)y$, we obtain

$$\begin{aligned}[\frac{1}{W(kj\omega)}I_N - M(\exp(-kj\omega\tau))& \\ - \text{diag}[K_k(\alpha_{0i},\alpha_i), ..., K_k(\alpha_{0N},\alpha_N)]]q_k = 0,&\end{aligned} \tag{4.20}$$

where $K_k(\cdot)$ is a describing function for $k = 0, 1$.
We now have two Multivariable Harmonic Balance equations for the networks with delay coupling from (4.20) for $k = 0, 1$, respectively. These can be expressed as

$$J_0(\alpha_0, \alpha)q_0 := [\frac{1}{W(0)} I_N - M(1) - \text{diag}[K_0(\alpha_{0i}, \alpha_i), ..., K_0(\alpha_{0N}, \alpha_N)]]q_0 = 0, \quad (4.21)$$

and

$$J_1(\alpha_0, \alpha, \omega)q_1 := [\frac{1}{W(j\omega)} I_N - M(\exp(-j\omega\tau)) - \text{diag}[K_1(\alpha_{0i}, \alpha_i), ..., K_1(\alpha_{0N}, \alpha_N)]]q_1 = 0. \quad (4.22)$$

All parameters of the oscillatory profile are encoded in the relations (4.21) and (4.22). These equations are nonlinear due to the describing functions (2.18). In order to solve the equations above, we consider two cases: a special case called equal amplitude case, which is semi-analytical, exploits the structure of the network, but can be applied only to networks exhibiting oscillations with equal amplitudes, and a general amplitude case.

4.3.1 Equal amplitude case

In this section we introduce the special case of the MHB method for delay-coupled systems where all amplitudes and offset components are the same. We consider the case where networks exhibit special patterns with $\alpha_{0i} = \alpha_{0e},\ \alpha_i = \alpha_e \forall i$. Such patterns often occur in regular network. Networks, whose structure is represented by symmetric unweighed graph, are referred to as regular if each node has exactly the same number of links [124]. Regularity is not a necessary condition for existence of equal amplitudes but favours the occurrence of stable oscillations with equal amplitudes.

Since we seek for $\alpha_{0i} = \alpha_{0e},\ \alpha_i = \alpha_e \forall i$, the pattern analysis can be substantially simplified by exploiting the structural properties of the network. Recall equations (4.21) and (4.22) and modify the describing function matrices $K_0(\alpha_0, \alpha) = k_0(\alpha_{0e}, \alpha_e)I_N$ and $K_1(\alpha_0, \alpha) = k_1(\alpha_{0e}, \alpha_e)I_N$ according to new conditions $\alpha_{0i} = \alpha_{0e},\ \alpha_i = \alpha_e \forall i$. With these new the describing function matrices (4.21) and (4.22) are reduced to

$$\left[\frac{1 - k_0(\alpha_{0e}, \alpha_e)W(0) + \gamma W(0)}{W(0)} I_N - \gamma \exp(0)\Gamma\right] q_0 = 0, \quad q_0 = \alpha_{0e} \quad (4.23)$$

and

$$\left[\frac{1-k_1(\alpha_{0e},\alpha_e)W(j\omega)+\gamma W(j\omega)}{W(j\omega)}I_N-\gamma\exp(-j\omega\tau)\Gamma\right]q_1=0,\quad q_1=|\alpha_e|e^{j\phi_i}. \tag{4.24}$$

Solutions $q_0=0$ and $q_1=0$ to (4.21) and (4.22) correspond to zero offset and equilibrium, respectively, and are not the point of interest. Therefore, we solve

$$\det\left[\frac{1-k_0(\alpha_{0e},\alpha_e)W(0)+\gamma W(0)}{W(0)}I_N-\gamma\exp(0)\Gamma\right]=0, \tag{4.25}$$

$$\det\left[\frac{1-k_1(\alpha_{0e},\alpha_e)W(j\omega)+\gamma W(j\omega)}{W(j\omega)}I_N-\gamma\exp(-j\omega\tau)\Gamma\right]=0. \tag{4.26}$$

We diagonalize the coupling matrix Γ and use the property of the determinant product in order to arrive at

$$\frac{1-k_0(\alpha_{0e},\alpha_e)W(0)+\gamma W(0)}{W(0)}-\gamma\lambda_{\Gamma i}=0, \tag{4.27}$$

$$\frac{1-k_1(\alpha_{0e},\alpha_e)W(j\omega)+\gamma W(j\omega)}{W(j\omega)}-\gamma\exp(-j\omega\tau)\lambda_{\Gamma i}=0, \tag{4.28}$$

where $\lambda_{\Gamma i}$ is an eigenvalue of matrix Γ.
Unlike the delay-free case, presented in Chapter 3, where we took a look only at maximal eigenvalue of Γ, here equations (4.27)-(4.28) must be solved for all eigenvalues of the coupling matrix. Due to two bifurcation parameters γ and τ, several eigenvalues can have positive real part and be responsible for different oscillatory patterns. Since $k_0(\alpha_{0e},\alpha_e)$ and $k_1(\alpha_{0e},\alpha_e)$ are real valued, solutions to (4.27)-(4.28) exists only for eigenvalues of Γ which satisfy oscillatory conditions of the given network. According to this the value of $k_0(\alpha_{0e},\alpha_e)$ can be computed as follows

$$k_0(\alpha_{0e},\alpha_e)=\frac{1-\gamma\lambda_{\Gamma i}W(0)+\gamma W(0)}{W(0)}. \tag{4.29}$$

One can easily see that this condition corresponds to offset components and the solution has to be computed only for $\lambda_{\Gamma i}\in\mathbb{R}$.
In order to compute the value of $k_1(\alpha_{0e},\alpha_e)$, we consider equation (4.28). Substituting $W(j\omega)=C(j\omega I_n-A)^{-1}B$ in (4.28), we obtain

$$1-k_1(\alpha_{0e},\alpha_e)C(j\omega I_n-A)^{-1}B+\gamma C(j\omega I_n-A)^{-1}B-\gamma\exp(-j\omega\tau)\lambda_{\Gamma i}C(j\omega I_n-A)^{-1}B=0,$$

$$1 + (j\omega I_n - A)^{-1} B[\gamma C + k_1(\alpha_{0e}, \alpha_e) C - \gamma \exp(-j\omega\tau)\lambda_{\Gamma i} C] = 0.$$

Since the isolated system (4.1) is exponentially stable $\det(j\omega I_n - A) \neq 0 \ \forall \omega > 0$, we arrive at

$$(j\omega I_n - A)[1 + (j\omega I_n - A)^{-1} B[\gamma C + k_1(\alpha_{0e}, \alpha_e) C - \gamma \exp(-j\omega\tau)\lambda_{\Gamma i} C]] = 0. \tag{4.30}$$

Using Schur's lemma [125], we obtain

$$\det[j\omega I_n - A + B(\gamma C + k_1(\alpha_{0e}, \alpha_e) C - \gamma \exp(-j\omega\tau)\lambda_{\Gamma i} C)] = 0. \tag{4.31}$$

Parameters γ, τ are fixed and frequency ω is known from the magnitude of the imaginary part of an unstable eigenvalue computed using the characteristic equation of the network. Thus equation (4.31) has one unknown $k_1(\alpha_{0e}, \alpha_e) \in \mathbb{R}$, which is computed for each eigenvalue $\lambda_{\Gamma i}$ of matrix Γ. If an oscillatory pattern exists for given $\lambda_{\Gamma i}$, $k_1(\alpha_{0e}, \alpha_e) \in \mathbb{R}$ can be computed. In other words, matrix $A - B(\gamma C + k_1(\alpha_{0e}, \alpha_e) C - \gamma \exp(-j\omega\tau)\lambda_{\Gamma i} C)$ has a pair of pure imaginary eigenvalues for $\pm j\omega$, where ω stands for oscillation frequency and all other eigenvalues are in the open left-half plane

$$\mathrm{Re}(\lambda_{1,2}(A - B(\gamma C + k_1(\alpha_{0e}, \alpha_e) C - \gamma \exp(-j\omega\tau)\lambda_{\Gamma i} C))) = 0, \tag{4.32}$$

where $\lambda_{1,2}$ is a pair of pure imaginary eigenvalues of the given matrix.
One can say that $k_1(\alpha_{0e}, \alpha_e)$ can be derived from the condition when the matrix is marginally stable. It is necessary to perform this procedure for all eigenvalues $\lambda_{\Gamma i}$. If there exists an oscillatory pattern, the marginal stability condition will be satisfied for selected $\lambda_{\Gamma i}$. Then, using the describing functions (2.18), the components α_{0e} and α_e can be computed. Note that describing functions (2.18) are coupled and it is necessary to solve the system of equations simultaneously. The phases ϕ_i are encoded in the eigenvector corresponding to the eigenvalue $\lambda_{\Gamma i}$ for which the solution is found.
Substituting $(1 - k_1(\alpha_{0e}, \alpha_e) W(j\omega) + \gamma W(j\omega))/W(j\omega) = \lambda_{\Gamma i}$ in (4.24), we arrive at

$$[\lambda_{\Gamma i} I_N - \gamma \exp(-j\omega\tau)\Gamma] q_1 = 0. \tag{4.33}$$

Since we seek for equal amplitudes, it is required that vector q_1 has the entries which are represented as $q_{1i} = \alpha_i \exp(j\phi_i)$ such that all components of q_{1i} share the same modulus α_e. The phases are computed using the following equation

$$\phi_i = \arg(q_{1i}). \tag{4.34}$$

All components of the oscillatory profile are computed and an approximation of the oscillations can be constructed using (4.19).
This special case of the MHB method is a useful tool due to several reasons: firstly, the method is analytical and gives solutions without employing numerical methods; secondly, the equal amplitude case is scalable in the sense that it exploits the structural properties of the network and greatly decreases the number of equations to solve; and the method can be used to verify results of the general MHB method which involves the numerical methods.

4.3.2 General amplitude case

In order to obtain the oscillatory profile with arbitrary amplitudes, we have to equip numerical methods. To determine components (offset α_0, amplitudes α, phases ϕ and frequency ω) of the oscillatory profile, we formulate an optimization problem. Solution $q_0 = 0$ and $q_1 = 0$ to (4.21) and (4.22) correspond to zero offset and equilibrium, respectively, and are not considered in this chapter. Thus we look for a set of phases ϕ_i, amplitudes α_i, offset components α_{0i} and frequency ω, which solve nonlinear equations (4.21) and (4.22). We define the objective function to minimize as

$$F(g) := Q_0^* Q_0 + Q_1^* Q_1 + p^\top p, \tag{4.35}$$

where

$$g := [\phi; \alpha; \alpha_0; \omega] \in \mathbb{R}^{3N+1}, \qquad p := \alpha - |q_1| \in \mathbb{R}^N,$$
$$Q_0 := J_0(\alpha_0, \alpha) q_0 \in \mathbb{C}^N, \qquad Q_1 := J_1(\alpha_0, \alpha, \omega) q_1 \in \mathbb{C}^N,$$

where $|q_1| = [|q_{11}|, |q_{12}|, ..., |q_{1N}|]^\top$.
Vector g consists of phases, amplitudes, offset components and frequency, the component p represents the second equation of (4.19). To simplify the problem, the phase of the first node is fixed at $\phi_1 = 0$ without loss of generality, and boundaries are chosen as: $\phi_i \in [0, 2\pi] \ \ \forall i \neq 1$, $\alpha_i \in [0, \beta_1] \ \ \forall i$, $\alpha_{0i} \in [-\beta_2, \beta_2] \ \ \forall i$, $\omega \in [0, 2\omega_{bif}]$, where β_1 and β_2 are user defined numbers that bound the region of interest in the search space.
It is worth mentioning, that the relative phases in ring networks can be extracted from the symmetry argument [144] [145]. An advantage of the MHB approach is that it is not limited only to the networks with a ring structure and aiming at computing the whole oscillatory profile (i.e.

the offset, amplitudes, phases and frequency) in one shot. Another large advantage of the Multivariable Harmonic balance method is the small number of parameters of the harmonic approximation looked for (at the price of a possible over-approximation of the solution's profile). This makes the method particularly suitable for the efficient detection of coexisting patters, given the reduced small space.
Solutions to nonlinear equations (4.21) and (4.22) are found by minimizing the squared residual norm of the objective function (4.35). The local solver `fmincon` included in `MATLAB` is used. The solver uses the *interior-point* algorithm [127] in order to find a minimum of a constrained nonlinear multivariable function satisfying the imposed constraints. Since equations (4.21) and (4.22) are nonlinear and multiple solutions exist, these solutions depend on the initial conditions. Multiple values of the initial conditions are generated by the `MultiStart` algorithm within the defined region of interest [128].
A big advantage of the `MultiStart` method is that starting points for the minimization procedure are not needed to be specified. A set of random points choosing from the feasible region, is used as initial conditions. The key point in the procedure is to choose the correct boundaries for the starting points and the unknown variables. Moreover, the approach can deal with co-existed periodic solution. Stable and unstable solutions can be simultaneously found. Having a set of parameters g, oscillatory profiles can be reconstructed using (4.19).

4.4 Numerical examples

In this section, it is shown how the Multivariable Harmonic Balance method is applicable to networks consisting of dynamical systems of Lur'e form interacting via linear time delay coupling functions. We present two different networks in terms of individual system dynamics, which illustrate the onset of instability of the network equilibrium via a supercritical and a subcritical Hopf bifurcation, respectively. Illustrative examples are given with the same network structure which is a directed ring [Fig.4.2] in order to show different possibilities of the MHB approach. We present both semi-analytical and numerical results. Semi-analytical results in these chapter, are used to verify the results of an optimization routine. Note that the MHB method can be easily applied for different networks in terms of structure.

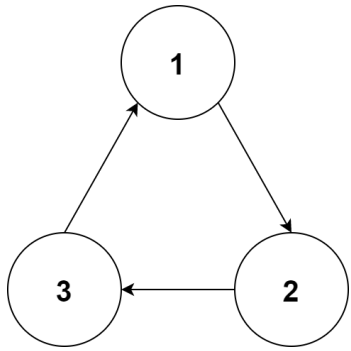


Figure 4.2: Network structure for numerical examples.

The graph topology is described by the following adjacency matrix,

$$\Gamma = \begin{bmatrix} 0 & 1 & 0 \\ 0 & 0 & 1 \\ 1 & 0 & 0 \end{bmatrix}. \tag{4.36}$$

The software package with demo examples, which are presented below, can be downloaded by the following link `https://github.com/RogovKO/DMHB.git`.

4.4.1 Network with a supercritical Hopf bifurcation

In this section, we present the example of coupled nonlinear systems of Lur'e type that we studied in [92] with delay-free coupling. In this chapter, the coupling has a time-delay component and is given by (4.2). The goal is to show that the MHB method for delayed systems gives a very accurate approximation when oscillations emerge as a result of a supercritical Hopf bifurcation. The individual dynamics of the nodes, as in [75], are given by

$$\begin{aligned} \dot{x}_i &= Ax_i + Bu_i, \\ u_i &= u_{ci} - \psi(z_i), \\ z_i &= Zx_i, \\ y_i &= Cx_i, \end{aligned} \tag{4.37}$$

with

$$A = \begin{pmatrix} 1 & -1 & 1 \\ 1 & 0 & 0 \\ -4 & 2 & -3 \end{pmatrix},$$

$$B = \begin{pmatrix} 0 & 0 & 1 \end{pmatrix}^\top,\ C = \begin{pmatrix} 0 & 0 & 1 \end{pmatrix},\ Z = B^\top P,$$

where P is the solution to the Lyapunov equation

$$A^\top P + PA = -I_3.$$

The nonlinear function $\psi(\cdot)$ is given as follows

$$\psi(z_i) = z_i^3;$$

and computing the describing functions using (2.18), we obtain

$$K_0(\alpha_{0i}, \alpha_i) = \alpha_{0i} + \frac{3}{2}\alpha_i^2, \quad K_1(\alpha_{0i}, \alpha_i) = 3\alpha_{0i} + \frac{3}{4}\alpha_i^2.$$

Note that nonlinearity $\psi(z_i)$ is odd and, due to this, the offset component satisfies $\alpha_{0i} = 0$. See Chapter 3 for additional information.
For coupled systems (4.37) and (4.2), MHB equations (4.21) and (4.22) become as follows:

$$J_0(\alpha_0, \alpha) q_0 := \left[\frac{1}{W_y(0)} I_N + M(0) + \frac{W_z(0)}{W_y(0)} K_0(\alpha_0, \alpha) I_N \right] q_0 = 0, \qquad (4.38)$$

and

$$J_1(\alpha_0, \alpha, \omega) q_1 := \left[\frac{1}{W_y(j\omega)} I_N + M(j\omega) + \frac{W_z(j\omega)}{W_y(j\omega)} K_1(\alpha_0, \alpha) I_N \right] q_1 = 0, \quad (4.39)$$

with vectors

$$K_0(\alpha_0, \alpha) = [K_0(\alpha_{01}, \alpha_1), ..., K_0(\alpha_{0N}, \alpha_N)]^\top,$$
$$K_1(\alpha_0, \alpha) = [K_1(\alpha_{01}, \alpha_1), ..., K_1(\alpha_{0N}, \alpha_N)]^\top,$$

and frequency response functions $W_y(j\omega)$ and $W_z(j\omega)$ defined as

$$W_y(j\omega) = C(j\omega I_3 - A)^{-1} B,$$
$$W_z(j\omega) = Z(j\omega I_3 - A)^{-1} B.$$

With equations (4.38) and (4.39), the cost function to solve for our optimization routine can be constructed.
In order to apply semi-analytical MHB method, we omit (4.38) since $\alpha_0 = 0$ due to the odd nonlinearity and consider (4.39). Since the trivial solution $q_1 = 0$ is not discussed in this chapter, (4.39) is rewritten as

$$\det\left[\frac{1}{W_y(j\omega)} I_N + M(j\omega) + \frac{W_z(j\omega)}{W_y(j\omega)} K_1(\alpha_0, \alpha) I_N\right] = 0. \tag{4.40}$$

Now the describing function $K_1(\alpha_0, \alpha)$ has arguments $\alpha_0 = 0$ and $\alpha_i = \alpha_e \forall i$ and becomes $K_1(\alpha_e)$. According to this, we now can exploit the structure of our network and diagonalize (4.40) as follows

$$\frac{1 + W_z(j\omega)K_1(\alpha_e) - \gamma W_y(j\omega)}{W_y(j\omega)} + \gamma \exp(-j\omega\tau)\lambda_i = 0. \tag{4.41}$$

Following the procedure which is described in Section 4.3.1, the amplitude can be found from the marginal stability condition of the matrix

$$\mathrm{Re}(\lambda_{1,2}(A - B(K_1(\alpha_e)Z + \gamma C - \gamma \exp(-j\omega\tau)\lambda_i C))) = 0,$$

in a sense that the matrix has a pair of eigenvalues with real part equals to zero and the rest eigenvalues are in the open left-half plane. The phases can be computed following the procedure in Section 4.3.1.

As the first step of the MHB procedure for delay systems, the critical values of coupling strength γ and time delay τ are computed by means of Lemma 4.2 and (4.9) in order to detect a Hopf bifurcation point. It is found that $\nu = \inf_{\omega>0} \mathscr{R}(\mathscr{H}(i\omega)) = -0.771$, which is attained at $\omega = \omega^* = 0.8146$. Thus the minimal coupling strength to have characteristic roots on the imaginary axis for some $\tau > 0$, is $\gamma_{min} = 0.6481$. The critical value of time delay $\tau_c = 1.5304$ is computed by solving quadratic eigenvalue problem (4.11). The Hopf bifurcation point is detected for the parameter values $\gamma_{min} = 0.6481$ and $\tau_c = 1.5304$.
In order to verify our calculations, we compute rightmost characteristics roots of our coupled systems described by DDEs using the method described in [146]. Fig.4.3 shows that the rightmost characteristic roots are located on the imaginary axes. They correspond to a Hopf bifurcation of the nonlinear system. (Note that the bifurcation leading to instability of the network equilibrium must be a Hopf bifurcation because otherwise the condition of Lemma 4.3 would be violated.)

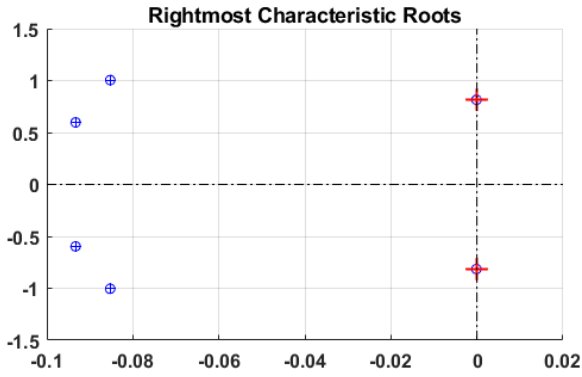


Figure 4.3: Rightmost characteristic roots computed for fixed $\gamma_{min} = 0.6481$ and $\tau_c = 1.5304$.

Now we fix the time delay parameter at $\tau = 1.5304$ and increase the coupling strength to make sure that there is a pair of eigenvalues with a positive real part. Fig.4.4 shows that there is one pair of unstable eigenvalues with the magnitude of imaginary part 0.8162 which is used in the MHB analysis to set up the search space for the frequency of oscillations. For this pair of parameters, there is one pair of eigenvalues with $\mathrm{Re}(\lambda) > 0$ while all others are confined to the open left half plane $\mathrm{Re}(\lambda) < 0$.
The oscillatory profile obtained by simulating the system of DDEs is shown in the Fig.4.5. The results are obtained by simulating DDEs using the `dde23` solver in `MATLAB` environment. The standard set of options is used and the initial data is chosen as a constant vector function defined on $[-\tau, 0]$ whose values are (uniformly distributed) random numbers. The oscillatory pattern emerges from the supercritical Hopf bifurcation and has the sinusoidal-like form close to the bifurcation point. It implies that effects of high-order harmonics is small enough to say the MHB method provides an accurate approximation of the pattern. In Table 4.1 one can see the oscillatory profiles derived from the DDE simulation and computed by the general MHB approach for delay-coupled systems and by the equal amplitude case (EAC) approach.
In order to measure the accuracy of two MHB approaches we provide the value of objective function (4.35) in the computed minimum (if any), and compare the offset components, amplitudes and frequency with the ones

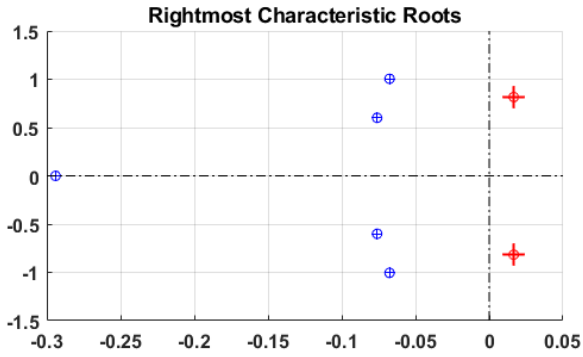


Figure 4.4: Rightmost characteristic roots computed for fixed $\gamma = 0.7129$ and $\tau_c = 1.5304$.

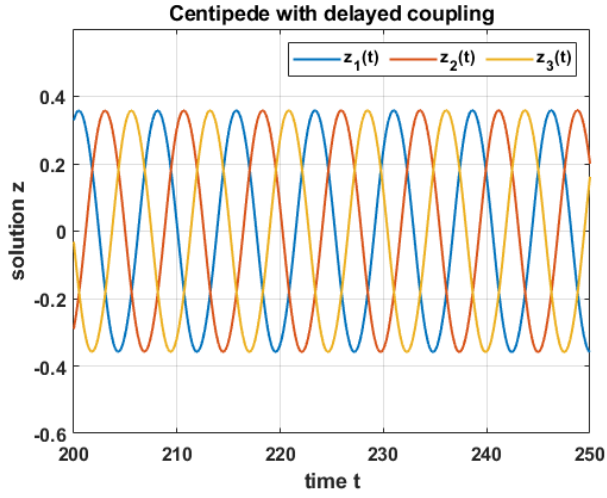


Figure 4.5: Network behavior obtained by simulating DDEs.

that are extracted from the DDE simulation as follows,

$$\Delta\alpha_0 = 100||\alpha_0 - \alpha_{0s}||/||\alpha_{0s}||;$$
$$\Delta\alpha = 100||\alpha - \alpha_s||/||\alpha_s||;$$
$$\Delta\omega = 100(\omega - \omega_s)/\omega_s,$$

Method	ω	α_0	α_e	ϕ_1	ϕ_2	ϕ_3
DDE Sim	0.8239	0	0.3992	0	240	120
MHB	0.8242	0	0.3624	0	240	120
MHB(EAC)	0.8162	0	0.3249	0	240	120

Table 4.1: Oscillatory profiles of the network extracted from the DDE simulation, computed by the general MHB method and by the EAC MHB method.

where α_{0s}, α_s and ω_s are obtained from the numerical simulation.

Method	Residual	$\Delta\omega$ in %	$\Delta\alpha_0$ in %	$\Delta\alpha$ in %
MHB	2.87e-8	0.02	0	0.94
MHB(EAC)	NaN	0.93	0	9.53

Table 4.2: Comparison of the DDE simulation, and the general MHB method and special case of the MHB method outputs.

This result shows that the numerical MHB approach for delay-coupled Lur'e systems accurately predicts oscillatory patterns in the neighbourhood of a Hopf bifurcation point. Inaccuracy of the EAC MHB comparing to the MHB can be explained by the fact frequency ω is not derived from equation (4.31), but is taken as a magnitude of the imaginary part of unstable root, which is computed using characteristic equation (4.8). Despite this inaccuracy, the EAC MHB method is much faster for large networks, which will be shown in Table 4.3.

In order to show that the MHB approaches for delay-coupled Lur'e systems are numerically efficient, we perform the pattern analysis of 3 nodes, 10 nodes, 20 nodes and 50 nodes networks (the structure is given in Fig. 4.6) with node's individual dynamics (4.37) and coupling (4.2). Bifurcation parameter values are chosen as $\gamma = 0.7129$ and $\tau = 1.5304$ for all networks. The results are presented in Table 4.3. The direct simulation results depends on initial conditions and contain only one pattern. Since there are co-existing patterns, it is nontrivial to find the initial conditions for each mode. The numerical MHB approach deals with multistability. In our

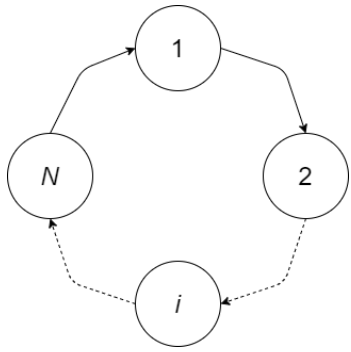


Figure 4.6: Ring network structure with N nodes.

example, we have 10 starting points distributed in the region of interest and this allows to simultaneously compute co-existent patterns (even if some of these patterns are unstable) in the network for selected parameters. Note that the search space is low dimensional, which crucially decreases computational time and MHB computational time in Table 4.3 is given for all starting points together.

Size of the ring	3	10	20	50
MHB (EAC), [sec]	1.72	7.91	8.734	14.02
MHB, [sec]	2.14	10.07	35.07	629.5
dde23, [sec]	2.45	35.29	355.7	4455
$\Delta\omega$ in %	0.02	0.02	0.04	0.89
$\Delta\alpha$ in %	0.94	8.47	14.35	20.82
Multistability	No	Yes	Yes	Yes

Table 4.3: Computational time of EA MHB, MHB and dde23 and comparison of the numerical MHB approach and the direct simulation.

Data in Table 4.3 shows that the MHB approaches (especially EAC MHB) is more numerically efficient than the direct simulation by `dde23` solver when we need to analyse the behavior of complex networks with many agents. The accuracy is computed only for a pair of the methods: the MHB and `dde23`. The value of $\Delta\alpha$ increases as we take larger network. It can be

explained by the fact that amplitudes becomes smaller when the amount of nodes increases. It is necessary to say that frequency and phases are accurately computed for all patterns.

4.4.2 Network with a subcritical Hopf bifurcation

In this section, we consider a collection of three inert FitzHugh-Nagumo (FHN) model neurons interconnected by a linear time-delay coupling functions [147]. The network structure is depicted in Fig. 4.2 and the adjacency matrix is given by (5.3). The bifurcation analysis is performed using the `ddebiftool` software package and shows that relaxation oscillations, observed in simulations, are emerged from a subcritical Hopf bifurcation. The MHB analysis is used to show that both stable and unstable oscillatory patterns exist for the same set of parameters and can be simultaneously computed by our approach. The EAC MHB is used to verify the results of the numerical MHB. The EAC MHB is limited only to stable solutions, so the verification is performed only for the stable solution.
The dynamics of this model neuron are given by the following equations:

$$\begin{aligned} \dot{x}_{i1} &= 0.08(x_{i2} - 0.8x_{i1}), \\ \dot{x}_{i2} &= x_{i2} - (x_{i2})^3/3 - x_{i1} - 0.559 + u_i, \\ y_i &= x_{i2}. \end{aligned} \tag{4.42}$$

One can easily verify that the FHN model has a locally exponentially stable equilibrium at $\bar{x}_i = (-1.225 - 0.980)^\top$. Moreover, the FHN model neuron is strictly C^∞-semipassive with a quadratic storage function, see [148]. Hence, the solutions of any network consisting of FHN neurons are uniformly bounded for any nonnegative γ and τ.
In order to simplify the MHB analysis of the network of FHN neurons, we perform a change of coordinates. For that, we define new variables $z_{i1} = x_{i1} - \bar{x}_{i1}$ and $z_{i2} = x_{i2} - \bar{x}_{i2}$. The system (4.42) is equivalent to the system:

$$\begin{aligned} \dot{z}_{i1} &= -0.064z_{i1} + 0.08z_{i2}, \\ \dot{z}_{i2} &= -z_{i1} + (1 - \bar{x}_{i2}^2)z_{i2} - (z_{i2}^3 + 3\bar{x}_{i2}z_{i2}^2)/3 + u_i, \\ y_i &= z_{i2}. \end{aligned} \tag{4.43}$$

It is easy to see that this system has an equilibrium at the origin and is of form (4.1) with

$$A = \begin{bmatrix} -0.064 & 0.08 \\ -1 & 0.0391 \end{bmatrix}, \qquad B = \begin{bmatrix} 0 & 1 \end{bmatrix}^\top, \qquad C = \begin{bmatrix} 0 & 1 \end{bmatrix},$$
$$\psi(y_i) = -y_i^3/3 + 0.98 y_i^2,$$

and $i = 1,2,3$. The network topology is defined by (5.3).
The nonlinear function $\psi(y_i)$ is not odd, which leads to a nonzero offset component of signal y_i. This implies that $y_0 \neq 0$ and both equations (4.21) and (4.22) have to be solved.
The describing functions for nonlinearity $\psi(y_i)$ are given as

$$K_{0i}(\alpha_{0i}, \alpha_i) = 0.98\alpha_{0i} - 0.5\alpha_i^2 - 0.33\alpha_{0i}^2 + 49\alpha_i^2/(100\alpha_{0i}),$$
$$K_{1i}(\alpha_{0i}, \alpha_i) = -0.25\alpha_i^2 - \alpha_{0i}^2 + 1.96\alpha_{0i}.$$

In order to determine the bifurcation point, we recall the condition from Lemma 4.2. It is found that $\nu = \inf_{\omega>0} \mathbb{R}(\mathscr{H}(i\omega)) = -0.197$, which is attained at $\omega = \omega^* = 0.4202$. Thus the minimal coupling strength to have characteristic roots on the imaginary axis for some $\tau > 0$, is $\gamma_{min} = 2.5376$. The critical value of time delay $\tau_c = 4.7643$ is computed by solving generalized eigenvalue problem (4.11). We verify the calculations by computing rightmost characteristic roots by means of the method described in [146]. Fig. 4.7 shows that a couple of characteristic roots is located on the imaginary axis, which corresponds to the Hopf Bifurcation.
The basic MHB analysis of the given network was performed in [93]. It was found that the simulation output consists of oscillations of the relaxation type. According to normal form theory [77], oscillations in the neighbourhood of the Hopf bifurcation must be sinusoidal like with zero offset. One may think that the Hopf bifurcation of the subcritical type occurs in the example under consideration. In order to verify this, a bifurcation analysis of the FHN neuron network is performed by means of the software package `ddebiftool`[143].
As a first step we compute Hopf bifurcation curves in the parameter space (γ, τ) which are shown in Fig. 4.8.
These curves computed for the (τ, γ) bifurcation parameter space for network (4.43),(4.2). The gray area stands for the region in which the network equilibrium is stable. When a bifurcation curve is crossed, the Hopf bifurcation occurs and the network equilibrium loses stability. The red dot represents a previously computed pair of parameters (τ_c, γ_{min})

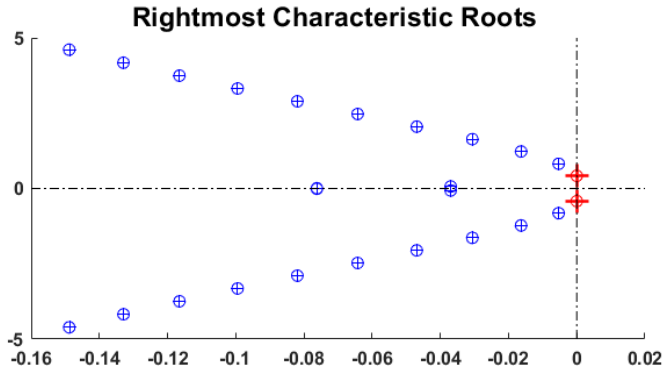


Figure 4.7: Rightmost characteristic roots computed for fixed $\gamma_{min} = 2.5376$ and $\tau_c = 4.7643$.

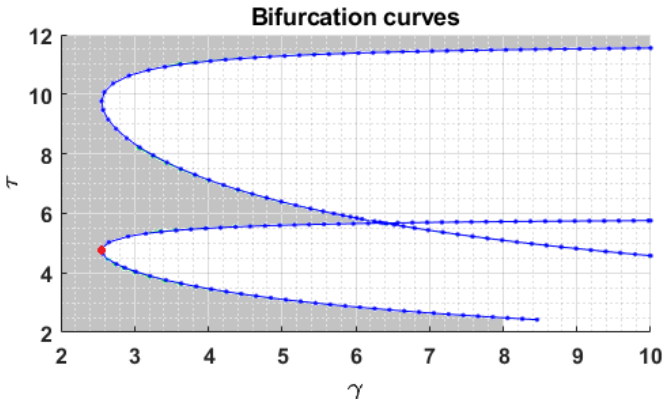


Figure 4.8: Bifurcation curves in (τ, γ) parameter space.

and lies on a bifurcation curve, which is also verifies our computations of γ_{min} and τ_c.
The second step of our analysis is the continuation procedure. We start from bifurcation point ($\tau = 4.4063$, $\gamma = 2.6733$), compute the first point of a branch of periodic solutions, and then we fix bifurcation parameter τ and change parameter γ with an adaptive step in order to compute the

next point of the branch. The computed branch of periodic solutions is shown in Fig.4.9. Each dot (320 in total) on this plot is a periodic solution computed by means of `ddebiftool`. The branch is represented in the (γ, amplitude) space. The blue line and dots stand for the unstable periodic solutions that emerges from the subcritical Hopf bifurcation. The brushed green line and dots stand for the stable periodic solutions. This confirms that the hypothesis, made in [93] about the subcritical type of the Hopf bifurcation.
In order to show that the MHB for delay-coupled systems deals with coexisting patterns, we choose two periodic solutions (red dots in Fig.4.9). These solutions coexist for the same set of parameters ($\tau = 4.4063$, $\gamma = 2.383$). Oscillatory profiles, obtained by bifurcation analysis software, are shown in Fig.4.10. One can see that the unstable periodic solution, located in a neighbourhood of the bifurcation point, has a sinusoidal-like shape. The stable periodic solution that co-exists with the unstable one for the same pair of parameters, is represented by relaxation oscillations. We employ the MHB method to simultaneously compute the oscillatory profiles of these two regimes. The oscillatory patterns are given in Table 4.4.

Periodic solution	ω	α_0	α_e	ϕ_1	ϕ_2	ϕ_3
Unstable	0.4491	0.0011	0.0529	0	120	240
Stable	0.4491	0.7063	1.8803	0	120	240

Table 4.4: Stable and unstable co-existing oscillatory patterns which are computed by the MHB method.

Using data from Table 4.4 and (4.19), the oscillations can be reconstructed. The MHB approach gives good approximation of the harmonic-like oscillation which are in the neighbourhood of the bifurcation point.

Periodic solution	Residual	$\Delta\omega$ in %	$\Delta\alpha_0$ in %	$\Delta\alpha$ in %
Unstable	3.67e-10	1.60	1.85	2.02
Stable	2.94e-13	2.25	26.04	4.95

Table 4.5: Comparison of the DDE simulation and the MHB method outputs.

It is clear that the accuracy of the MHB approach cannot be good when it is applied for oscillations of relaxation type (See Table 4.5), but it gives an accurate prediction in terms of phases of the oscillations and good starting points for tools to accurately compute periodic solutions such as collocation based approaches. The MHB method for delay coupled systems deals with co-existing patterns even if some of them are unstable. In addition one may say that since oscillatory profiles presented in Table 4.4 share the phases and the frequency and belong to one branch of periodic solutions (Fig. 4.9), the MHB approach can be used for basic bifurcation analysis. This branch of periodic solutions arises from the subcritical Hopf bifurcation point and connects two oscillatory patterns, presented in Fig. 4.10 and Table 4.4.

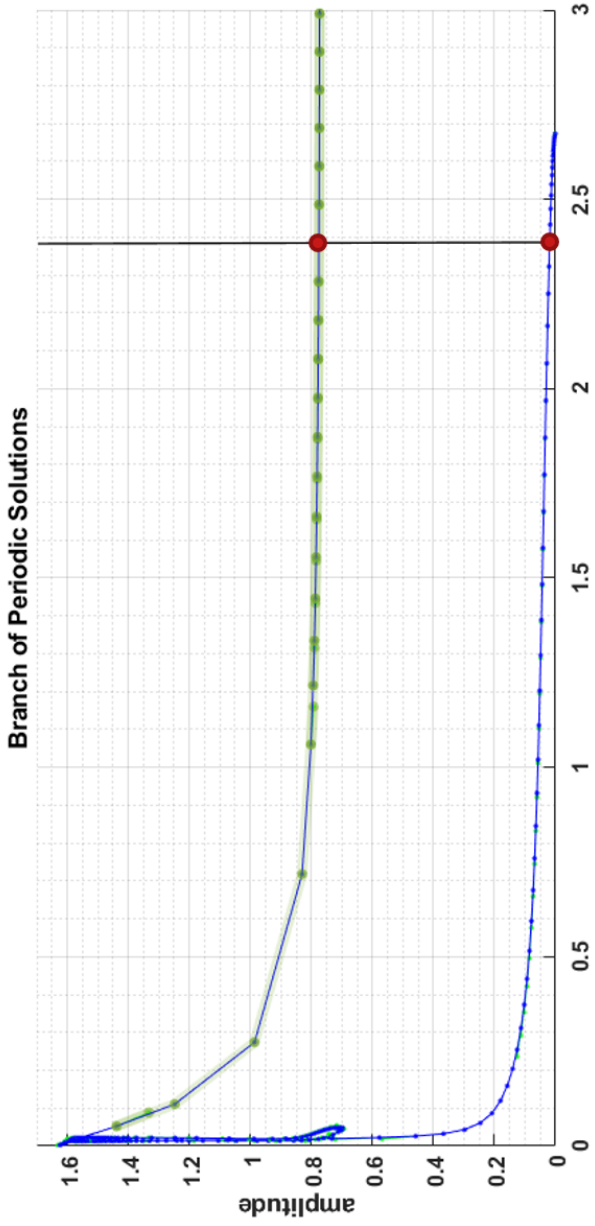


Figure 4.9: Branch of periodic solutions that emerges from the subcritical Hopf bifurcation.

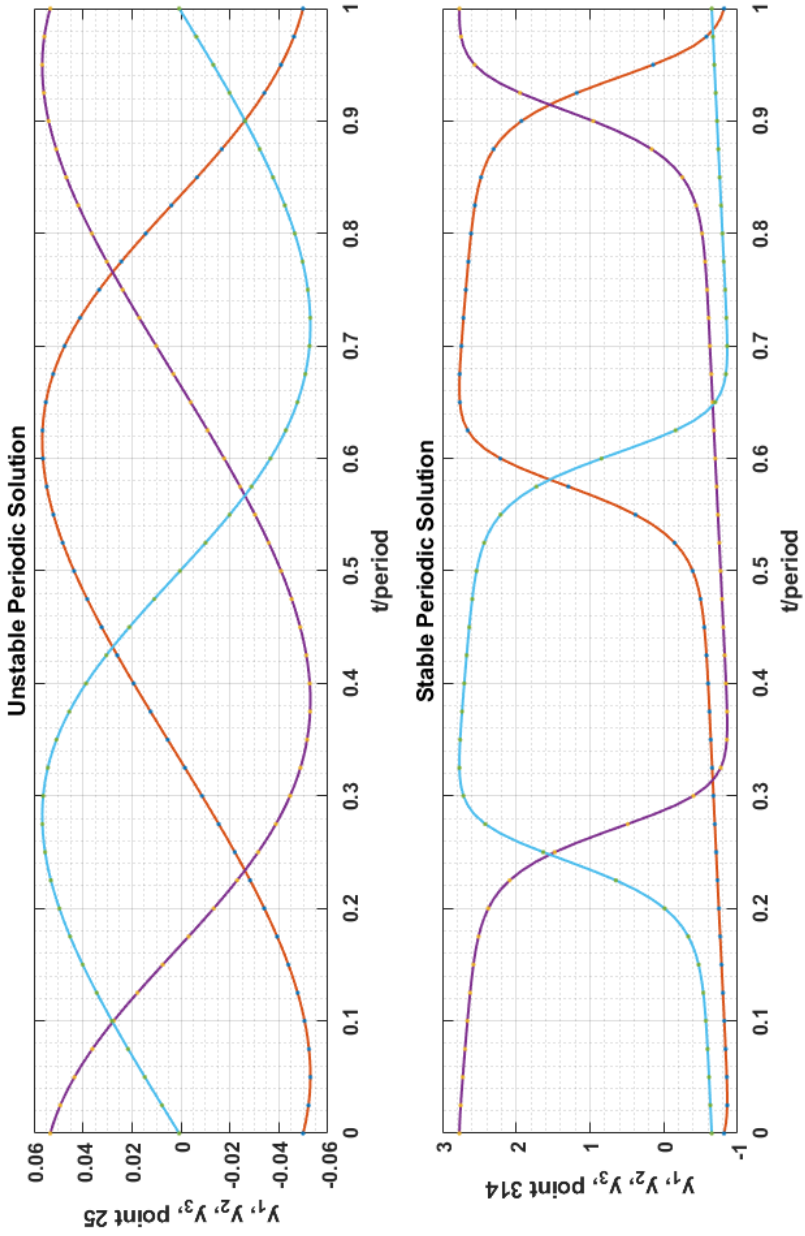


Figure 4.10: Oscillatory profiles of the periodic solutions represented by red dots in Fig. 4.9.

In order to verify the computations of stable oscillations which are accomplished by the numerical MHB approach, we use the semi-analytical EAC MHB. We perform the analysis and compare the accuracy with the results of the direct simulations which are performed by `dde23`. The results and the accuracy of the EAC MHB analysis, comparing with direct simulations, are presented in the table below.

ω	α_0	α_e	ϕ_1	ϕ_2	ϕ_3
0.42	0.7073	1.8843	0	120	240

Table 4.6: Stable oscillatory patterns computed by the EAC MHB method.

$\Delta\omega$ in %	$\Delta\alpha_0$ in %	$\Delta\alpha$ in %
0.84	25.81	4.51

Table 4.7: Comparison of the DDE simulation and the EAC MHB method outputs.

We can see that the MHB method for equal amplitudes computes a very similar pattern as the general MHB approach. For our particular example the results of the EAC MHB are more accurate than results computed by the numerical MHB method.

4.5 Concluding remarks

This chapter addresses the problem of detecting (coexisitng) oscillatory patterns in networks of delay-coupled nonlinear systems of Lur'e form. We focused on cases where oscillatory patterns appear in the networks via both subcritical and supercritical Hopf bifurcations. We developed fast and efficient numerical tools which help to avoid time inefficient simulations of DDEs and can handle co-existing periodic solutions. The Multivariable Harmonic Balance method was modified and extended for

systems described by DDEs, and applied to two examples with subcritical and supercritical Hopf bifurcations in order to show that the method can successfully compute a good approximation of periodic solutions which appear in such networks, even if the periodic solution does not occur in the neighbourhood of the bifurcation point. In addition, a special case (namely equal amplitude case) of the MHB analysis was presented. The EAC MHB is semi-analytical and exploits the structure of the networks, which helps crucially decrease the number of equations to solve. This semi-analytical method was used as a verification tool for our numerical procedures. We showed that the methods are numerically efficient, especially the EAC MHB, in comparison with the direct simulation approach. Moreover, the MHB method for delay coupled systems can simultaneously compute co-existing periodic solutions even if some of them are unstable and perform basic bifurcation analysis. In addition, we performed a bifurcation analysis of the delay coupled systems with the subcritical Hopf bifurcation by means of `ddebiftool`, using MHB results as starting points.

Chapter 5

Delay Induced Full Synchronization: A case-study

5.1 Introduction

Synchronization is an important phenomenon in delay-coupled nonlinear dynamical systems, which is motivated by different applications in engineering and science. Complex networks formed by identical nonlinear systems show rich dynamical behavior and may exhibit different oscillatory patterns, such as synchronization, partial synchronization or so-called rotating waves. It is worth noting, that for some interaction parameters (i.e. coupling strengths γ and/or time-delays τ), the network dynamics can be multistable and different oscillatory patterns may locally coexist. The analysis of such complex behavior requires a combination of tools in order to obtain complete insight in network behavior depending on the values of parameters. In this chapter, a case study is presented in which a numerical bifurcation analysis is performed to determine the dynamics of a delay-coupled nonlinear system in the vicinity of its equilibrium points as function of the interaction parameters. The analysis is then complemented with the MHB-based pattern analysis, which can detect co-existing oscillations, including those that are not a result from a bifurcation of an equilibrium point.

A directed ring network consisting of delay-coupled identical Lur'e systems, is the subject of study in this chapter. The considered Lur'e systems are globally asymptotically stable in isolation (being uncoupled). The interconnection between the nodes is defined by linear coupling

with time delay of the $u_i(t) = \gamma \sum_l \gamma_{il}[y_l(t-\tau) - y_i(t)]$. Basic pattern and bifurcation analysis of this directed ring network is performed in Chapter 4. It is known from that analysis that the origin of oscillations in this network is a Hopf bifurcation of supercrtitical type (i.e. the bifurcation results in a stable limit circle emanating from the equilibrium). The coupling strength and time-delay are chosen to be bifurcation parameters.

In absence of time-delay, the coupling functions vanish on the synchronization manifold as $y_l(t) = y_i(t)$. Thus the dynamics within the synchronization manifold are identical to the individual node dynamics. But these node dynamics have an asymptotically stable equilibrium and therefore no oscillatory synchronized solutions are possible in absence of delay.

The phenomenon of the *delay induced full synchronization* was firstly observed in the considered system in the three nodes ring-like complex network with directed time-delayed coupling in Chapter 4. In that chapter, the coupling strength parameter was fixed and the time-delay parameter was the subject to change. Varying the time-delay parameter, the network exhibited different behavior, such as a stable synchronized equilibrium [134], a rotating wave, a full synchronization mode and coexisting modes for the same values of parameters. In order to analyse the phenomenon and answer the question whether the *delay induced full synchronization* mode is a result of a bifurcation of synchronized equilibria or not, the following study is performed.

The possible patterns (modes) that may emanate from the synchronized network equilibrium can be analytically computed by the approach based on stability analysis of the synchronized equilibria [134]. The coexisting patterns are not covered by the synchronized equilibria approach, which leads to the need of additional analysis. The local picture of the regions of coexisting patterns (if any) can be obtained by the pattern analysis performed by the multivariable harmonic balance method (MHB) for delay coupled systems introduced in [93]. The approach is able to simultaneously compute coexisting patterns, which is cumbersome using the common methods of analysis, helps to avoid the initial conditions search problem, and, as the result, gives good initial conditions for a conducted continuation procedure, which is used to obtain a picture of the network behavior for a larger range of parameters. This more global picture can be obtained by the numerical bifurcation analysis performed in `ddebiftool` software package [143]. These tools can be used to construct a bifurcation diagram in (coupling strength, time-delay)-parameter space. Such analysis can be done in order to support and complement the results of analytical

approach and pattern analysis. In order to perform the analysis of the *delay induced full synchronization* and the network behavior, the combination of the pattern and bifurcation analysis is essential because it gives both local and more global pictures of the network behavior, which is shown in the chapter.

The chapter is organized as follows. In Section 5.2, the case-study network, in which the phenomenon is observed, is introduced. The phenomenon of delay induced full synchronization is described in detail in Section 5.3. Both the analytical and numerical analysis is done in Section 5.4. In Section 5.5, concluding remarks are given.

5.2 Network representation

The complex network is formed by delay-coupled Lur'e systems. The individual dynamics of N network nodes is described by:

$$\begin{aligned} \dot{x}_i &= Ax_i + Bu_i, \\ u_i &= u_{ci} - \psi(z_i), \\ z_i &= Zx_i, \\ y_i &= Cx_i, \end{aligned} \tag{5.1}$$

where $i = 1,...,N$ stands for the node number, $x_i(t) \in \mathbb{R}^3$ is the state of a i-th node, $u_i(t) \in \mathbb{R}^1$ is the combined input of a i-th node, consisting of two components: $\psi(\cdot)$ is a continuously differentiable scalar nonlinear sector-bounded function and $u_{ci} \in \mathbb{R}^1$ is the input receiving data from the coupling of multiple nodes, $y_i(t) \in \mathbb{R}^1$ is the output of the i-th system used for the coupling, $z_i \in \mathbb{R}^1$ is the argument of the nonlinearity of the i-th node.
Matrices A, B, C, Z are as follows:

$$\begin{aligned} A &= \begin{pmatrix} 1 & -1 & 1 \\ 1 & 0 & 0 \\ -4 & 2 & -3 \end{pmatrix}, \\ B &= \begin{pmatrix} 0 & 0 & 1 \end{pmatrix}^\top, \\ C &= \begin{pmatrix} 0 & 0 & 1 \end{pmatrix}, \\ Z &= B^\top P, \end{aligned}$$

where P is the solution to the Lyapunov equation

$$A^\top P + PA = -I_3.$$

The nonlinear function $\psi(\cdot)$ is provided as follows

$$\psi(z_i) = z_i^3.$$

The Lur'e systems are interconnected via directed time-delay coupling via output y_i and the coupling function is

$$u_{ci}(t) = \gamma \sum_l \gamma_{il}[y_l(t-\tau) - y_i(t)], \tag{5.2}$$

where positive constant γ stands for the overall coupling gain, positive constant τ represents the time delay (both γ and τ will be used as bifurcation parameters later on). Nonnegative constants γ_{il} are the interconnection weights which can be either 0 or 1, with $\gamma_{il} = 1$ if and only if there is a connection from system l to system i. Graphically, the connection between the nodes l and i is represented by a directed edge (arrow) between l and i.
The Delay Induced Full Synchronization phenomenon was observed for the first time in the network of size $N = 3$ [Fig. 5.1]. The network is connected, i.e. for any two nodes there exists a path (sequence of edges) connects them, and regular, i.e. each node has exactly the same number of links.

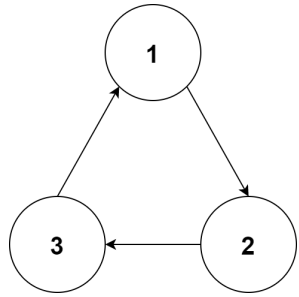


Figure 5.1: Network structure for the case study.

The graph topology $\Gamma = (\gamma_{il}) \in \mathbb{R}^{3\times 3}$ is described by the following adjacency matrix,

$$\Gamma = \begin{bmatrix} 0 & \gamma_{12} & \gamma_{13} \\ \gamma_{21} & 0 & \gamma_{23} \\ \gamma_{31} & \gamma_{22} & 0 \end{bmatrix} = \begin{bmatrix} 0 & 1 & 0 \\ 0 & 0 & 1 \\ 1 & 0 & 0 \end{bmatrix}. \tag{5.3}$$

The coupling matrix satisfies the following condition:

i) The sum of each row of the matrix Γ equals 1.

This condition implies, by the Gershgorin Disc Theorem [120], that all eigenvalues of Γ are located in the closed unit disc in $\mathbb{C}$. In other words, all eigenvalues of Γ have absolute value smaller or equal to 1. Moreover, matrix Γ has a simple eigenvalue equal to 1 and $[1\ 1\ 1]^\top$ is the corresponding eigenvector and there exist a vector $\epsilon = [\epsilon_1\ \epsilon_2\ \epsilon_3]^\top$ such that

$$\epsilon_i > 0, \quad i \in \{1,2,3\}, \quad \sum_{i=1}^{3} \epsilon_i = 1, \quad \epsilon^\top(\Gamma - I) = 0.$$

The condition i) ensures that a synchronous (oscillatory) state exists in such networks [134] [135].
The coupled systems (5.1)-(5.2) satisfy the following conditions for exhibiting oscillatory behavior imposed in Chapter 4:

ii) The isolated ($u_{ci} \equiv 0$) system (5.1), described by $\dot{x}_i := f(x_i) := Ax_i - B\psi(Zx_i)$, has a unique equilibrium point x_{i0}, which is globally asymptotically stable and locally exponentially stable;

iii) The solutions of the network (5.1)-(5.2) are uniformly bounded and uniformly ultimately bounded [136];

iv) The coupled systems (5.1)-(5.2) have a unique but hyperbolically unstable equilibrium at $x_0 = \mathbf{1}_N \otimes x_{10}$ for values of parameters γ, τ for which oscillatory behaviour is present.

Note that (local) exponential stability of the equilibrium of the isolated system is equivalent to the Jacobian matrix $J_0 = J(x_{i0}) = \partial f / \partial x_i(x_{i0})$ being Hurwitz, i.e. all eigenvalues of J_0 have negative real part. For the considered system $J_0 = A$.
Under the conditions ii)-iv), the coupled Lur'e systems exhibit oscillatory behavior in the sense of Yakubovich [121]. Pattern analysis by means of the MHB method is performed in the frequency domain and according to this, the network is rewritten into a transfer function representation as follows (note that s stands for the differential operator). Recall the MHB method presented in Chapter 3 and Chapter 4.

$$\begin{aligned} y_i &= W_y(s)u_i, \\ z_i &= W_z(s)u_i, \\ u_i &= \gamma \sum_{l=1}^{N} \gamma_{il}[y_l(t-\tau) - y_i(t)] - v_i, \\ v_i &= \psi(z_i), \end{aligned} \tag{5.4}$$

with $W_y(s)$ and $W_z(s)$ defined as

$$W_y(s) = C(sI - A)^{-1}B = \frac{s^2 - s + 1}{s^3 + 2s^2 + 2s + 1}, \tag{5.5}$$

$$W_z(s) = Z(sI - A)^{-1}B = \frac{s^2 + 1.5s + 1}{s^3 + 2s^2 + 2s + 1}. \tag{5.6}$$

Transfer functions $W_y(s)$ and $W_z(s)$ satisfy the following conditions imposed in Chapter 3:

v) The transfer function $W_y(s)$ is non-degenerate, has an even number of zeros with positive real part and relative degree one, and $W_y(0) > 0$;

vi) The transfer function $W_z(s)$ is such that $W_z(0) > 0$.

The graphical representation of the network is shown in Fig. 5.2. $F(s) = \begin{pmatrix} W_y(s) \\ W_z(s) \end{pmatrix}$ is the transfer matrix representing the linear time invariant part of the individual dynamics, output y is used for the coupling, matrix Γ represents the coupling structure for delayed signals, u is a combined input of u_c and output of nonlinear block, and output z is an input for the nonlinear block and is measured to read the behavior of each node.

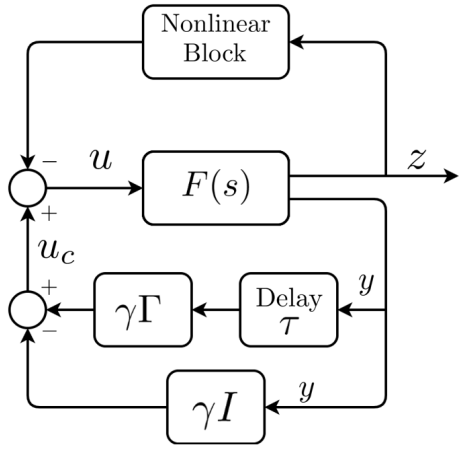


Figure 5.2: Block scheme representation of the network.

In the next section, the phenomenon of Delay Induced Full Synchronization is introduced.

5.3 Delay Induced Full Synchronization

Networks of Lur'e systems with individual dynamics described by (5.1) with a delay-free diffusive coupling, were thoroughly studied in a number of papers [75],[91],[92]. The numerical analysis performed in [91],[92] and Chapter 3 showed that the full synchronization oscillatory regime cannot be reached for the given configuration ($N = 3$) with a delay-free coupling function.

The network formed by (5.1)-(5.2) was introduced in [94] as an example of a complex network with time delay in the coupling and a supercritical Hopf bifurcation occurring in the network. Parameters γ and τ are bifurcation parameters and, in the given setting, a Hopf bifurcation is the origin of oscillations, so is it needed to detected Hopf bifurcation points in order to find the values of parameter for which the networks exhibits the oscillatory behavior.

Using Lemma 4.2 (Instability) from Chapter 4, $\gamma_{min} = 0.6481$ is computed for which the characteristic equation (4.8)

$$\Delta(\lambda;\gamma,\tau) := \det(\lambda I_{Nn} - I_N \otimes (A - \gamma BC) - (\gamma\Gamma \otimes BC)e^{-\lambda\tau}) = 0$$

has at least one root in $\mathbb{C}_+$ for some $\tau > 0$. In that case, the network equilibrium is unstable.

Using an approach based on a generalized eigenvalue problem presented in Section 4.2.3, and solving the auxiliary characteristic equation (ACE)(4.11)

$$ACE(\mathscr{P}) := \det[(\mathscr{A} + \mathscr{B}\mathscr{P}) \oplus (\mathscr{A}^\top + \mathscr{B}^\top \bar{\mathscr{P}})] = 0,$$

with $\mathscr{A} = I_n \otimes (A - \gamma_{min}BC)$, $\mathscr{B} = (\gamma_{min}\Gamma) \otimes (BC)$, and $\mathscr{P} := \exp(-j\omega\tau_c)$, two values of critical time delay $\tau_{c1} = 1.5304$ and $\tau_{c2} = 1.5314$ are computed for γ_{min}. These two critical values of τ are the endpoints of an interval for which the network equilibrium is unstable. Note that for $\gamma = \gamma_{min}$, the critical value τ_c is a point, not belonging to an interval. Moreover, at this critical point $\lambda = j\omega$.

In order to increase the region of instability to observe richer dynamical behavior of the network, γ is set as follows, $\gamma = 1.1 \cdot \gamma_{min} = 0.7110$, and the procedure is repeated for new γ. From now the parameter representing the coupling gain is fixed at $\gamma = 0.7110$ and τ is the only parameter to change in the network. The set of values of critical time delay for the interval

$\tau \in [0, 8]$ is computed as

$$\tau_c = \begin{bmatrix} \tau_{c1} \\ \tau_{c2} \\ \tau_{c3} \\ \tau_{c4} \\ \tau_{c5} \end{bmatrix} = \begin{bmatrix} 0.4364 \\ 2.7521 \\ 2.8534 \\ 5.0922 \\ 5.7406 \end{bmatrix}. \tag{5.7}$$

From the characteristic equation, which is periodic in τ, one can observe that critical values of τ_{cp} are periodically repeated with $\tau_{cp} + k2\pi/\omega_p$, where k is a natural number. The dimension of vector τ_c implies that a Hopf bifurcation occurs at each point (γ, τ_{cp}) where $p = 1, 2, 3, 4, 5$.
In order to verify the calculations, the rightmost characteristic roots are computed by means of the method described in [146]. Fig. 5.3 shows that a couple of characteristic roots is located on the imaginary axis, which corresponds to the Hopf Bifurcation and matches our calculations.

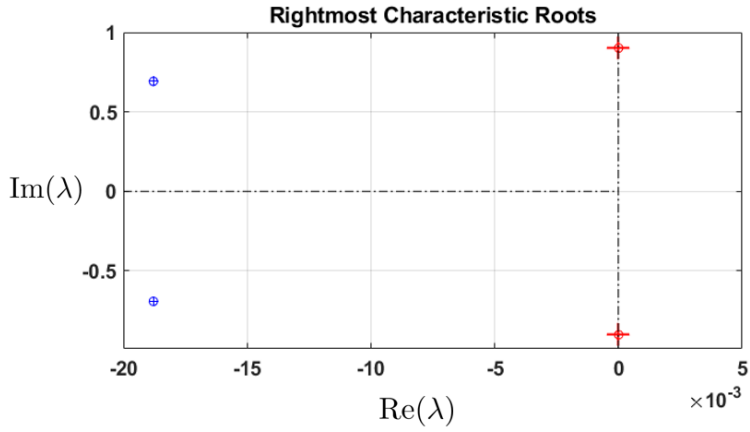


Figure 5.3: Rightmost characteristic roots computed for fixed $\gamma = 0.7110$ and $\tau_{c1} = 0.4364$.

From the analysis in Chapter 4, it is known that the network equilibrium point is stable for $\gamma = 1.1\gamma_{min}$ and $\tau \in [0, 0.4364)$. At each point $[\gamma, \tau_{cp}]$, a Hopf bifurcation occurs, changing stability of the equilibrium point. The first Hopf bifurcation happens at the point $(0.7110, 0.4364)$ in (γ, τ)-parameter space and the network (5.1)-(5.2) starts exhibiting oscillatory pattern corresponding to "travelling wave" with phase difference between

systems 1 and 2, 2 and 3, 3 and 1 equal to $2\pi/3$.

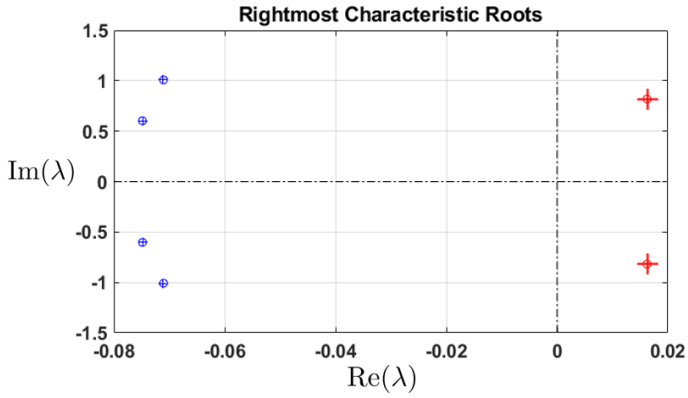


Figure 5.4: Rightmost characteristic roots computed for $\gamma = 0.7110$ and $\tau = 1.5$.

Fig. 5.4 and Fig. 5.5 illustrate the rightmost characteristic roots of the characteristic equation and the results of the direct simulation of DDEs using the `dde23` solver in `MATLAB R2020` environment, respectively, for the parameter values for $\gamma = 0.711$ and $\tau = 1.5$. The default set of options for `dde23` solver is used and the initial conditions are chosen as a constant vector function defined on $[-\tau, 0]$ whose values are (uniformly distributed) random numbers. An oscillatory pattern with equal amplitudes and phase shift of $2\pi/3$ on the time interval $[400, 500]$ is shown after some transition time.
The MHB analysis shows the very similar result with small mismatch. In Table 5.1 the components of the harmonic profile, namely frequency ω, offset component α_0, amplitudes α_e, and phases ϕ_i, are provided.

ω	α_0	α_e	ϕ_1	ϕ_2	ϕ_3
0.8262	0	0.3574	0	120	240

Table 5.1: Oscillatory pattern computed by the MHB method for $\gamma = 0.7110$ and $\tau = 1.5$.

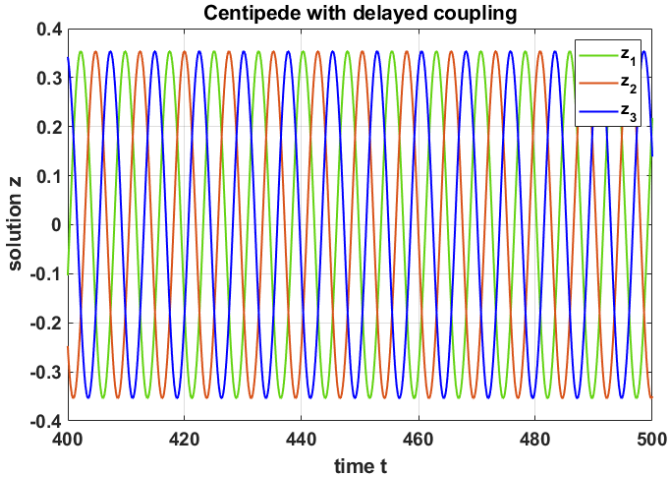


Figure 5.5: Output of direct simulation of the given network for a pair of parameters $\gamma = 0.7110$ and $\tau = 1.5$.

Now the time-delay parameter is changed to $\tau = 3.5$ in order to satisfy the following inequality $\tau_{c3} < \tau < \tau_{c4}$ from (5.7). The interval $[\tau_{c2}, \tau_{c3}]$ is not of interest for now and will be studied later on. The rightmost characteristic roots of (4.8) are presented in Fig. 5.6.
One can see that there is a pair of roots with positive real parts exactly as in the $\gamma = 0.7110$ and $\tau = 1.5$ configuration, so an oscillatory pattern with $2\pi/3$ phase shift is expected. The MHB analysis and the direct simulation show a new phenomenon, which we call *delay induced full synchronization*. The results of the MHB is given in Table 5.2 and Fig. 5.7 shows the output of numerical integration of coupled systems (5.1)-(5.2).
The data in Table 5.2 shows that all three nodes have the same phase (note that the value of the initial phase is arbitrary), amplitude and frequency, which implies that the node are synchronized.

In order to show that full synchronization mode exist for some range of parameter τ, the time-delay is selected as $\tau = 6 \in [\tau_{c5}, 8]$. The procedure above is repeated. The rightmost characteristic roots of (4.8) for $\gamma = 0.7110$ and $\tau = 6$ are depicted in Fig. 5.8.
There is a pair of roots with positive real parts exactly as in the previous

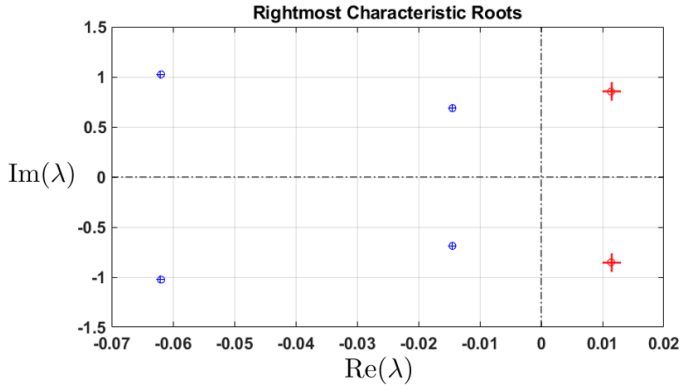


Figure 5.6: Rightmost characteristic roots computed for $\gamma = 0.7110$ and $\tau = 3.5$.

ω	α_0	α_e	ϕ_1	ϕ_2	ϕ_3
0.8589	0	0.3318	174	174	174

Table 5.2: Oscillatory pattern computed by the MHB method for $\gamma = 0.7110$ and $\tau = 3.5$.

configurations, so now it is hard to say what kind of pattern is expected. In order to obtain the oscillatory profile of the pattern, the MHB analysis is used. The results of the MHB analysis are given in Table 5.3 and the output of direct simulations is shown in Fig. 5.9.

ω	α_0	α_e	ϕ_1	ϕ_2	ϕ_3
0.8557	0	0.3372	0	240	120

Table 5.3: Oscillatory pattern computed by the MHB method for $\gamma = 0.7110$ and $\tau = 6$.

Summarizing the observations above, one may say that full synchronization

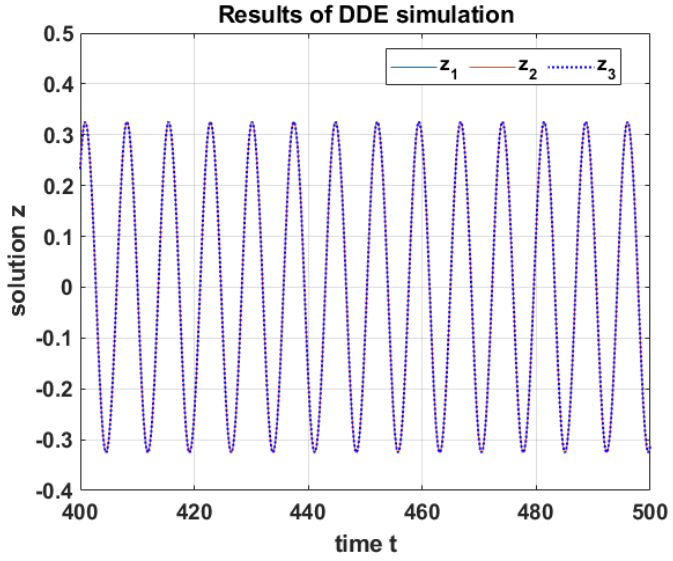


Figure 5.7: Delay Induced Full Synchronization. Output of direct simulation of the given network for a pair of parameters $\gamma = 0.7110$ and $\tau = 3.5$.

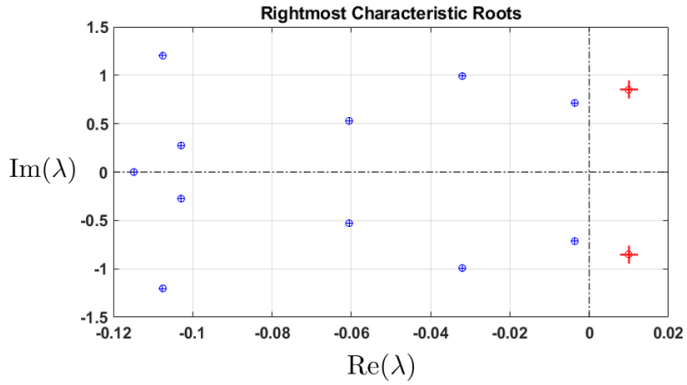


Figure 5.8: Rightmost characteristic roots computed for $\gamma = 0.7110$ and $\tau = 6$.

mode is an unexpected phenomenon, which is not present in such networks when the coupling is delay-free. There are two bifurcation parameters

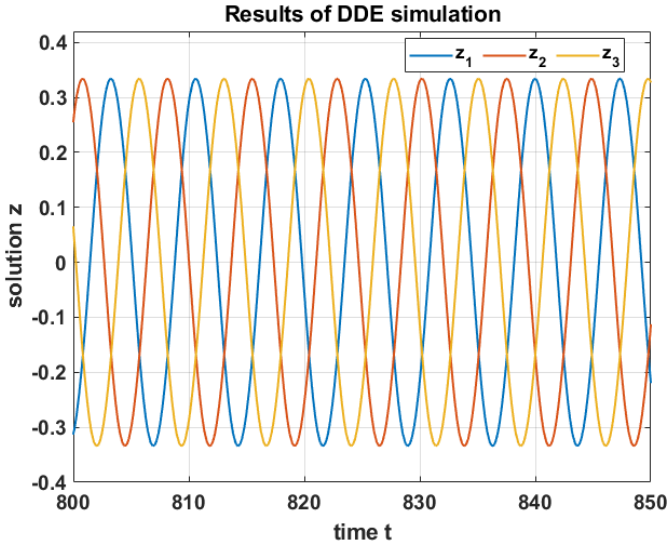


Figure 5.9: 240 phase shift rotating wave. Output of direct simulation of the given network for a pair of parameters $\gamma = 0.7110$ and $\tau = 6$.

γ, τ in our complex network. Parameter γ is fixed and τ is the subject to change. Moreover, the phenomenon is observed for some range of parameter τ. There are five (periodically repeating) critical values of $\tau \in [0,8]$ which correspond to Hopf bifurcation points, and bifurcation analysis is required in order to understand the phenomenon of delay induced full synchronization. In the next sections, the theoretical results, which explains the occurrence of the synchronized mode and supporting the theory numerical analysis, will be presented.

5.4 Analytical and numerical analysis of the case-study

In order to explain the phenomenon of the delay induced full synchronization, a combination of different approaches for analysis is used. Stability analysis of synchronized equilibria is performed in order to determine possible patterns that may appear in the case-study network. The method-

ology, described in [134], instead of directly computing synchronization conditions for the complex network (5.1)-(5.2), first considers the linearized stability problem around a synchronized equilibrium, which can be exactly solved. Such an approach directly leads to insights in the problem, due to its ability to characterize the stability regions in the (γ, τ) parameter space. In order to support the analytical results, local pattern analysis and numerical bifurcation analysis by means of the MHB method and `ddebiftool`, respectively, are performed.

5.4.1 Stability Analysis of Synchronized Equilibria

Following [134], the analysis starts with the linearization around equilibria. For the network (5.1)-(5.2), according to condition iv) in Section 5.2, there exists only one equilibrium point at the origin $x_0 = \mathbf{1}_3 \otimes (0,0,0)^\top$. After linearization the network takes the following form:

$$\begin{bmatrix} \dot{v}_1(t) \\ \dot{v}_2(t) \\ \dot{v}_3(t) \end{bmatrix} = I_3 \otimes (A - \gamma BC) \begin{bmatrix} v_1(t) \\ v_2(t) \\ v_3(t) \end{bmatrix} - (\gamma\Gamma \otimes BC) \begin{bmatrix} v_1(t-\tau) \\ v_2(t-\tau) \\ v_3(t-\tau) \end{bmatrix}, \tag{5.8}$$

where v_i is a vectorfunction.
The characteristic equation of (5.8) is given by

$$\varphi(\lambda; \gamma, \tau) := \det \Phi(\lambda; \gamma, \tau),$$

where the characteristic equation Φ is defined as

$$\Phi(\lambda; \gamma, \tau) = \lambda I_9 - I_3 \otimes (A - \gamma BC) - (\gamma\Gamma \otimes BC) e^{-\lambda\tau}. \tag{5.9}$$

If we factorize the coupling matrix $\Gamma = T\Lambda T^{-1}$, where $\Lambda \in \mathbb{C}^{3\times 3}$ is triangular and $T \in \mathbb{C}^{3\times 3}$, the characteristic function becomes

$$\begin{aligned} \varphi = (\lambda; \gamma, \tau) &= \det(\lambda I_9 - I_3 \otimes (A - \gamma BC) - (\gamma T\Lambda T^{-1} \otimes BC) e^{-\lambda\tau}) \\ &= \det(T^{-1} \otimes I_9) \det(\lambda I_9 - I_3 \otimes (A - \gamma BC) - (\gamma T\Lambda T^{-1} \\ &\otimes BC) e^{-\lambda\tau}) \det(T \otimes I_9) \\ &= \det(\lambda I_9 - I_3 \otimes (A - \gamma BC) - (\gamma\lambda_i(\Gamma) \otimes BC) e^{-\lambda\tau}) \\ &= \prod_{i=1}^{3} \varphi(\lambda; \gamma, \tau), \end{aligned}$$

where

$$\varphi_i(\lambda;\gamma,\tau) := \det F_i(\lambda;\gamma,\tau),$$
$$\Phi_i(\lambda;\gamma,\tau) := \lambda I_3 - A + \gamma BC - \gamma\lambda_i(\Gamma)BCe^{-\lambda\tau},\ i = 1,...,3.$$

The next step is an investigation of the eigenspace of the characteristic matrix (5.9), corresponding to a characteristic root. In our case all eigenvalues of the coupling matrix Γ are simple. Let E_i be the eigenvector of Γ corresponding to the eigenvalue $\lambda_i(\Gamma)$, $i = 1,2,3$. According to properties following from the condition i) in Section 5.2, we have $E_1 = [1\ 1\ 1]^\top$ for $\lambda_1(\Gamma) = 1$.
If for some $i \in \{1,2,3\}$, the equation

$$\varphi_i(\lambda;\gamma,\tau) = 0$$

has a simple root at $\lambda = \hat{\lambda}$ such that

$$\varphi_i(\hat{\lambda};\gamma,\tau)V = 0, \quad V \in \mathbb{C}^{3\times 1} \tag{5.10}$$

then it can be verified that

$$\Phi_i(\hat{\lambda};\gamma,\tau)(E_i \otimes V) = 0. \tag{5.11}$$

According to this, the linearized system (5.8) has an exponential solution

$$\begin{bmatrix} v_1(t) \\ v_2(t) \\ v_3(t) \end{bmatrix} = c(E_i \otimes V)\exp(\hat{\lambda}t) = c \begin{bmatrix} e_{i,1}V \\ e_{i,2}V \\ e_{i,3}V \end{bmatrix} \exp(\hat{\lambda}t), \tag{5.12}$$

where c is a constant depending on the initial conditions.
In conclusion, the relations between the corresponding state variables of the different nodes of the linearized complex network (5.1)-(5.2) are solely determined by the eigenvector E_i, corresponding to the ith eigenvalue of the coupling matrix Γ. It means that all possible modes can be classified in at most 3 types based on the relations between the behavior of the different nodes. The classification of the bifurcations of the synchronized equilibria of the original nonlinear system , described by (5.1)-(5.2), can be done in the same way [134].
For coupled systems (5.1)-(5.2), whose topology is represented by a three node ring with unidirectional coupling, the adjacency matrix (5.3)

$$\Gamma = \begin{bmatrix} 0 & 1 & 0 \\ 0 & 0 & 1 \\ 1 & 0 & 0 \end{bmatrix}.$$

has the following properties:

$$\lambda_i(\Gamma) = \exp(-j[2\pi(i-1)/3]), \quad E_i = \begin{bmatrix} 1 \\ \exp(-j[2\pi(i-1)/3]) \\ \exp(-j[4\pi(i-1)/3]) \end{bmatrix}$$

for $i = 1, ..., 3$.
Using the approach above, we compute the eigenpairs (note that the eigenvectors are normalized):

$$\lambda_1(\Gamma) = 1, \qquad E_1 = \begin{bmatrix} 1 \\ 1 \\ 1 \end{bmatrix}, \tag{5.13}$$

$$\lambda_2(\Gamma) = -\frac{1}{2} - j\frac{\sqrt{3}}{2}, \qquad E_2 = \begin{bmatrix} 1 \\ -\frac{1}{2} - j\frac{\sqrt{3}}{2} \\ -\frac{1}{2} + j\frac{\sqrt{3}}{2} \end{bmatrix}, \tag{5.14}$$

$$\lambda_3(\Gamma) = -\frac{1}{2} + j\frac{\sqrt{3}}{2}, \qquad E_3 = \begin{bmatrix} 1 \\ -\frac{1}{2} + j\frac{\sqrt{3}}{2} \\ -\frac{1}{2} - j\frac{\sqrt{3}}{2} \end{bmatrix}. \tag{5.15}$$

When equation (5.10) is satisfied for $\hat{\lambda} = j\omega$, $\omega > 0$, then the emanating solution (5.12) becomes

$$\begin{bmatrix} v_1(t) \\ v_2(t) \\ v_3(t) \end{bmatrix} = c \begin{bmatrix} V\exp(j\omega t) \\ V\exp(-j\omega t[2\pi(i-1)/3]) \\ V\exp(-j\omega t[4\pi(i-1)/3]) \end{bmatrix}. \tag{5.16}$$

Such solution can be interpreted as a "travelling wave", where the nodes follow each other with a phase shift of $2\pi(i-1)/3$ radians ($360(i-1)/3$ in degrees). Therefore, if the characteristic root $\hat{\lambda}$, which is located on the imaginary axis, corresponds to a Hopf Bifurcation of the delay-coupled Lur'e systems, described by (5.1) and (5.2), for a critical value of free parameter τ, this bifurcation is referred as a "Hopf $360(i-1)/3$" bifurcation. This terminology was introduced in [134].
The analysis above implies that all possible modes can be determined from the eigenpairs (the eigenvalue and the corresponding eigenvector) of the coupling matrix Γ for the given network.
From eigenpairs (5.13)-(5.15), one can see that there exist three possible modes emerging at a Hopf bifurcation of the synchronized equilibrium,

namely full synchronization (Hopf 0), which is described in Section 5.3, clockwise (Hopf 120) and counterclockwise (Hopf 240) travelling waves with phase shift of ±120 degrees.

5.4.2 Pattern analysis by MHB

Using the stability analysis of the synchronized equilibria, the structurally possible modes for the complex network (5.1)-(5.2) of three nodes with unidirectional coupling (5.3), are found. In Section 5.3, the critical values of the free parameter τ for the interval $\tau \in [0,8]$ are computed as

$$\tau_c = \begin{bmatrix} 0.4364 \\ 2.7521 \\ 2.8534 \\ 5.0922 \\ 5.7406 \end{bmatrix}.$$

It is shown that for $\tau \in [0.4364, 2.8534]$ the pattern with the phase shift of 120 degrees is present, which corresponds to Hopf 120, whereas for $\tau \in [2.7521, 5.7406]$ the full synchronization mode (Hopf 0) is observed. It is expected that the oscillatory pattern associated with Hopf 240 would be present in the interval $\tau \in [5.0922, 8]$. In order to have a complete understanding of the network behavior for the fixed $\gamma = 0.7110$ and free τ, the analysis of the network behavior has to be done for time delay intervals $\tau \in [2.7521, 2.8534]$ and $\tau \in [5.0922, 5.7406]$.
For this, the bifurcation parameter τ is selected to be $\tau = 2.8$ from the first interval $\tau \in [2.7521, 2.8534]$. From the stability analysis of synchronized equilibria it is known that different oscillatory patterns are related to unstable (with a positive real part) eigenvalues of the characteristic equation (5.9). Computation of rightmost characteristic roots for the pair of parameters $\gamma = 0.7110$ and $\tau = 2.8$ shows that there are two pairs of unstable eigenvalues (Fig. 5.10), which implies that two different modes coexist for the same pair of parameters (γ, τ). See Chapter 4 for details.
The unstable eigenvalues and the corresponding (normalized) eigenvectors are

$$\lambda_1 = 0.001 \pm j0.8990, \qquad \lambda_2 = 0.001 \pm j0.7317, \tag{5.17}$$

$$E_1 = \begin{bmatrix} 1 \\ 1 \\ 1 \end{bmatrix}, \qquad E_2 = \begin{bmatrix} 1 \\ -\frac{1}{2} + j\frac{\sqrt{3}}{2} \\ -\frac{1}{2} - j\frac{\sqrt{3}}{2} \end{bmatrix},$$

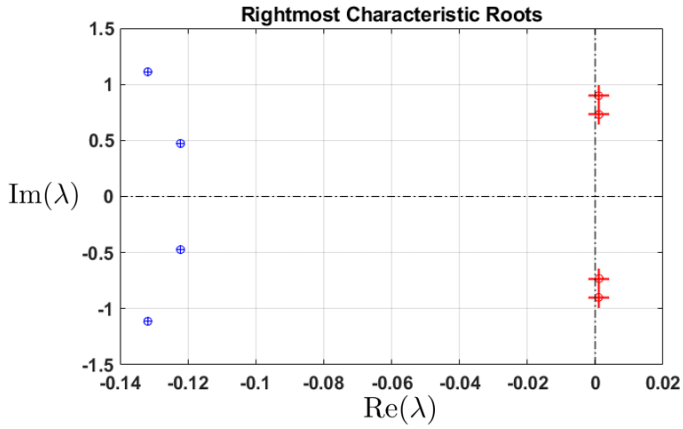


Figure 5.10: Rightmost characteristic roots computed for $\gamma = 0.7110$ and $\tau = 2.8$.

which satisfy modes of the full synchronization and the travelling wave with 120 degrees phase shift, respectively. Note that the magnitude of the imaginary part of the eigenvalues equals to the frequency of oscillations.
The results of the direct simulations of DDEs (5.1)-(5.2) show that for different initial conditions the network behavior converges to one of two modes, namely the full synchronization (Fig. 5.11) and the travelling wave (Fig. 5.12).
Although the coexisting oscillatory patterns can be computed by the direct simulation approach using `dde23` solver in MATLAB environment, the problem of finding the initial conditions arises.
In order to avoid numerically solving an initial value problem and simultaneously obtain oscillatory profiles (frequency ω, offset component α_0, amplitudes α_e, and phases ϕ_i) of coexistent patterns, the Multivariable Harmonic Balance (MHB) method for delay-coupled systems is employed. The method is presented in Chapter 4.
The coexisting oscillatory patterns, computed by means of the MHB approach, are given in Table 5.4.
The MHB approach computed coexisting oscillatory profiles for parameters $\gamma = 0.7110$ and $\tau = 2.8$. The computed values of the frequency of oscillations match the magnitude of imaginary part of the unstable eigenvalues (5.17), which relates the patterns with the corresponding roots of the characteristic equation (5.9).

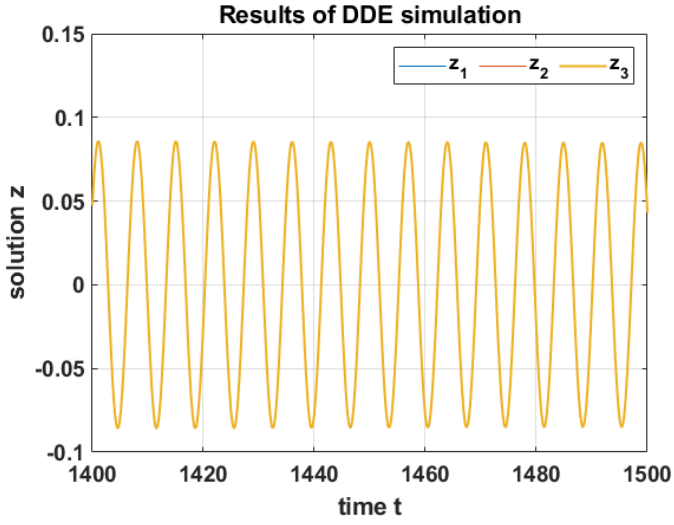


Figure 5.11: Output of direct simulation for a pair of parameters $\gamma = 0.7110$ and $\tau = 2.8$. The full synchronization regime.

Mode	ω	α_0	α_e	ϕ_1	ϕ_2	ϕ_3
Full Synch	0.8998	0	0.1013	0	0	0
$2\pi/3$ Wave	0.7320	0	0.0947	0	120	240

Table 5.4: Two stable coexisting oscillatory patterns which are computed by the MHB method for $\gamma = 0.7110$ and $\tau = 2.8$.

In order to verify the results of the MHB approach, the MHB output is compared with the results of the direct DDE simulation, which is used the MHB results as the initial conditions. The data is provided in Table 5.5 Now the value of parameter τ is selected from the second interval $\tau \in [5.0922, 5.7406]$ and the procedure is repeated for $\tau = 5.3$. Two pairs of unstable eigenvalues are computed for $\gamma = 0.7110$ and $\tau = 5.3$, which indicates the coexistence of two oscillatory patterns. The rightmost characteristic roots are depicted in Fig. 5.13.

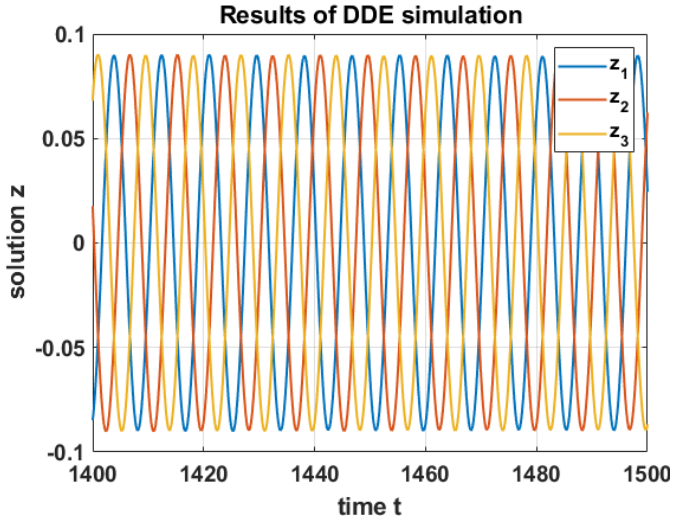


Figure 5.12: Output of direct simulation for a pair of parameters $\gamma = 0.7110$ and $\tau = 2.8$. The $2\pi/3$ phase shift travelling wave regime.

Mode	$\Delta\omega$ in %	$\Delta\alpha_0$ in %	$\Delta\alpha$ in %
Full Synch	0.009	0	11.63
$2\pi/3$ Wave	0.006	0	4.48

Table 5.5: Comparison of the DDE simulation and the MHB method outputs.

The unstable eigenvalues and the corresponding (normalized) eigenvectors are given as follows

$$\lambda_1 = 0.0051 \pm j0.7506, \qquad \lambda_2 = 0.0034 \pm j0.8887, \tag{5.18}$$

$$E_1 = \begin{bmatrix} 1 \\ 1 \\ 1 \end{bmatrix}, \qquad E_2 = \begin{bmatrix} 1 \\ -\frac{1}{2} - j\frac{\sqrt{3}}{2} \\ -\frac{1}{2} + j\frac{\sqrt{3}}{2} \end{bmatrix},$$

In order to compute oscillatory profiles of the coexisting modes, the MHB approach is used. The results of the analysis are given in Table 5.6.

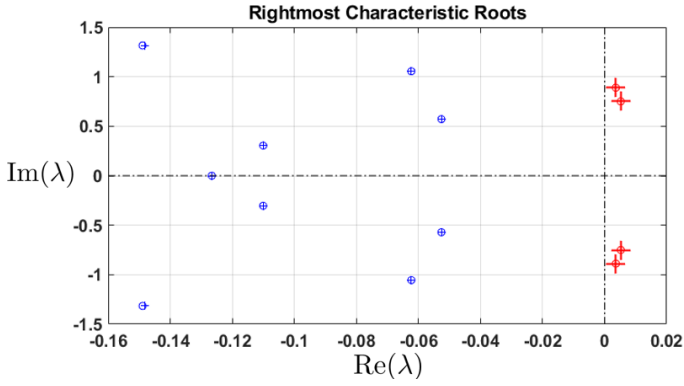


Figure 5.13: Rightmost characteristic roots computed for $\gamma = 0.7110$ and $\tau = 5.3$.

Mode	ω	α_0	α_e	ϕ_1	ϕ_2	ϕ_3
Full Synch	0.7519	0	0.2230	0	0	0
$4\pi/3$ Wave	0.8914	0	0.2019	0	240	120

Table 5.6: Two stable coexisting oscillatory patterns which are computed by the MHB method for $\gamma = 0.7110$ and $\tau = 5.3$.

The relation between the unstable eigenvalues and the computed oscillatory patterns is due to frequency (phases) and magnitude of the imaginary part of the eigenvalue (corresponding eigenvector) match.
The data shows that it is more convenient to use the MHB method for the pattern analysis due to the facts that the MHB approach can compute coexisting patterns and helps to avoid the search of the initial conditions. The pattern analysis performed in this section shows that there are coexisting patterns in the the network and explains what happens when the free parameter τ is taken from one of the intervals $[2.7521, 2.8534]$ and $[5.0922, 5.7406]$. The coexistence of different patterns, namely 120, 240 phase shift rotating waves and full synchronization mode shows the importance of the pattern analysis for understanding complex network behavior.

5.4.3 Numerical Bifurcation Analysis

Using the stability analysis of the synchronized equilibria and the pattern analysis by means of the MHB method, the structurally possible modes of oscillatory behavior and coexisting stable oscillatory modes for the same bifurcation parameters (γ, τ), are found. In this section, a numerical bifurcation analysis by means of `ddebiftool` is performed in order to explain the phenomenon of Delay Induced Full Synchronization in the network (5.1)-(5.2).
It was shown that there exist three oscillatory modes, namely the $2\pi/3$ phase shift mode, the $4\pi/3$ phase shift mode, and the full synchronization mode, and for some regions of free parameter τ the modes coexist. In order to explain this result, the branches of periodic solutions and a bifurcation diagram are constructed by means of the `ddebiftool` toolbox. Using the toolbox, the bifurcation points of the branch of equilibria are computed for fixed $\gamma = 0.7110$ and free τ. The computed bifurcation points are shown in Table 5.7.

Hopf type	Hopf 120	Hopf 0	Hopf 120_{end}	Hopf 240	Hopf 0_{end}
γ	0.7110	0.7110	0.7110	0.7110	0.7110
τ	0.4364	2.7521	2.8534	5.0922	5.7406

Table 5.7: Bifurcation points and types of bifurcation.

It is worth mentioning that the pair eigenvalues crosses the imaginary axis towards instability at the Hopf 120 (Hopf 0) and become stable at the Hopf 120_{end} (Hopf 0_{end}). Note that for this analysis, only part of the interval $\tau \in [0, 8]$ is used.
The stability of the branch of equilibria is depicted in Fig. 5.14. The curves represent how the real parts of the rightmost eigenvalues change as a function of τ. We can see that the network equilibrium loses its stability exactly at the Hopf 120 point at $\tau = 0.4364$ and then there exist a region $\tau \in [2.7521, 2.8534]$ where there are two pairs of unstable eigenvalues.
One can see from the figure that in the chosen region of τ, the unique network equilibrium is unstable for all $\tau > 0.4364$ in the interval $\tau \in [0, 5]$.
The next step is to compute branches of periodic solutions which exist in the given network. The procedure starts from constructing an initial small-amplitude orbit near a Hopf bifurcation. Then, using a continuation

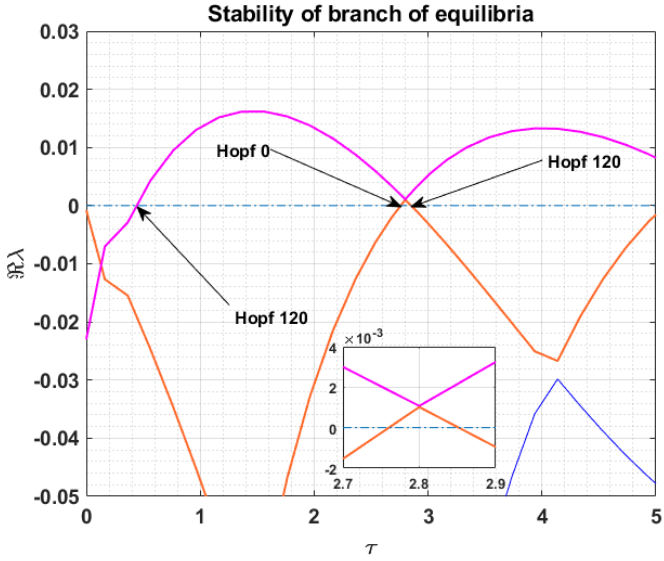


Figure 5.14: Stability of the branch of trivial equilibria for $\gamma = 0.7110$. Note that in the bottom right part of the figure, the numerical artifact is observed.

method with τ as a free parameter, a periodic solutions branch is computed.

The vertical axis in Fig. 5.15 shows the Euclidean norm of all state variables which is called amplitude. The horizontal axis represent bifurcation parameter τ. One observes two branches of periodic solutions (120 wave is orange and Full Synchronization is purple) and each blue dot is a periodic solution computed by a numerical procedure. Branches emanate from bifurcation points Hopf 120 $(0.7110, 0.4364)$ and Hopf 0 $(0.7110, 2.7521)$, respectively. Each branch of periodic solutions starts in a Hopf bifurcation and ends in a Hopf bifurcation, while the periodic solution is stable along the whole branch.
The final step of the analysis is to construct the stability crossing curves of the synchronized equilibrium, which describe the network behavior in (γ, τ)-parameter space. The procedure is the follows:

i) Locating the first Hopf Bifurcation. In our case it is Hopf 120 at $(0.7110, 0.4364)$;

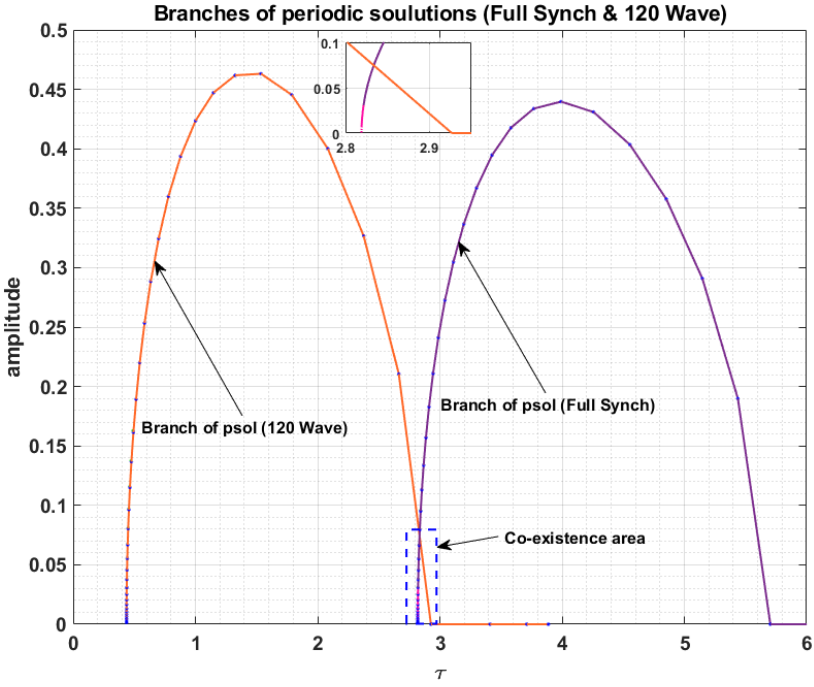


Figure 5.15: Branches of periodic solutions. 120 wave mode and full synchronization mode. The purple dots represent computed periodic solutions from which form the branches.

ii) Initialize and continue the first Hopf bifurcation to construct a branch;

iii) Hopf curve continuation and detection of a double Hopf bifurcation point [149]. The double Hopf bifurcation occurs at $(0.7045, 2.8191)$ (Fig. 5.16);
Existence of such points shows the importance of the constructing more global picture than can be provided by only pattern analysis.

iv) Switch to the second Hopf bifurcation at double Hopf bifurcation;

v) Continuation of the second Hopf bifurcation;

vi) Repeat the procedure with the second branch as initial one (due to periodicity of time delay systems).

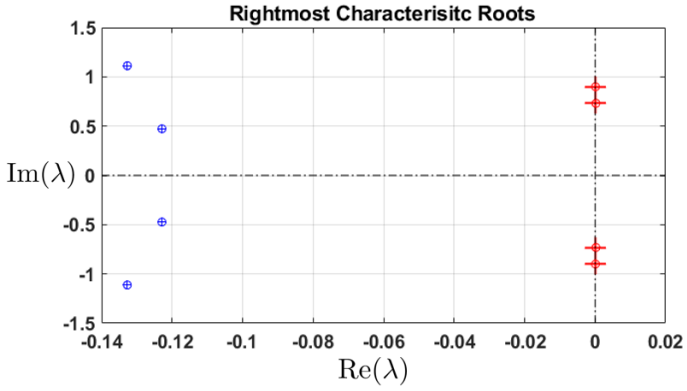


Figure 5.16: Rightmost characteristic roots computed for double Hopf bifurcation at $\gamma = 0.7045$ and $\tau = 2.8191$.

The bifurcation diagram, describing the behavior of the network (5.1)-(5.2) and explaining the phenomenon of Delay Induced Full Synchronization, is shown in Fig. 5.17.
The bifurcation diagram is constructed for the parameter intervals $\gamma \in [0,1]$ and $\tau \in [0,8]$. The dotted vertical black line shows the minimal value of the coupling strength $\gamma_{min} = 0.6481$. The blue curves represent branches of Hopf bifurcation points. There are four curves: two branches of Hopf 240, a Hopf 120 branch, and a branch of Hopf 0. The bifurcation diagram matches the results of the stability analysis of synchronized equilibria and, moreover, provides information of the regions of multistability. Numbers $0,1,2,3$ indicate the number of unstable pairs of eigenvalues and, in this case, stable oscillatory patterns in a region. Nevertheless, in general, there is not strong relation between the number of unstable eigenvalues along the branch of equilibria, and the number of periodic regimes. The match between the theoretical results obtained by synchronized equilibria analysis and the number of unstable eigenvalues is verified by the pattern analysis performed by the MHB approach. The red vertical line stands for the fixed parameter $\gamma = 0.7110$ for which the analysis of the delay induced full synchronization is performed. The colored regions indicate patterns or coexisting patterns which are observed in each region. Apart from the phenomenon of delay induced full synchronization, the golden region attracts attention because, according to the diagram, all three possible pat-

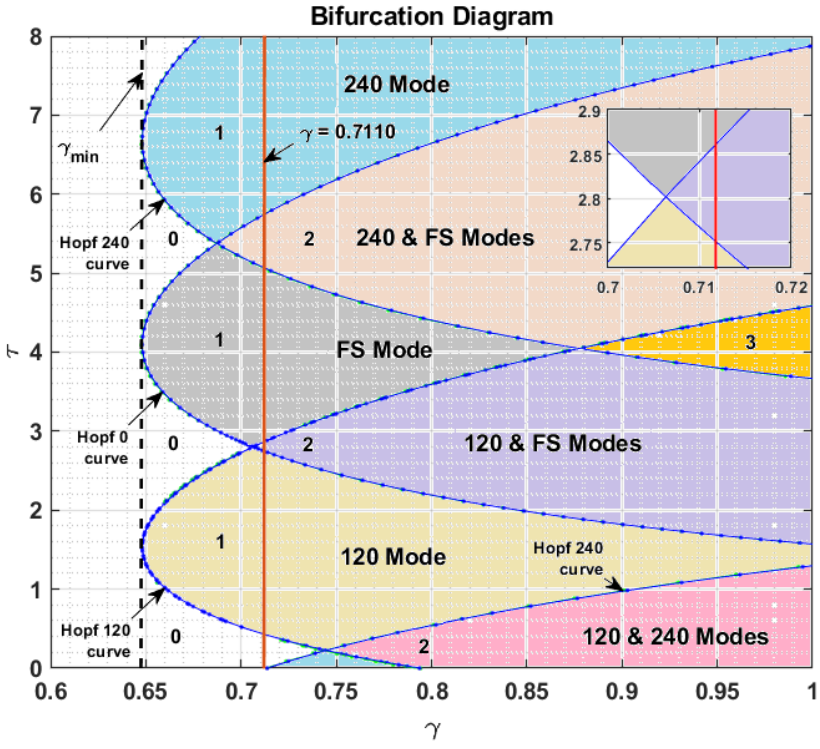


Figure 5.17: Bifurcation diagram in (γ, τ)-parameter space. Red vertical line is $\gamma = 0.7110$. Golden region 3 contains three coexisting modes, namely 120, 240 and FS.

terns, namely 120, 240 travelling waves and full synchronization, should coexist in the region. For values of parameters within this region, the characteristic equation of the network has 3 pairs of unstable eigenvalues, which is depicted in Fig. 5.18.

In order to support the bifurcation diagram, the local pattern analysis by means of the MHB method is performed for parameter values $\gamma = 0.95$ and $\tau = 4$, i.e. parameters within the golden region. The results of the MHB approach are provided in Table 5.8

The phenomenon of the delay induced full synchronization is a result of a bifurcation of the synchronized equilibria of the network. Full synchroniza-

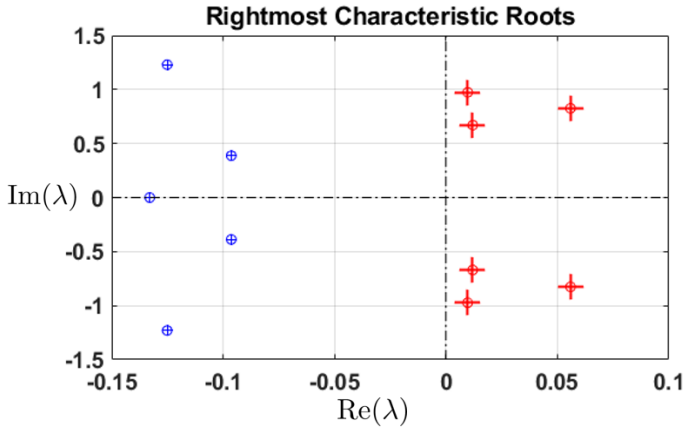


Figure 5.18: Rightmost characteristic roots at $\gamma = 0.95$ and $\tau = 4$.

Mode	ω	α_0	α	ϕ_1	ϕ_3	ϕ_3
Full Synch	0.8491	0	0.7711	0	0	0
$2\pi/3$ Wave	0.9848	0	0.3643	0	120	240
$4\pi/3$ Wave	0.6702	0	0.3247	0	240	120

Table 5.8: Three coexisting patterns simultaneously computed by the MHB method.

tion can be achieved by manipulating the time-delay parameter τ, while the coupling strength remains fixed. In order to illustrate this, the analysis of the network behavior is performed along the red line, which represents fixed parameter $\gamma = 0.7110$. Starting at $\tau = 0$ and moving along the red line, first the network is stable, then the Hopf 120 bifurcation occurs at $\tau = 0.4364$, where one pair of eigenvalues becomes unstable and oscillatory pattern emanates from the unstable equilibrium. At $\tau = 2.7521$ the second pair of eigenvalues crosses the imaginary axis and the area of coexisting 120 and full synchronization patterns is entered (zoomed plot in Fig. 5.17). The pair of eigenvalues, corresponding to the travelling waves pattern with 120 degree phase shifts, crosses the imaginary axis and becomes stable at $\tau = 2.8534$. The network exhibits only the fully synchronized oscillatory pattern in the grey area. Increasing τ, the Hopf 240 curve is crossed

and coexistence area of the fully synchronized mode and 240 phase shift travelling wave, is entered.

5.5 Concluding remarks

The chapter introduces and gives the analysis of the phenomenon of the *delay induced full synchronization* which was firstly observed in the particular complex network described by (5.1)-(5.2). Two coupling parameters γ and τ are selected as bifurcation parameters. It is shown that for the fixed γ, the full synchronization regime can be achieved by varying τ. The full synchronization regime cannot be observed in such networks with delay-free coupling. The analysis performed in the chapter is aiming at answering the question whether the phenomenon of the *delay induced full synchronization* is a result of a bifurcation of the synchronized equilibria. In order to show this, a combination of analytical and numerical approaches are used.

Analytical analysis, performed by the stability analysis of synchronized equilibria [134], shows the possible modes that may emerge in bifurcations of equilibria, when the network topology is defined by (5.3). This result also implies that, in the neighbourhood of the synchronized equilibrium, the individual dynamics of the nodes does not affect the regimes which can be observed in such networks. An oscillatory pattern (frequency and phases) is defined by an eigenpair (unstable eigenvalue and its corresponding eigenvector).

The local pattern analysis is performed by the Multivariable Harmonic Balance method for time delay systems, presented in Chapter 4. The MHB method is used to detect bifurcation points and to compute the oscillatory patterns avoiding the common methods of the analysis. Moreover, the pattern analysis by the MHB approach is the only simple way to simultaneously compute coexisting patterns for the same parameters, which is necessary for understanding the network behavior, especially in the case of three coexisting patterns. The pattern analysis output verifies the results of the stability analysis of synchronized equilibria and supports the results of the numerical bifurcation analysis by providing local behavioral analysis in the regions of interest.

The numerical bifurcation analysis, performed by `ddebiftool` software package, is used to support and complement the analytical results and the MHB approach. Using the method, the bifurcation diagram of the network behavior in (γ, τ)-parameter space is constructed, depicting more global

behavior of the network. In order to support the MHB method, the continuation procedure is used to construct branches of periodic solutions, which arise from the Hopf bifurcation points. It is shown that there is an area in which different patterns coexist for the same parameters, which matches with the results of the MHB analysis. As a main result, the bifurcation diagram (Fig. 5.17), illustrating and explaining the network behavior as a function of γ and τ, is constructed. The data in Fig. 5.17 matches with the results obtained by the stability analysis of synchronized equilibria and the Multivariable Harmonic Balance method. For fixed $\gamma = 0.7110$ and $\tau \in [2.8534, 5.093]$, the network exhibits an oscillatory pattern with all phases equal to each other (full Synchronization). In accordance with this pattern, unstable eigenvalue has a corresponding eigenvector with all entries corresponding to different subsystems matching.
In this chapter, the phenomenon of Delay Induced Full Synchronization is described and analysed. As a result of the analysis, we can say that the full synchronization mode, emanating from the network equilibrium, is a result of the Hopf bifurcation of the synchronized equilibria. The phenomenon shows the importance of combining the local pattern analysis and bifurcation analysis, showing more global picture, when the complex networks are studied.

Chapter 6

Conclusions and Future directions

6.1 Conclusions

Complex networks are omnipresent in nature and can be used to describe a large amount of natural phenomena. Motivated by various applications in different scientific fields, scientists study complex networks and their phenomenology. This thesis focuses on the phenomenon of pattern formation in coupled nonlinear systems with either delayed or delay-free coupling. The goal of the thesis is to develop numerically efficient and simple to use methods for analysis of patterns that may exist (coexist) in such networks. The following setting has been used. The individual systems are Lur'e systems that are globally asymptotically stable in isolation, i.e. when the coupling is absent. When we assemble these systems into the network, the stability of the (network) equilibrium may be changed under parameter variation in the coupling and (stable and unstable) limit cycles may occur. The focus of the thesis is on cases when a Hopf bifurcation is the origin of the stability change and birth of the periodic solution. In some cases, several limit cycles or patterns may emanate from a bifurcation point and coexist for the same values of coupling parameters. Such situations make the analysis of the network behavior by common methods (e.g. the Lyapunov (delay-free case) and Lyapunov-Krasovskii (time-delay case) methods or the analysis of Poincaré maps) cumbersome and increase the demand for simple and numerically efficient methods of analysis.
The thesis introduces semi-analytical and numerical approaches aiming at detecting and approximating oscillatory profiles of (coexisting) patterns

that can be observed in complex networks. The analysis is based on the Multivariable Harmonic Balance (MHB) method, which is an extension of the harmonic balance method that can be applied to networked systems. The MHB analysis is complemented by different numerical approaches in order to detect Hopf bifurcation points, regions of instability, and the number and type of patterns in the regions under consideration. The presented methods are simple to use, scalable (for a special case), and numerically efficient. In addition, the presented approaches provide accurate starting points for numerical continuation procedures in order to compute exact oscillatory profiles of patterns with large amplitudes.

The first contribution of the study, introduced in Chapter 3, is a novel developed method (MHB) for pattern analysis in complex networks consisting of nonlinear systems of Lur'e type, which interact via a delay-free diffusive coupling. These oscillatory patterns, called oscillatory profiles, are characterized by a set of parameters, i.e. frequency, amplitudes, and relative phases. The chapter focuses on the case when the oscillations arise at a Hopf bifurcation (equivariant Hopf bifurcation), which means that the oscillations are sinusoidal in a neighbourhood of the bifurcation point. This justifies the application of the describing function method for linearising the nonlinearities and to analyse the network behavior by means of the harmonic balance method. Moreover, these oscillatory patterns may coexist for the same coupling parameters, which implies multistability of the network dynamics. Multistability makes the usage of common analytical tools, such as the direct Lyapunov method, highly involved. Motivated by these facts, the Multivariabe Harmonic Balance method for diffusively coupled Lur'e systems has been developed. In Chapter 3, the MHB equation for a network of delay-free diffusion coupled nonlinear systems is derived and it is shown that the method can accurately predict oscillatory patterns in such networks, even if some of them coexist. Two variants demonstrate the efficiency of the method, the variant targeting the equal amplitude case, and the variant for the general amplitude case. The equal amplitude case results in a semi-analytical method that can easily be applied using structural properties of the network. The method has favorable scaling properties in terms of the number of nodes in the network. The general amplitude case is numerically more challenging. A numerical optimization routine has been developed which determines the local minima of the MHB equation and therewith predicts stable (due to the type of bifurcation) oscillatory patterns in the search region.

Chapter 4 introduces the second contribution in the natural development of the MHB method, in the sense that the approach is extended and modified for networks whose interconnections are represented by time-delay coupling. Physically, the adopted delay model represents the time that a signal takes to propagate from its source to its destination, while the nodes have access to their own outputs immediately. Taking into account time-delay components makes the method applicable to many real world systems, such as networks of neurons, electrical circuits, networked control systems, etc. The focus of the study in the chapter is on the case where the oscillatory patterns in the complex network appear via either a subcritical or supercritical Hopf bifurcation. In the selected setting, we have two bifurcation parameters, whose complexity necessitates a complementary bifurcation analysis. Fast and efficient numerical tools have been developed, which help to avoid time-inefficient simulations of delay differential equations (DDEs) and which are able to handle coexisting periodic solutions. The Multivariable Harmonic Balance method is modified and extended for networked systems described by DDEs. In order to demonstrate the possibilities and efficiency of the method, it is applied to two illustrative networks in which subcritical and supercritical Hopf bifurcations occur. The study shows that the MHB approach can successfully compute an approximation of periodic solutions which appear in such networks, even if the periodic solutions are not located in a neighbourhood of the bifurcation point. In addition, a special case (namely equal amplitude case) of the MHB analysis is presented. The MHB equations for the equal amplitude case can be solved in a semi-analytical way because they exploit the structure of the networks, which helps to reduce the number of equations to solve. This semi-analytical approach is used as a verification tool for the presented numerical procedures. It is shown that the methods are numerically efficient, especially the MHB approach for the equal amplitude case, in comparison with the direct simulation approach. Moreover, the MHB method for delay coupled systems can simultaneously compute co-existing periodic solutions even if some of them are unstable and perform basic bifurcation analysis. In addition, we executed a bifurcation analysis of the delay coupled systems with the subcritical Hopf bifurcation by means of the software tool `ddebiftool`, using the MHB results as starting point for the continuation procedures.

The third contribution of the thesis (Chapter 5) reveals the phenomenon of delay induced full synchronization in delay coupled nonlinear systems. The phenomenon has been firstly observed in the complex network in-

troduced in Chapter 4 and motivated us to perform a theoretical and numerical analysis of the phenomenon, which is presented in Chapter 5. The coupling function used in the network has two interaction parameters, namely coupling strength γ and time delay τ, which take the role of bifurcation parameters. It is shown that for fixed γ, the full synchronization regime can be achieved by varying the time-delay parameter τ. The full synchronization mode cannot be observed in such networks with delay-free coupling, which is shown in Chapter 3 for the network with the same individual node dynamics but delay-free diffusive coupling. The goal of the analysis is to study whether the phenomenon of delay induced full synchronization is a result of a bifurcation of the network equilibria. In order to give a positive answer to this question, the following analytical techniques and numerical approaches have been used.

The analytical approach, consisting of the stability analysis of synchronized equilibria presented in [134], shows the possible regimes that may emerge from bifurcations of equilibria. The result implies that, in the neighbourhood of the synchronized equilibrium, the network topology mostly affects the variety of the regimes which can be observed in such networks. An oscillatory pattern (frequency and relative phases) is defined by an eigenpair of the coupling matrix (unstable eigenvalue and its corresponding eigenvector), while amplitudes are mainly determined by the nonlinearity of the individual dynamics of a node.

The pattern analysis is performed isung the Multivariable Harmonic Balance method for time delay systems, presented in Chapter 4. Such an analysis by means of the MHB approach is the simplest way to compute simultaneously coexisting patterns for the same coupling parameters, which is essential for understanding the network behavior, especially in the case of two and more coexisting patterns. The pattern analysis confirms the results of the stability analysis of synchronized equilibria and supports the results of the numerical bifurcation analysis.

The numerical bifurcation analysis is performed using the `ddebiftool` software and is used to support and complement the analytical results and the MHB approach. By means of `ddebiftool`, the bifurcation diagram in the (γ,τ)-parameter space has been constructed, depicting the network behavior as a function of the selected parameter intervals. The `ddebiftool` analysis also shows that there exist regions in which different patterns coexist for the same parameter values, matching with the results of the MHB analysis. The bifurcation analysis by means of `ddebiftool` shows that for fixed γ and some interval of values of τ, the network exhibits a fully synchronized periodic solution, while outside of the interval another

patterns are observed. In accordance to such a pattern, the eigenvalue with positive real part has a corresponding eigenvector with all entries corresponding to different subsystems matching.
As a result of the combined analysis, it can be said that the full synchronization regime, emanating from the network equilibrium, is a result of the Hopf bifurcation of the synchronized equilibria. The study of the phenomenon shows the importance of combining the pattern analysis and bifurcation analysis, which complement and support each other and, in this way, lead to a more global picture of the dynamics.

In this thesis, we have presented the novel developed approaches for pattern and bifurcation analysis based on the MHB method. The MHB analysis is applicable for networks consisting of nonlinear systems of Lur'e type with delay and delay-free coupling. It has been shown that the method is simple to use, numericaly efficient and scalable (for cases where all amplitudes are equal in magnitude). We studied different possibilities of the MHB approach, namely detecting stable and unstable regimes, coexisting patterns and, we introduced and analysed a new phenomenon, called delay induced full synchronization.

6.2 Future directions

In this section, some possible future research directions, which are directly related to the work reported in this thesis, are described.

6.2.1 The generalized MHB method

So far, the Multivariable Harmonic Balance method has been developed and applied to complex networks whose individual dynamics of nodes have a scalar nonlinear function as an internal feedback structure. This limitation is due to the approach which is used to approximate the nonlinearity, called the describing function method. The main problem of the limitation is that the MHB method can only be applied to special type of systems, such as Lur'e systems. The generalization of the methods presented in this thesis to dynamical systems with not only scalar nonlinearity will highly increase the applicability of the developed approaches and simplify the investigation and analysis of emergent behavior observed in complex networks, for instance, by predicting synchronization and partial synchronization regimes in coupled Hindmarsh–Rose neurons [132] [150]. The

work presented in [151] can be taken as a starting point of the research in this direction.

6.2.2 Network structure synthesis

The purpose of the analysis is to gain insight into the behavior of a system or coupled systems. The next step is to use this knowledge to do something with the system, for instance, implement a system model directly, design a system showing the same phenomenology or to perform a control of the system or network. One possible future research direction for the methods, presented in this thesis, is to use the understanding of the pattern formation phenomenon in complex networks in order to design or synthesize a network showing desired behavior in terms of frequency, offset, amplitudes, and relative phases.
The numerical analysis presented in this thesis and the theoretical work on the stability analysis of synchronized equilibria [134] have shown that an oscillatory profile (frequency and relative phases) is related to a pattern in the eigenvectors of the graph Laplacian or adjacency matrix, depending on the coupling. Based on this observation, the Multivariable Harmonic Balance equation for delay-free systems (3.14) and the MHB equations for delay-coupled systems (4.21-4.22) may be used, when the desired pattern is chosen, to compute the network structure (Laplacian or adjacency matrix), which satisfies the desired pattern. These desired patterns may correspond to fully synchronization motion, a partial synchronization regime with two or more clusters, or rotating/travelling waves. Such an approach can find its applications in different fields, for example, in networked robotics [152]. It is worth mentioning that the possible patterns, partial synchronization manifolds, etc. are determined by the coupling matrix. Designing this matrix should be considered as only a first step. In order to observe these patterns in practise, they need to be stable. Here, the individual node dynamics and the parameters of the coupling come in.

6.2.3 Local controller for networks with coexisting patterns

Another possible direction of the research is to use the understanding of the behavior of the complex network for control purposes. There are many projects aiming at this objective, for example, the UCoCoS (Understanding and Controlling Complex Systems) project. In terms of

control of complex networks, I wish to highlight two main objectives, namely stabilizing the dynamics (patterns) of the networks by means of decentralized control strategies [153] [154] and "choosing" between coexisting patterns using a local control strategy [155] [156]. The idea behind the second objective is to design a local controller (applied to one node or a cluster of nodes in a network) to make one or more of coexisting patterns unstable. In Chapter 3 and Chapter 5, it has been observed in the case-studies that the number of unstable eigenvalues of the linearised network dynamics around the equilibrium point matches with the number of stable oscillatory profiles in the complex networks whose individual dynamics of nodes satisfy the assumptions presented in the chapters. Moreover, each oscillatory profile relates to the structure of the corresponding eigenvector. In Chapter 3, the case has been studied where two rotating waves (clockwise and counterclockwise) coexist. This situation is related to the condition that the unstable eigenvalue has algebraic and geometric multiplicity 2. Depending on the initial conditions, the network exhibits one of the coexisting patterns. In order to avoid selecting the initial conditions, a local controller can be designed to break the symmetry or to make the real part of one of the eigenvalues negative [157], which may render one of the coexisting patterns unstable.

References

[1] J. Goldstein. “Emergence as a Construct: History and Issues”. In: *Emergence* 1.1 (1999), pp. 49–72.

[2] S. Camazine, J.L. Deneubourg, N.R. Franks, J. Sneyd, E. Bonabeau, and G. Theraula. *Self-organization in Biological Systems*. Princeton Studies in Complexity. Princeton University Press, 2003.

[3] G. Flierl, D. Grünbaum, S. Levin, and D. Olson. “From individuals to aggregations: The interplay between behavior and physics”. In: *Journal of theoretical biology* 196.4 (1999), pp. 397–454.

[4] M. Dorigo and L. M. Gambardella. “Ant colony system: A cooperative learning approach to the traveling salesman problem”. In: *IEEE Transactions on Evolutionary Computation* 1.1 (1997), pp. 53–66.

[5] F. Cucker and S. Smale. “Emergent behavior in flocks”. English. In: *IEEE Transactions on Automatic Control* 52.5 (2007), pp. 852–862.

[6] H. Ling, G.E. Mclvor, J. Westley, K. van der Vaart, R. T. Vaughan, A. Thornton, and N.T. Ouellette. “Behavioural plasticity and the transition to order in jackdaw flocks”. In: *Nature Communications* 10 (2019).

[7] T. Vicsek, A. Czirk, E. Ben-Jacob, I. Cohen, and O. Shochet. “Novel type of phase transition in a system of self-driven particles”. In: *Physical Review Letters* 75.6 (1995), pp. 1226–1229.

[8] S. Haykin. “Cognitive radio: Brain-empowered wireless communications”. In: *IEEE Journal on Selected Areas in Communications* 23.2 (2005), pp. 201–220.

[9] W. Karwowski. “A review of human factors challenges of complex adaptive systems: Discovering and understanding chaos in human performance”. In: *Human factors* 54.6 (2012), pp. 983–995.

[10] T. E. Drabek and D. A. McEntire. “Emergent phenomena and the sociology of disaster: Lessons, trends and opportunities from the research literature”. In: *Disaster Prevention and Management: An International Journal* 12.2 (2003), pp. 97–112.

[11] G. Abramson and M. Kuperman. “Social games in a social network”. In: *Physical Review E - Statistical Physics, Plasmas, Fluids, and Related Interdisciplinary Topics* 63.3 (2001).

[12] J.M. Smith. *Evolution and the Theory of Games*. Cambridge University Press, 1982.

[13] A. Buka. “Pattern Formation in Liquid Crystals”. In: *Physica Scripta* 1989 (Feb. 2007), p. 114.

[14] D. M. Walker and A. Tordesillas. “Topological evolution in dense granular materials: A complex networks perspective”. In: *International Journal of Solids and Structures* 47.5 (2010), pp. 624–639.

[15] W. Wang, W. Duan, S. Ahmed, T. E. Mallouk, and A. Sen. “Small power: Autonomous nano- and micromotors propelled by self-generated gradients”. In: *Nano Today* 8.5 (2013), pp. 531–554.

[16] A. Barabasi and R. Albert. “Emergence of scaling in random networks”. In: *Science* 286.5439 (1999), pp. 509–512.

[17] I. Karamouzas, P. Heil, P. Van Beek, and M. H. Overmars. *A predictive collision avoidance model for pedestrian simulation*. Vol. 5884 LNCS. Lecture Notes in Computer Science (including subseries Lecture Notes in Artificial Intelligence and Lecture Notes in Bioinformatics). 2009, pp. 41–52.

[18] A. Filotheou, A. Nikou, and D. V. Dimarogonas. “Robust decentralised navigation of multi-agent systems with collision avoidance and connectivity maintenance using model predictive controllers”. In: *International Journal of Control* 93.6 (2020), pp. 1470–1484.

[19] A. Medina, A. Lakhina, I. Matta, and J. Byers. “BRITE: An approach to universal topology generation”. In: *IEEE International Workshop on Modeling, Analysis, and Simulation of Computer and Telecommunication Systems - Proceedings*. 2001, pp. 346–353.

[20] K. Aberer, P. Cudré-Mauroux, and M. Hauswirth. “The chatty web: Emergent semantics through gossiping”. In: *Proceedings of the 12th International Conference on World Wide Web, WWW 2003*. 2003, pp. 197–206.

[21] M. C. Schut. “On model design for simulation of collective intelligence”. In: *Information Sciences* 180.1 (2010), pp. 132–155.

[22] G. Deco, V. K. Jirsa, P. A. Robinson, M. Breakspear, and K. Friston. “The dynamic brain: From spiking neurons to neural masses and cortical fields”. In: *PLoS Computational Biology* 4.8 (2008).

[23] L. Perea, G. Gómez, and P. Elosegui. “Extension of the cucker-smale control law to space flight formations”. In: *Journal of Guidance, Control, and Dynamics* 32.2 (2009), pp. 526–536.

[24] J. S. Baras, X. Tan, and P. Hovareshti. “Decentralized Control of Autonomous Vehicles”. In: *Proceedings of the IEEE Conference on Decision and Control*. Vol. 2. 2003, pp. 1532–1537.

[25] K. M. Passino. “Biomimicry of Bacterial Foraging for Distributed Optimization and Control”. In: *IEEE Control Systems* 22.3 (2002), pp. 52–67.

[26] N. E. Leonard and E. Fiorelli. “Virtual leaders, artificial potentials and coordinated control of groups”. In: *Proceedings of the IEEE Conference on Decision and Control*. Vol. 3. 2001, pp. 2968–2973.

[27] R. Damper. “Editorial for the Special Issue on ’Emergent Properties of Complex Systems’: Emergence and levels of abstraction”. In: *International Journal of Systems Science* 31 (2000), pp. 811 –818.

[28] A. Mugler and B. Sun. “Special issue on emergent collective behaviour from groups of cells”. In: *Physical Biology* 15.6 (2018), p. 060202.

[29] R. Cox, R. Den Hartigh, M. Richardson, C. Yu, and T. Frank. “Complex Dynamical Systems in Human Development”. In: *Complexity* 2019 (July 2019).

[30] J. Na, Z. Yang, S. Kamal, L. Hu, W. Wang, and Y. Zhou. “Bio-Inspired Learning and Adaptation for Optimization and Control of Complex Systems”. In: *Complexity* 2019 (Apr. 2019), pp. 1–3.

[31] M. Qiu, S. Garg, R. Buyya, B. Yu, and S. Hu. “Special Issue on Scalable Cyber-Physical Systems”. In: *Journal of Parallel and Distributed Computing* (2017).

[32] M. Gardner. “Mathematical Games: The Remarkable Lore of the Prime Number”. In: *Journal of Applied Physics* 210 (1964), 120–128.

[33] J. Nittmann and H.E. Stanley. “Non-deterministic approach to anisotropic growth patterns with continuously tunable morphology: the fractal properties of some real snowflakes”. In: *Journal of Physics A: Mathematical and General* 20.17 (1987), pp. L1185–L1191.

[34] S. Marsland, J. Shapiro, and U. Nehmzow. “A self-organising network that grows when required”. In: *Neural Netw* 15 (2002), pp. 1041–1058.

[35] B.G. Elmegreen. “Star Formation Patterns and Hierarchies”. In: *EAS Publications Series* 51 (2011), 31–44.

[36] L. Shamir. *Multipole alignment in the large-scale distribution of spin direction of spiral galaxies*. 2020. arXiv: 2004.02963 [astro-ph.GA].

[37] S. Strogatz. *Sync: The Emerging Science of Spontaneous Order*. Hyperion Press, 2003.

[38] I.I. Blekhman. *Synchronization in science and technology*. ASME Press, 1988.

[39] M. Nagy, I. D. Couzin, W. Fiedler, M. Wikelski, and A. Flack. “Synchronization, coordination and collective sensing during thermalling flight of freely migrating white storks”. In: *Philosophical Transactions of the Royal Society B: Biological Sciences* 373.1746 (2018), p. 20170011.

[40] A. Ravignani, D. L. Bowling, and W. T. Fitch. “Chorusing, synchrony, and the evolutionary functions of rhythm”. In: *Frontiers in Psychology* 5 (2014), p. 1118.

[41] U. Amin, G. Ahmad, S. Zahoor, and F. Durrani. “Implementation of Parallel Synchronization Method of Generators for Power and Cost Saving in University of Gujrat”. In: *Energy and Power Engineering* 6 (2014), pp. 317–332.

[42] E. Rossoni, J. Feng, B. Tirozzi, D. Brown, G. Leng, and F. Moos. “Emergent Synchronous Bursting of Oxytocin Neuronal Network”. In: *PLOS Computational Biology* 4.7 (July 2008), pp. 1–12.

[43] V. Makarov. “Why is the Moon synchronously rotating?” In: *Monthly Notices of the Royal Astronomical Society* 434 (May 2013), p. L21.

[44] C.M. Gray. “Synchronous oscillations in neuronal systems: Mechanisms and functions”. In: *Journal of Computational Neuroscience* 1 (June 1994), pp. 11–38.

[45] D. M. Abrams and S. H. Strogatz. “Chimera States for Coupled Oscillators”. In: *Phys. Rev. Lett.* 93 (17 2004), p. 174102.

[46] Y. Kuramoto. *Chemical Oscillations, Waves, and Turbulence*. Springer Series in Synergetics. Springer-Verlag Berlin Heidelberg, 1984.

[47] L. Schmidt, K. Schönleber, K. Krischer, and V. García-Morales. “Coexistence of synchrony and incoherence in oscillatory media under nonlinear global coupling”. In: *Chaos: An Interdisciplinary Journal of Nonlinear Science* 24.1 (2014), p. 013102.

[48] A. M. Hagerstrom, T. E. Murphy, R. Roy, P. Hovel, I. Omelchenko, and Eckehard Schöll. “Experimental observation of chimeras in coupled-map lattices”. In: *Nature Physics* 8.9 (2012), pp. 658–661.

[49] J. Sawicki, I. Omelchenko, A. Zakharova, and E. Scholl. “Delay-induced chimeras in neural networks with fractal topology”. In: *The European Physical Journal B* 92.3 (2019).

[50] S. Shahal, A. Wurzberg, I. Sibony, E. Shniderman, D. Weymouth, N. Davidson, and M. Fridman. “Synchronization of complex human networks”. In: *Nature Communications* 11.1 (2020).

[51] T. Iwasaki, J. Chen, and W. O. Friesen. “Biological clockwork underlying adaptive rhythmic movements”. In: *Proceedings of the National Academy of Sciences* 111.3 (2014), pp. 978–983.

[52] V. M. Lauschke, C. D. Tsiairis, P. François, and A Aulehla. “Scaling of embryonic patterning based on phase-gradient encoding”. In: *Nature* 493 (2013).

[53] G.B. Ermentrout and D. Kleinfeld. “Traveling Electrical Waves in Cortex: Insights from Phase Dynamics and Speculation on a Computational Role”. In: *Neuron* 29.1 (2001), pp. 33 –44.

[54] M. Sebek, R. Tönjes, and I.Z. Kiss. “Complex Rotating Waves and Long Transients in a Ring Network of Electrochemical Oscillators with Sparse Random Cross-Connections”. In: *Phys. Rev. Lett.* 116 (6 2016), p. 068701.

[55] Y. Dou, S. Pandey, C. A. Cartier, O. Miller, and K. J. M. Bishop. “Emergence of traveling waves in linear arrays of electromechanical oscillators”. In: *Communications Physics* 1 (1 2018).

[56] L. Harnefors and H.P. Nee. “Power-Synchronization Control of Grid-Connected Voltage-Source Converters”. In: *Power Systems, IEEE Transactions on* 25 (June 2010), pp. 809 –820.

[57] L. M. Pecora and T. L. Carroll. “Synchronization of chaotic systems”. In: *Chaos: An Interdisciplinary Journal of Nonlinear Science* 25.9 (2015), p. 097611.

[58] P. Jiruska, M. de Curtis, J. G. Jefferys, C. A. Schevon, S. J. Schiff, and K. Schindler. “Synchronization and desynchronization in epilepsy: controversies and hypotheses”. In: *The Journal of physiology* 591.4 (2013), 787—797.

[59] L. B. Good, S. Sabesan, S. T. Marsh, K. Tsakalis, D. Treiman, and L. Iasemidis. “Control of synchronization of brain dynamics leads to control of epileptic seizures in rodents”. In: *International journal of neural systems* 19.3 (2009), 173—196.

[60] K.Y. Pettersen, J.T. Gravdahl, and H. Nijmeijer, eds. *Group coordination and cooperative control*. English. Lecture notes in control and information sciences. Germany: Springer, 2006.

[61] H. Nijmeijer and A. Rodriguez Angeles. *Synchronization of mechanical systems*. English. World Scientific series on nonlinear science : Series A. United States: World Scientific, 2003.

[62] G.J.L. Naus, R.P.A. Vugts, J. Ploeg, M.J.G. van de Molengraft, and M. Steinbuch. “String-stable CACC design and experimental validation, a frequency-domain approach”. In: *IEEE Transactions on Vehicular Technology* 59.9 (2010), pp. 4268–4279.

[63] A. Taylor, G.W. Cottrell, and W.B. Kristan. “A model of the leech segmental swim central pattern generator”. In: *Neurocomputing* 32-33 (2000), pp. 573 –584.

[64] P. Atoofi, F. H. Hamker, and J. Nassour. “Learning of Central Pattern Generator Coordination in Robot Drawing”. In: *Frontiers in Neurorobotics* 12 (2018), p. 44.

[65] J. Buchli and A. J. Ijspeert. “Distributed Central Pattern Generator Model for Robotics Application Based on Phase Sensitivity Analysis”. In: *Biologically Inspired Approaches to Advanced Information Technology*. Ed. by A. J. Ijspeert, M. Murata, and N. Wakamiya. Berlin, Heidelberg: Springer Berlin Heidelberg, 2004, pp. 333–349.

[66] S. Roth. “Mathematics and biology: A Kantian view on the history of pattern formation theory”. In: *Development genes and evolution* 221.5-6 (2011), pp. 255–279.

[67] A.M. Turing. “The Chemical Basis of Morphogenesis”. In: *Philosophical Transactions of the Royal Society of London. Series B, Biological Sciences* 237.641 (1952), pp. 37–72.

[68] S. Kondo and T. Miura. “Reaction-diffusion model as a framework for understanding biological pattern formation”. In: *Science* 329.5999 (2010), pp. 1616–1620.

[69] A. Gierer and H. Meinhardt. “A theory of biological pattern formation”. In: *Kybernetik* 12.1 (1972), pp. 30–39.

[70] G. Nicolis and A. D. Wit. “Reaction-diffusion systems”. In: *Scholarpedia* 2.9 (2007). revision #137222, p. 1475.

[71] S. Smale. “A Mathematical Model of Two Cells Via Turing’s Equation”. In: *The Hopf Bifurcation and Its Applications*. Springer New York, 1976, pp. 354–367.

[72] V. Yakubovich and E. Tomberg. “Conditions for auto-oscillations in nonlinear systems”. In: *Siberian Mathematical Journal* 30.4 (1989), pp. 641–653.

[73] E. Tomberg and V. Yakubovich. “On one problem of Smale”. In: *Siberian Mathematical Journal* 4.41 (2000), pp. 771–774.

[74] A. Pogromsky, T. Glad, and H. Nijmeijer. “on Diffusion Driven Oscillations in Coupled Dynamical Systems”. In: *International Journal of Bifurcation and Chaos* 09.04 (1999), pp. 629–644.

[75] A. Pogromsky, N. Kuznetsov, and G. Leonov. “Pattern generation in diffusive networks: How do those brainless centipedes walk?” In: *Proceedings of the IEEE Conference on Decision and Control* (2011), pp. 7849–7854.

[76] O.E. Lowenstein, Osborne M., and J. Wersäll. “Structure and innervation of the sensory epithelia of the labyrinth in the Thornback ray”. In: *Proceedings of the Royal Society of London. Series B. Biological Sciences* 160.978 (1964), pp. 1–12.

[77] M. Han and P. Yu. “Hopf Bifurcation and Normal Form Computation”. In: *Normal Forms, Melnikov Functions and Bifurcations of Limit Cycles*. Vol. 181. Springer London, 2012, pp. 7–58.

[78] Y.A. Kuznetsov. *Elements of Applied Bifurcation Theory (2Nd Ed.)* Berlin, Heidelberg: Springer-Verlag, 1998.

[79] W. Hahn. “The Direct Method of Liapunov”. In: *Stability of Motion*. Berlin, Heidelberg: Springer Berlin Heidelberg, 1967, pp. 93–165.

[80] E. Fridman. *Introduction to Time-Delay Systems*. Systems and Control: Foundations and Applications. Springer International Publishing, 2014.

[81] J.K. Hale. “Diffusive coupling, dissipation, and synchronization”. In: *Journal of Dynamics and Differential Equations* 9.1 (1997), pp. 1–52.

[82] E. Steur and A. Pogromsky. “Emergence of Oscillations in Networks of Time-Delay Coupled Inert Systems”. In: *Nonlinear Systems: Techniques for Dynamical Analysis and Control*. Ed. by Nathan van de Wouw, Erjen Lefeber, and Ines Lopez Arteaga. Cham: Springer International Publishing, 2017, pp. 137–154.

[83] M. Dhamala, V.K. Jirsa, and M. Ding. “Enhancement of Neural Synchrony by Time Delay”. In: *Phys. Rev. Lett.* 92 (7 2004), p. 074104.

[84] D. V. Ramana Reddy, A. Sen, and G. L. Johnston. “Experimental Evidence of Time-Delay-Induced Death in Coupled Limit-Cycle Oscillators”. In: *Phys. Rev. Lett.* 85 (16 2000), pp. 3381–3384.

[85] R. Sipahi, S. Niculescu, C. T. Abdallah, W. Michiels, and K. Gu. “Stability and Stabilization of Systems with Time Delay”. In: *IEEE Control Systems Magazine* 31.1 (2011), pp. 38–65.

[86] W.A. Zuniga-Galindo. “Reaction-diffusion equations on complex networks and Turing patterns, via p-adic analysis”. In: *Journal of Mathematical Analysis and Applications* 491.1 (2020), p. 124239.

[87] E. Schöll. “Synchronization patterns and chimera states in complex networks: Interplay of topology and dynamics”. In: *The European Physical Journal Special Topics* 225 (Sept. 2016), pp. 891–919.

[88] B. Yang, J. Liu, and D. Liu. “Characterizing and Extracting Multiplex Patterns in Complex Networks”. In: *IEEE Transactions on Systems, Man, and Cybernetics, Part B (Cybernetics)* 42.2 (2012), pp. 469–481.

[89] A. Mees and A. Bergen. “Describing functions revisited”. In: *IEEE Transactions on Automatic Control* 20.4 (1975), pp. 473–478.

[90] T. Iwasaki. “Multivariable harmonic balance for central pattern generators”. In: *Automatica* 44.12 (2008), pp. 3061–3069.

[91] K. Rogov, A. Pogromsky, E. Steur, W. Michiels, and H. Nijmeijer. "Pattern Prediction in Networks of Diffusively Coupled Nonlinear Systems". In: *IFAC-PapersOnLine* 51.33 (2018). 5th IFAC Conference on Analysis and Control of Chaotic Systems CHAOS 2018, pp. 62 –67.

[92] K. Rogov, A. Pogromsky, E. Steur, W. Michiels, and H. Nijmeijer. "Pattern Analysis in Networks of Diffusively Coupled Lur'e Systems". In: *International Journal of Bifurcation and Chaos* 29.14 (2019), p. 1950200.

[93] K. Rogov, A. Pogromsky, E. Steur, W. Michiels, and H. Nijmeijer. "Pattern Analysis in Networks of Delayed Coupled Nonlinear Systems". In: *2020 European Control Conference (ECC)*. 2020.

[94] K. Rogov, A Pogromsky, E. Steur, W. Michiels, and H. Nijmeijer. "Detecting coexisting oscillatory patterns in delay coupled Lur'e systems". In: *Chaos: An Interdisciplinary Journal of Nonlinear Science* 31.3 (2021), p. 033114.

[95] A. Pavlov, N. Wouw, van de, and H. Nijmeijer. *Uniform output regulation of nonlinear systems : a convergent dynamics approach*. Systems and control : foundations and applications. Switzerland: Birkhäuser Verlag, 2006.

[96] H. K. Khalil. *Nonlinear Systems*. Prentice-Hall, New Jersey, 1996.

[97] C. Koch. *Biophysics of computation: Information processing in single neurons*. New York: Oxford University Press, 1999.

[98] D. Arrowsmith and C.M. Place. *Dynamical Systems*. Taylor and Francis, 1992.

[99] J. C. Willems. "Dissipative dynamical systems part I: General theory". In: *Archive for Rational Mechanics and Analysis* 45.5 (1972), pp. 321–351.

[100] J. C. Willems. "Dissipative dynamical systems Part II: Linear systems with quadratic supply rates". In: *Archive for Rational Mechanics and Analysis* 45.5 (1972), pp. 352–393.

[101] A. Pogromsky. "Passivity Based Design of Synchronizing Systems". In: *International Journal of Bifurcation and Chaos* 8 (Feb. 1998).

[102] R. Lozano, B. Maschke, B. Brogliato, and O. Egeland. *Dissipative Systems Analysis and Control: Theory and Applications*. Berlin, Heidelberg: Springer-Verlag, 2000.

[103] D. Hill and P. Moylan. “The stability of nonlinear dissipative systems”. In: *IEEE Transactions on Automatic Control* 21.5 (1976), pp. 708–711.

[104] J.K. Hale and S. Verduyn Lunel. “Introduction to Functional Differential Equations”. In: vol. 99. Springer-Verlag, Jan. 1993.

[105] A. Halanay. *Differential Equations: Stability, Oscillations, Time Lags*. Vol. 23. Mathematics in Science and Engineering. Elsevier, 1966.

[106] E. Fridman. “New Lyapunov–Krasovskii functionals for stability of linear retarded and neutral type systems”. In: *Systems and Control Letters* 43.4 (2001), pp. 309–319.

[107] E. Fridman. “Tutorial on Lyapunov-based methods for time-delay systems”. In: *Eur. J. Control* 20 (2014), pp. 271–283.

[108] K. Gu, V.L. Kharitonov, and J. Chen. *Stability of Time-Delay Systems*. Control Engineering. Birkhäuser Basel, 2003.

[109] Y. A. Kuznetsov. “Andronov-Hopf bifurcation”. In: *Scholarpedia* 1.10 (2006), p. 1858.

[110] J. Guckenheimer. “Bifurcations of Dynamical Systems”. In: *Dynamical Systems*. Ed. by C. Marchioro. Berlin, Heidelberg: Springer Berlin Heidelberg, 2011, pp. 5–123.

[111] J.K. Hale. *Theory of Functional Differential Equations*. Springer-Verlag New York, 1977, p. 366.

[112] T. Faria and L. Magalhaes. “Normal Forms for Retarded Functional Differential Equations with Parameters and Applications to Hopf Bifurcation”. In: *Journal of Differential Equations* 122 (Nov. 1995), pp. 181–200.

[113] T. Faria. “Normal forms for periodic retarded functional differential equations”. In: *Proceedings of the Royal Society of Edinburgh: Section A Mathematics* 127.1 (1997), 21–46.

[114] A. Pikovsky, M. Rosenblum, and J. Kurths. *Synchronization*. Cambridge Nonlinear Science Series. Cambridge University Press, 2001.

[115] A. Pogromsky and H. Nijmeijer. “Cooperative oscillatory behavior of mutually coupled dynamical systems”. In: *IEEE Transactions on Circuits and Systems I: Fundamental Theory and Applications* 48.2 (2001), pp. 152–162.

[116] M. Golubitsky, I. Stewart, P. Buono, and J. J. Collins. “Symmetry in locomotor central pattern generators and animal gaits”. In: *Nature* 401.6754 (1999), pp. 693–695.

[117] H. Nakao and A. S. Mikhailov. “Turing patterns in network-organized activator-inhibitor systems”. In: *Nature Physics* 6 (2010), pp. 544–550.

[118] A. Gorban, N. Jarman, E. Steur, C. van Leeuwen, and I. Tyukin. “Leaders Do Not Look Back, or Do They?” In: *Math. Model. Nat. Phenom.* 10.3 (2015), pp. 212–231.

[119] A. Gorban, N. Jarman, E. Steur, H. Nijmeijer, C. van Leeuwen, and I. Tyukin. “Directed cycles and multi-stability of coherent dynamics in systems of coupled nonlinear oscillators”. In: *IFAC-PapersOnLine* 48.18 (2015). 4th IFAC Conference on Analysis and Control of Chaotic Systems CHAOS 2015, pp. 19 –24.

[120] S. Gershgorin. “Uber die Abgrenzung der Eigenwerte einer Matrix”. In: *Bulletin de l’Académie des Sciences de l’URSS. Classe des sciences mathématiques et na* 6 (1931), pp. 749–754.

[121] V. Yakubovich. “Frequency conditions for auto-oscillations in nonlinear systems with one stationary nonlinearity”. In: *Siberian Mathematical Journal* 14.5 (1973), pp. 768–788.

[122] Z. Balanov. “Equivariant Hopf Theorem”. In: *Nonlinear Analysis: Theory, Methods and Applications* 30 (1997), 3463—3474.

[123] T. Glad and L. Ljung. *Control theory - multivariable and nonlinear methods*. Taylor and Francis, 2000.

[124] W.K. Chen. *Graph Theory and Its Engineering Applications*. Advanced series in electrical and computer engineering. World Scientific, 1997.

[125] D.S. Dummit and R.M. Foote. *Abstract Algebra (2nd ed.)* New York: Wiley, 1999, pp. 336–337.

[126] MATLAB. *MATLAB Optimization Toolbox (R2017a)*. Natick, Massachusetts: The MathWorks Inc., 2017.

[127] R.H. Byrd, Jean Charles Gilbert, and Jorge Nocedal. “A trust region method based on interior point techniques for nonlinear programming”. In: *Mathematical Programming* 89.1 (2000), pp. 149–185.

[128] Z. Ugray, L. Lasdon, J. Plummer, F. Glover, J. Kelly, and R. Martí. "Scatter Search and Local NLP Solvers: A Multistart Framework for Global Optimization". In: *INFORMS Journal on Computing* 19.3 (2007), pp. 328–340.

[129] J. R. Dormand and P. J. Prince. "A family of embedded Runge-Kutta formulae". In: *J. Comp. Appl. Math.* 6 (1980), 19–26.

[130] M. Golubitsky, M. Nicol, and I. Stewart. "Some Curious Phenomena in Coupled Cell Networks". In: *Journal of Nonlinear Science* 14 (2004), 207—236.

[131] J.S. Climaco and A. Saa. "Optimal global synchronization of partially forced Kuramoto oscillators". In: *Chaos: An Interdisciplinary Journal of Nonlinear Science* 29.7 (2019), p. 073115.

[132] L. Su, Y. Wei, W. Michiels, E. Steur, and H. Nijmeijer. "Robust partial synchronization of delay-coupled networks". In: *Chaos: An Interdisciplinary Journal of Nonlinear Science* 30.1 (2020), p. 013126.

[133] D. J. Allwright. "Harmonic balance and the Hopf bifurcation". In: *Mathematical Proceedings of the Cambridge Philosophical Society* 82.3 (1977), 453–467.

[134] W. Michiels and H. Nijmeijer. "Synchronization of delay-coupled nonlinear oscillators: An approach based on the stability analysis of synchronized equilibria". In: *Chaos: An Interdisciplinary Journal of Nonlinear Science* 19.3 (2009), p. 033110.

[135] E. Steur and H. Nijmeijer. "Synchronization in Networks of Diffusively Time-Delay Coupled (Semi-)Passive Systems". In: *IEEE Transactions on Circuits and Systems I: Regular Papers* 58.6 (2011), pp. 1358–1371.

[136] T.A. Burton. "Limit Sets, Periodicity, and Stability". In: *Stability and Periodic Solutions of Ordinary and Functional Differential Equations*. Ed. by T.A. Burton. Vol. 178. Mathematics in Science and Engineering. Elsevier, 1985, pp. 197 –324.

[137] E. Steur, T. Oguchi, C. van Leeuwen, and H. Nijmeijer. "Partial synchronization in diffusively time-delay coupled oscillator networks". In: *Chaos: An Interdisciplinary Journal of Nonlinear Science* 22.4 (2012), p. 043144.

[138] J. Kato. "An autonomous system whose solutions are uniformly ultimately bounded but not uniformly bounded". In: *Tohoku Math. J. (2)* 32.4 (1980), pp. 499–504.

[139] W. Michiels and S. Niculescu. *Stability and Stabilization of Time-Delay Systems*. Society for Industrial and Applied Mathematics, 2007.

[140] E. Jarlebring. "Critical delays and polynomial eigenvalue problems". In: *Journal of Computational and Applied Mathematics* 224.1 (2009), pp. 296 –306.

[141] J. Brewer. "Kronecker products and matrix calculus in system theory". In: *IEEE Transactions on Circuits and Systems* 25.9 (1978), pp. 772–781.

[142] A. Ergenc, N. Olgac, and H. Fazelinia. "Extended Kronecker Summation for Cluster Treatment of LTI Systems with Multiple Delays". In: *SIAM Journal on Control and Optimization* 46.1 (2007), pp. 143–155.

[143] J. Sieber, K. Engelborghs, T. Luzyanina, G Samaey, and D. Roose. *DDE-BIFTOOL Manual - Bifurcation analysis of delay differential equations*. 2014. arXiv: `1406.7144 [math.DS]`.

[144] Martin Golubitsky and Ian Stewart. "Rigid patterns of synchrony for equilibria and periodic cycles in network dynamics". In: *Chaos: An Interdisciplinary Journal of Nonlinear Science* 26.9 (2016), p. 094803.

[145] Martin Golubitsky, Leopold Matamba Messi, and Lucy E. Spardy. "Symmetry types and phase-shift synchrony in networks". In: *Physica D: Nonlinear Phenomena* 320 (2016), pp. 9 –18. ISSN: 0167-2789.

[146] Zh. Wu and W. Michiels. "Reliably computing all characteristic roots of delay differential equations in a given right half plane using a spectral method". In: *Journal of Computational and Applied Mathematics* 236.9 (2012), pp. 2499 –2514.

[147] R. FitzHugh. "Impulses and Physiological States in Theoretical Models of Nerve Membrane". In: *Biophysical Journal* 1.6 (1961), pp. 445 –466.

[148] E. Steur, I. Tyukin, and H. Nijmeijer. "Semi-passivity and synchronization of diffusively coupled neuronal oscillators". In: *Physica D: Nonlinear Phenomena* 238.21 (2009), pp. 2119 –2128.

[149] J. Guckenheimer and Y.A. Kuznetsov. "Bogdanov-Takens bifurcation". In: *Scholarpedia* 2.1 (2007), p. 1854.

[150] D.M. Semenov and A.L. Fradkov. “Adaptive synchronization for the heterogeneous network of Hindmarsh-Rose neurons”. In: *European Control Conference 2020, ECC 2020*. 2020, pp. 306–308.

[151] V. Vander, E. Wallace, and A. Gelb. *Multiple-input describing functions and nonlinear system design*. New York : McGraw-Hill, 1968.

[152] A. Sanfeliu, N. Hagita, and A. Saffiotti. “Network robot systems”. In: *Robotics and Autonomous Systems* 56 (Oct. 2008), pp. 793–797.

[153] D. Dileep, J. Thomas, L. Hetel, N. van de Wouw, J.-P. Richard, and W. Michiels. “Design of L2 stable fixed-order decentralised controllers in a network of sampled-data systems with time-delays”. In: *European Journal of Control* 56 (2020), pp. 73 –85.

[154] D. Dileep, R. Van Parys, G. Pipeleers, L. Hetel, J.-P. Richard, and W. Michiels. “Design of robust decentralised controllers for MIMO plants with delays through network structure exploitation”. In: *International Journal of Control* 93.10 (2020), pp. 2275–2289.

[155] J. Zhou, X. Yu, and J.-A. Lu. “Node Importance in Controlled Complex Networks”. In: *IEEE Transactions on Circuits and Systems II: Express Briefs* 66.3 (2019), pp. 437–441.

[156] S.A. Plotnikov and A.L. Fradkov. “Desynchronization control of FitzHugh-Nagumo networks with random topology”. In: *IFAC-PapersOnLine* 52.16 (2019). 11th IFAC Symposium on Nonlinear Control Systems NOLCOS 2019, pp. 640–645.

[157] W. Michiels and S. Niculescu. *Stability and Stabilization of Time-Delay Systems: Advances in Design and Control*. Society for Industrial and Applied Mathematics, 2007.

Acknowledgments

One of my Russian friends always told me «Боишься обжечься - не зажигай, но если зажёг - иди до конца», which can be interpreted as «if you are afraid of failing - do not even start, but if you have started something - you have to do your best to accomplish it». When I came to the Netherlands to start my PhD project, I was a different person with a different mindset. I was not the most educated or the smartest guy in the room, but I was and still am a very curious person. I think that my curiosity, the need and itch to know and understand how things around me work, and my stubbornness and determination are the drivers that have brought me to this moment.

Applying for this PhD position was one of the most defining moments, or bifurcation points, of my life. Since childhood, I had always asked myself: «How and what is it like to be a scientist?» And now, 4 years later I have a better understanding of what it is like to be able to partially answer this questioning. It has not been fully as I imagined back then but these years have definitely given me a lot in terms of knowledge, experience and personal development. I strongly believe that I will always refer to these years as to one of the best periods of my life. Of course, it became possible thanks to people around me. That is why, I am very grateful to the European Union for funding this project. I truly hope that the knowledge gained during these years spent in the Netherlands, Belgium and France will be of great service to my future research pursuits.

First of all, I would like to express my gratitude to my promoters Henk Nijmeijer and Wim Michiels, and my co-promoters Erik Steur and Sasha Pogromsky for giving me the opportunity of being a part of the UCoCoS project. I am deeply grateful for your guidance, mentoring, support and patience. Sasha, thank you for your support with research and cultural adaptation, and abundance of interesting and enlightening discussions we

had. Your broad and deep knowledge together with a diplomatic attitude are delightful, and I am grateful for time and effort you spent answering thousands of my questions. Erik, thank you for being patient and supportive, always asking questions that trigger me to look at a problem from different angles and to "see a bigger picture". Your mastery of teaching, attention to details together with sharp mathematical skills helped me to improve the presented thesis a lot. Wim, thank you for your enthusiasm, broad knowledge and always being willing to help, I appreciate your time and effort you spent explaining to me different concepts and challenging my findings. Special thanks for coordinating this project, I am glad and proud to having been a part of it. Henk, thank you for being my promoter and giving me this opportunity. I respect and admire your rigorous attitude and critical view, and I am grateful for your sense of humor, patience and support. I would also like to wish you a long, healthy, and happy retirement! It is really honor that I have had a chance to work with all of you and learn from you.

My sincere gratitude also goes to Bob Puers and Philip de Goey, who agreed to be the chairs of my doctoral committee for preliminary and public defenses, respectively, and Giovanni Samaey, Jaap den Toonder and Emilia Fridman, who agreed to be the members of my examination committee and review this thesis in detail.

During my PhD, I had the chance to visit and collaborate with the Control and Scientific Computing group of the CNRS lab CRIStAL at Centrale Lille, France. I would like to thank Jean-Pierre Richard and Laurentiu Hetel for arranging this visit. I have spent great and productive time in Lille.

I would like to express my gratitude to my fellow early stage researchers in the UCoCoS project: comrade Libo Su, Haik Jan Davtyan (Silm), my favourite Deesh, Dr. Thomas and tovarish Quentin Voortman. I am happy to have met you, guys, and have had a chance of working, partying and becoming friends with you. I enjoyed every gathering we have had over the past years and hope that we will keep gathering in future. Mr. Q, thank you for being a great office mate in Eindhoven. Furthermore, I am grateful to the colleagues whom I met during my stay at KU Leuven, Emil, Joris, Francesco, Luca, Pieter, Koen and Marco, and whom I met during my stay at TU/e, Andy, Fahim, Brandon, Wouter, Frans, Robin, Haitao, Sebastiaan and Timo. Thanks for sharing your expertise and experiences during colloquiums, lunches and coffee breaks. I would also like to extend my

gratitude to the staff of the Computer Science Department at KU Leuven (especially Stella) and the Mechanical Engineering Department at TU/e (especially Geertje) for their administrative support.

In addition, I would also like to thank my dear friends and close people in Eindhoven, Lille and Leuven, Lena, Tatiana, Ramina, Artem, Fedor, Anatolii, Alex, Isaac, Anastasia, thank you for making my spare time great! Special thanks goes to my dearest Daniel, Ksenia, Nika, Ronis and Mariia, with whom I have shared so many memorable moments, trips and dinners. You are amazing, thank you for being with me during my PhD journey. It would not be fair not to express my gratitude to Dima and Vlada, two amazing and very close people who supported me on this road distantly. I am so lucky to have all of you in my life. Without you, my stay in the Netherlands, France and Belgium would not have been so enjoyable.

The last but not least, I would like to dedicate this thesis to my family. Especially to my mother Natalia Rogova, my father Oleg Rogov, my little sister Elizaveta Rogova and my grandparents Nikolay and Ira Meda. Thank you for always being by my side! I would not have accomplished this project without your love and support!

Kirill Rogov
June 2021
Leuven, Belgium

Curriculum Vitae

Kirill Rogov was born on 28-06-1992 in Saint-Petersburg, Russia. After finishing High School in 2009, he studied Aerospace Engineering at Saint-Petersburg State University of Aerospace Instrumentation (SUAI), in Saint-Petersburg, Russia, where he did an engineering diploma project on modeling MEMS and NEMS sensors. After obtaining his engineering degree (BSc and MSc) in 2014, he started an international master program at Polytechnic University of Catalonia (UPC). In 2016 Kirill graduated from UPC, obtaining the Master of Science degree in Aerospace Science and Technology, supervised by Prof. J. J. Masdemont, with a thesis on computation of libration point orbits and manifolds using collocation methods. In 2016 he started a joint PhD as a Marie Skłodowska-Curie fellow and a member of the UCoCoS (Understanding and Controlling Complex Systems) project at Eindhoven University of Technology (TU/e), the Netherlands, and Katholieke Universiteit te Leuven (KU Leuven), Belgium, the results of which are presented in this dissertation.